CONDITION MONITORING OF BEARING DAMAGE: TEST IMPLEMENTATION AND DATA ACQUISITION

by

Adrian Gomez

Submitted to the Department of Mechanical Engineering in partial fulfillment of the requirements for the Degrees of

Bachelor of Science in Mechanical Engineering

and

Master of Science

at the

Massachusetts Institute of Technology

June 2000

Signature of Author .....
Department of Mechanical Engineering
May 5th, 2000

Certified by .....
Sanjay E. Sarma
Thesis Supervisor
Cecil and Ida Green Associate Professor of Mechanical Engineering

Accepted by .....
Ain A. Sonin
Chairman, Department Committee on Graduate Students

DISCLAIMER OF QUALITY

Due to the condition of the original material, there are unavoidable flaws in this reproduction. We have made every effort possible to provide you with the best copy available. If you are dissatisfied with this product and find it unusable, please contact Document Services as soon as possible.

Thank you.

Some pages in the original document contain text that runs off the edge of the page.

CONDITION MONITORING OF BEARING DAMAGE: TEST IMPLEMENTATION AND DATA ACQUISITION

by

Adrian Gomez

Submitted to the Department of Mechanical Engineering on May 5th, 2000
in partial fulfillment of the requirements for the Degrees of
Bachelor of Science in Mechanical Engineering and Master of Science

ABSTRACT

The field of preventive maintenance has seen continued interest in the condition monitoring of roller element bearings. The push towards creating "smart bearings" has led many to develop instrumented solutions to existing applications. Unfortunately, there is a lack of data when trying to correlate bearing damage to a particular signal signature. Therefore, this project will conduct a condition monitoring study of bearing damage. The study will create a test procedure to accelerate, isolate, and evaluate damage in different bearing components. In addition, the design and construction of an automated data acquisition system will aim to capture incipient bearing degradation. In the end, it is the author's intent to create a capacity for conducting damage mapping tests using a standardized procedure. Hence, it is hoped that once a bearing defect can be associated with a particular signal, the instrumented bearing can be used to provide useful as well as vital information to customers.

Keywords: damage mapping, condition monitoring, bearing DAQ system.

Thesis Supervisor: Sanjay E. Sarma

Title: Cecil and Ida Green Associate Professor of Mechanical Engineering

To my parents,

I am here at MIT because one day you decided to embark on an adventure. You did it for your sons and I cannot find the words to thank you. We have survived this journey and we are eager to begin once more. Please, never forget that I am indebted to you always.

Los quiere mucho,

Adrián

Acknowledgements

The author would like to thank the following individuals:

- Rosendo Fuquen. For his guidance and support during the length of the project and during my other internships with the Timken Company. His advice and friendship are privileges that extend beyond any experience in the program.

- Sanjay Sarma. For his tireless enthusiasm and help in the past years. Especially, for his trust and concern not only for my work but also for my well being.

- Ryan Anderson. For his friendship during my stay at Timken Research. His help and unconditional support have made him a friend for life.

- Mike French. For his constant advice and guidance on the project and for his ability to always make me laugh.

- Dave Lawrentz. For his help and patience to explain the details of the test components. Also, for his time and interest in helping me learn.

- Brian Palmer, Joel Russell, and Gary Trompower for their guidance, patience and friendship in the life-test lab.

- Michelle Cadile. For her advice on how to handle work and life in general, but also for her friendship.

- Al Pierce, Mark Ostapack, and James Nisly for the support in the instrumentation of the bearings.

- Mike Miller. For inheriting the project and carrying out the proposed test work.

- Doug Clouse. For his help in obtaining the orthographic plots for the damaged

- Marisela Morales. For her continuous support and care. Especially for letting me share my dreams and goals in her laughter and joy. Also, for simply being there to help and accompany me in the toughest moments these past years.
- Socrates Gomez. For his continuous life-long support. Thank you for your constant affection in all aspects of life, especially in my college years.
- Milos Komarcevic. For simply listening so many times and for his sincere friendship all these past five years. Also a friend for life.
- David Schiller, Jim Maltese, Brittany Harmon, and Erica Klacik. For making my stay in Ohio a memorable one and for your continued friendship.

Table of Contents

List of Figures

List of Tables

1 Introduction

This project project describes the design of equipment and process for a condition monitoring study of bearing damage. The following section will outline the scope of the project, previous work carried out in this field and the sate of the bearing industry today.

1.1 The bearing industry

The modern day bearing industry has carried out application research, technological innovation and development for more than a century. As it stands today, numerous companies compete for the world bearing market. The following four companies are an example of global competition and technical expertise.

NSK (headquarters located in Ann Arbor, Michigan)

In 1913, NSK Corporation was created from two old names in the bearing industry, Hoover Ball Bearing and Nippon Seiko Kabushiki Kaisha (NSK Ltd.). Presently, NSK Corporation is a world-class producer of ball and roller bearings. Established in 1916, NSK has nearly 70 years experience in design, development and manufacture of nearly every kind of anti-friction bearing. This experience combined with up-to-date research methods and close attention to quality control have made NSK a world-class supplier of bearings, automotive components, and linear motion products to all major industries.

NTN (headquarters located in Osaka, Japan)

NTN's founders began research and manufacture of ball bearings at Nishizono Ironworks establishment of the Iwata Works in 1960, which enabled NTN to commence mass production of ball bearings. Subsequently, NTN came to lead the industry in the domestic needle bearing market. Presently, NTN's products include: bearings, automotive equipment (CV Joints), automated production equipment used in flexible intelligent manufacturing systems (FIMS), and precision processing equipment such as air slides with linear motors and preload multi-control bearing units.

SKF (headquarters located in Gothenburg, Sweden)

In 1907 Sven Wingqvist marked the start of a major industrial development, the world's first self-aligning ball bearing. One of the most important SKF advances of the immediate years after the First World War was the introduction of the spherical roller bearing. 1926 Production of experimental cars was started by AB Volvo, a subsidiary of SKF and becomes independent by 1935. In 1975 SKF further strengthened its position as a supplier to the aerospace industry by acquiring a 66 per cent shareholding in Société Anonyme de Recherches de Mécanique Appliquée (SARMA). By 1995 SKF had 90 factories, 44,000 employees of whom 84% are working outside Sweden. Hence, SKF has grown to be a world leader in rolling bearings

The Timken Company (headquarters located in Canton, Ohio)

In 1887, at 56 years old, Henry Timken retired as a successful carriage builder. By 1892 he had achieved three new patents on carriage springs. After 100 years, The Timken Company continues to serve every major manufacturing industry. Timken has produced more than six billion bearings since 1899. Its steel-melting capacity is 1.4 million tons annually. The Timken Company is a leading international manufacturer of highly engineered bearings and alloy steels (see figure 1.1). The company employs about 21,000 people worldwide and reported 1998 sales of more than $2.6 billion.

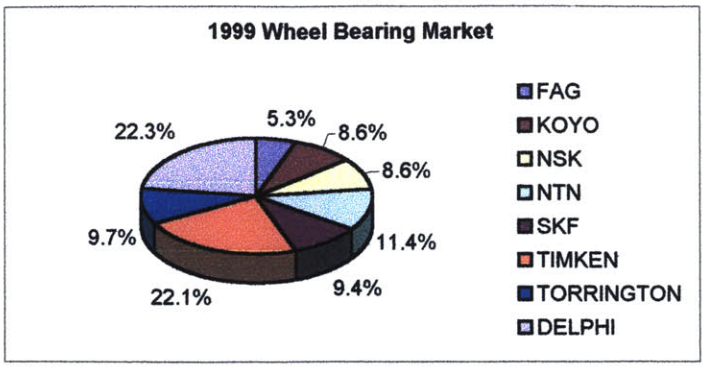

Figure 1.1: 1999 Component Forecast Market Report. Source: CSM Worldwide

1.2 Motivation

The project objective is to design a machine to test bearings under various load and speed conditions to detect bearing damage. This machine will allow the mapping of bearing damage in order to know the threshold of detection to certain confidence levels. Furthermore, it will enable the engineer to test and configure signal-processing algorithms for bearing damage. This project can be therefore split into two sections. First of all, a technical capacity is required with which to study bearing damage progression. Secondly, a laboratory test procedure is needed to allow for the collection of sensor data at the early stages of bearing degradation. Once these two sections are completed, the damage mapping of bearings through signals can begin.

Damage needs to be clearly understood in order to carry out a comprehensive risk analysis of a particular rotating system. The problem's complexity grows because damage can occur in a variety of forms and in different components. Hence, this experiment is needed to validate the use of sensors to monitor bearing life. Once this validation is established, future decisions can be made such as whether to continue or cease operation due to the damage severity. In addition, the data from these test trials can be used to create bounds around the damage field of a particular bearing application.

Intended Scope

The intended scope of this project is to establish the proposed sensor evaluation system and carry out several damage tests. The project will touch on the following aspects: hydraulics, mechanical design, sensor technology, signal processing, data acquisition software/hardware, and material properties. Each section will be needed in order to understand how bearing damage evolves and propagates. Furthermore, the final goal is to pinpoint incipient bearing damage through a criterion for damage signals. This monitoring, also known as preventive-maintenance, will be able to predict various damage levels: incipient, tolerable, in need of replacement, or catastrophic. At some poin in the future it may be possible to place sensors inside mechanisms and to detect failure.

Actual Scope

The actual scope of this project is only to establish the testing procedure for bearing damage mapping. Numerous time constraints prevented any test work from being carried out. On the other hand, the sensor selection and baseline tests have been completed and prove satisfactory. Furthermore, an automated data acquisition system has been developed to monitor changes in the signals.

1.3 Outline of thesis and previous work

This thesis will present and explain the testing capacity and procedure for bearing damage mapping. It will describe how the test bearing, tooling, lubricant, and sensors were selected. It will also describe the modifications made to the load system, bearing tooling, and test machine housing in order to accommodate the selected sensors. In addition, the accelerated bearing damage will be described along with the test machine assembly procedure. Finally, this study will present the development of an automated data acquisition system, as well as explain the baseline and proposed tests.

As previously mentioned, "rolling element bearings form an important part of machine tools. Consequently, regular monitoring of their performance is essential to ensure manufacturing quality and operation safety." [1] The word "smart bearing" is being frequently used today throughout the bearing industry. Everything from helicopters to heavy machinery is a candidate for these mechatronic components. In a study by Robert X. Gao, Brian T. Holm-Hansen, and Changting Wang from the University of Massachusetts, they state that "an advanced condition monitoring system often consists of a variety of sensing, controlling, and actuating components. Their effective and efficient integration requires the application of mechatronic design principles to achieve the desired synergy". [2] A smart bearing system includes the following component sections: electrical, electro-mechanical, and mechanical. Microelectronics is an example of the purely electrical part of the condition monitoring system. The electro-mechanical component is perhaps a piezoelectric sensor, while the mechanical element is the component to be monitored (bearings). Thus, "mechatronic design principles provide a systematic approach to effectively integrate various engineering aspects for the implementation of advanced machine condition monitoring system". [2]

In a study by SKF, it was concluded stated that "preventive maintenance holds the key to plant optimization . . . Condition monitoring allows for the detection of machinery, equipment and bearing problems at an early stage through noise and vibration analysis". [3] Furthermore, the most favored methods for "in-depth diagnosis of machine failure modes are spectral analysis and discrete frequency analysis". [4] It was also concluded that 16% of bearing failure originates during mounting, while 30% of all bearing failures were due to lubrication problems. [4]

On a slightly different note, instrumented bearings are currently being used in the market. For example, electrical sensors are placed on mechanical bearings for better control of antilock braking systems. The Sensor-Pac from the Timken Co. is such an example. Other examples make use of a variety of sensor technologies including magnetoresistant sensors and Hall-effect sensors.[5] These current condition monitoring solutions are proof that combining electrical and mechanical components create an added advantage and incentive in the bearing industry.

In regards to health maintenance for machines, there are three different approaches. First, breakdown maintenance refers to machines that run until they fail or are producing 100% scrap. Although failure can be catastrophic, tooling or replacement parts are rarely available. Secondly, scheduled maintenance carries out routine checkups that completely shut down the machine. Usually, machines are disassembled and worn parts are replaced, making it an expensive process. Finally, predictive maintenance combines early detection and real-time analysis. Shut downs can be scheduled and the necessary can be allocated accordingly, making it an inexpensive alternative.[6]

At the 12th International Congress on Condition Monitoring and Diagnostic Engineering Management (1999), Roger W. Hutton stated in his paper, "for many years condition monitoring has claimed to be able to deliver significant benefits in terms of reduced maintenance costs, and increased production output. The reality is that the expectations have rarely been fully met, leaving skepticism and confusion as to what has gone wrong".

He goes on to conclude that in order to improve these shortcomings, industry must set for itself the following goals: integrate condition monitoring with business and financial goals, carry out reliability studies to determine which machines should be maintained, and integrate condition monitoring systems with maintenance management systems.[7]

At the same conference, Scott E. Dow presented a paper dealing with the future of training for condition based monitoring. Condition monitoring can be divided into four main categories: vibration analysis, lubrication analysis, temperature analysis, and electrical testing. He goes on to conclude that the future of training is in the hands of companies. He adds that as companies move towards standardization of processes and procedures, evaluation techniques must be developed to measure an operator's ability to improve machine reliability, reduces downtime, and correct machinery problems. [8]

2 Bearing Types

Bearings are mechanical elements that reduce friction between moving machine parts. Most bearings consist of an inner ring, a number of rolling elements, an outer ring, and a cage. For rolling bearings, they are differentiated by the type of rolling elements such as: ball, cylindrical, needle, spherical, and roller. The first four types of rolling elements will be subsequently described, while roller bearings will be presented in the next section.

Ball Bearings

Ball bearings have a point contact between the balls and the inner and outer races. Therefore, it is necessary to specify a larger ball bearing for a specific load capacity in contrast to a tapered roller bearing, which distributes the load over the length of the roller. The deep groove ball bearing seen in Figure 2.1 is suitable for light radial loads only.

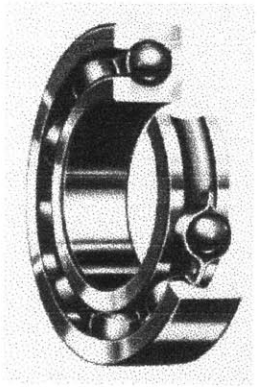

Figure 2.1: Deep groove ball bearing. Source: NSK-RHP

For deep groove ball bearings, axial load conditions should be avoided since this can lead to rapid failure. Furthermore, thrust ball bearings, as seen Figure 2.2, support only axial loads acting in one direction.

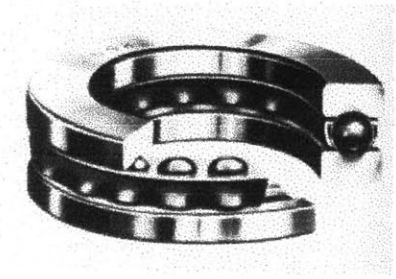

Figure 2.2: Thrust ball bearings. Source: NSK-RHP

Hence, low shaft speeds are needed. If this criterion cannot be met, then angular contact bearings are preferable instead.

The angular contact ball bearing is designed to take combined radial and thrust loads. Thus, its load capacity is increased when compared to the deep grooved ball bearing, but it's still lower than the equivalent tapered roller bearing. The single row angular contact ball bearing shown in Figure 2.3 does not allow for any misalignment between the shaft and the housing, which in turn severely affects bearing life.

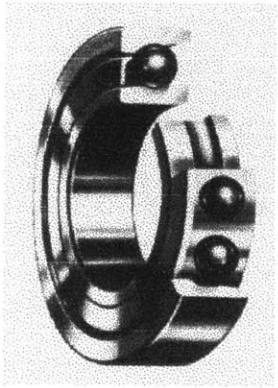

Figure 2.3: Angular contact ball bearing. Source: NSK-RHP

Cylindrical Roller Bearings

Cylindrical roller bearings (see Figure 2.4) are used to accommodate for thermal expansion effects by allowing axial displacement of the shaft relative to the housing.

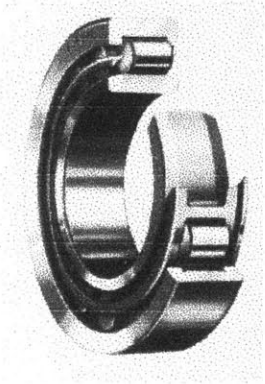

Figure 2.4: Cylindrical Roller Bearing. Source: NSK-RHP

In addition, inner and outer races are separable, facilitating mounting and dismounting. As opposed to ball bearings, cylindrical rollers have a higher load carrying capacity due to their line contact with the races. In comparison with a tapered roller bearing of similar size, the cage from a cylindrical bearing is therefore heavier and has fewer rollers, lowering its load capacity.

Needle Roller Bearings

Although similar to cylindrical roller bearings, needle roller bearings have a compact cross-section using long, thin rollers (see Figure 2.5).

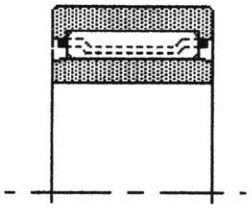

Figure 2.5: Cross-section of Needle Roller Bearing. Source: NSK-RHP

These bearings have a high radial load capacity, but limited capacity in the axial direction. Some typical applications include the synchromesh mechanisms of automotive gearboxes, and the planetary gear bearings in light duty epicyclic hub-reduction units.

Spherical Roller Bearings

Spherical roller bearings (see Figure 2.6) have a self-aligning feature, which allows for minor angular displacements between the shaft and housing.

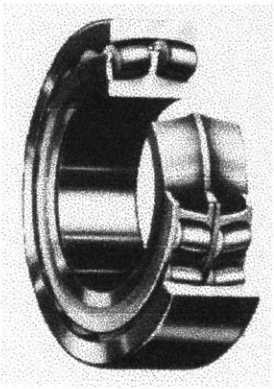

Figure 2.6: Spherical Roller Bearings. Source: NSK-RHP

These bearings have a high radial load capacity, but under heavy load the stress is not evenly distributed. Therefore, true rolling motion only occurs at two contact points on each roller. Consequently, this induces skidding along the roller length, giving the spherical roller bearing a higher coefficient of friction with lower speed capabilities when compared to other bearings. To counteract the roller skidding condition, the cage is much heavier, increasing the moment of inertia and limiting the number of rollers.

In addition, a variety of industries depend on the previously mentioned bearing types as well as many others, such as: aircraft, magneto, pump, rolling mill, super precision, miniature, high-speed, and instrument bearings (see Figure 2.7).

a) 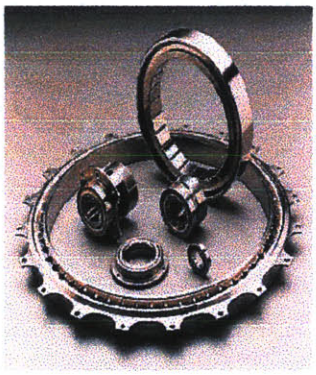 b) 

Figure 2.7: Various bearing types for a) medical/dental and b) aerospace industries. Source: The Timken Co.

The automotive industry requires a large number of bearings for its passenger, light-truck, and heavy-duty vehicles. Bearings are primarily used in wheels, trailers, and drive lines, which include transmissions and differentials. The consumer equipment industry also requires the use of bearings for all types of products: boats, motors, golf carts, snowmobiles, etc. Furthermore, all industries such as: construction, mining, agriculture, mass-transit, government, and process equipment require the use of bearings for any type of rotating machinery.

2.1 Tapered Roller Bearings

The main difference between ball and tapered roller bearings is that ball bearings have a lower coefficient of friction, but tapered roller bearings have a higher load capacity. With this in mind, tapered roller bearings can be grouped into the following different categories:

Single-row bearings

The single-row bearing (see Figure 2.8) is the most widely used type of tapered roller bearing. It has two main, separable parts: the inner race assembly (or cone/roller assembly) and the outer race (or cup).

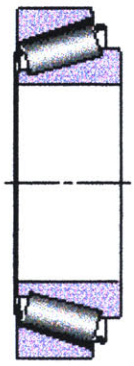

Figure 2.8: Single-row tapered roller bearing. Source: The Timken Co.

Single row bearings can be "set" to a required "endplay" or "preload" condition during equipment assembly to optimize the rotating system's performance.

Two-row bearings

The two single-row assemblies are often referred to as 'spacer assemblies', which are comprised of two basic single-row bearings. The assemblies have both inner and outer race spacers, giving a pre-determined bearing setting according to the application. A snap ring is also sometimes used as the outer race spacer. There are three different mounting configurations for double-row bearings. As seen in Figure 2.9, indirect mounting uses two single-row bearings with an inner and an outer race spacer.

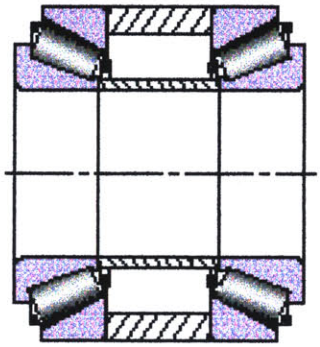

Figure 2.9: Indirect mounting of two-row tapered roller bearing. Source: The Timken Co.

In the case of direct mounting, two single-row bearings are used again. This time, only an outer race spacer is used with the inner races abutting. This type of mounting seen in figure 2.10 is mostly used at fixed positions on rotating shaft applications.

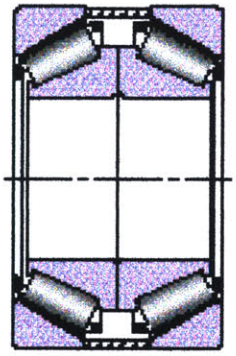

Figure 2.10: Direct mounting of two-row tapered roller bearing. Source: The Timken Co.

When the thrust component is beyond the load carrying capacity of a single bearing, two single-row bearings can be used in tandem mounting (see Figure 2.11). Inner and outer spacers must also be used to carry the combined radial and thrust loads.

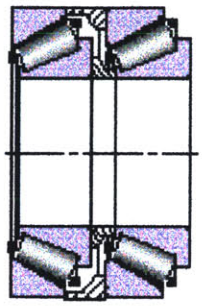

Figure 2.11: Tandem mounting of two-row tapered roller bearing. Source: The Timken Co.

These pre-set assemblies give a wide effective bearing spread and the same time the bearings can be used in fixed positions or allow floating in the housing bore in the event of any shaft expansion. Furthermore, there are several variations of two-row tapered roller bearings, such as: double outer race, double inner race with tapered bore, non-adjustable, non-adjustable with lubricant slots, or non-adjustable with lubricant slots and extended races. These last three variations are made up of one outer race and two inner races. In this case, the inner faces are extended so that there is no need for an inner race spacer.

Four-row bearings

Four-row bearings are assemblies of maximum load rating in a minimum space. These combine high-load, radial/thrust capacity and direct/indirect mounting variables of tapered roller bearings. The bearings' main application is on the roll necks of rolling mill equipment. All four-row bearings are supplied as pre-set matched assemblies. As seen in Figure 2.12, the four-row bearings are designed to take thrust loads at a) semi-static or oscillating applications and b) heavy-duty applications at high speeds.

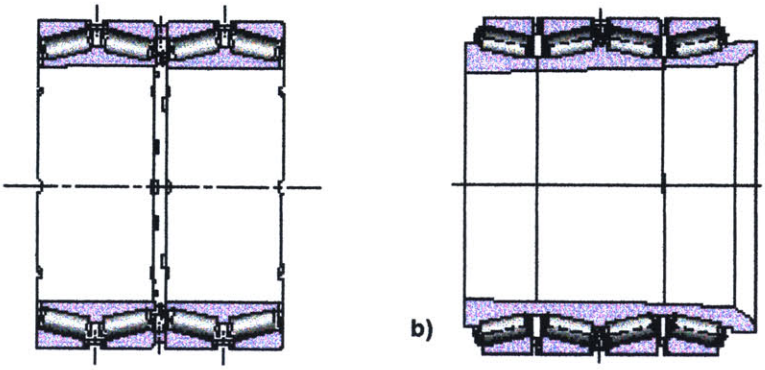

Figure 2.12: Four-row tapered roller bearings. Source: The Timken Co.

Railroad bearings

This bearing is a self-contained assembly comprised of two single inner races, a counterbored double outer race, a backing ring, two radial seals, an end cap and cap screws. This rail bearing is a pre-set, pre-lubricated and sealed package.

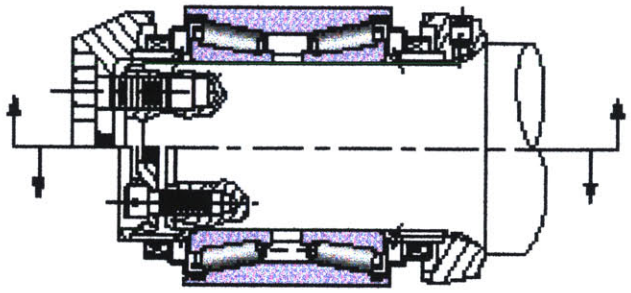

Figure 2.13: Railroad tapered roller bearing application. Source: The Timken Co.

Once the bearing type study was conducted, it was decided that based on product availability as well as the testing apparatus, a tapered roller bearing would be the ideal candidate for carrying out the damage mapping tests. The following section will therefore outline the selection criteria for this particular bearing.

2.2 Selection Criteria

A tapered roller bearing reduces friction as either the cup or cone rotates while the other remains stationary. Figure 2.14 shows the different components: cup, cone, cage and rollers.

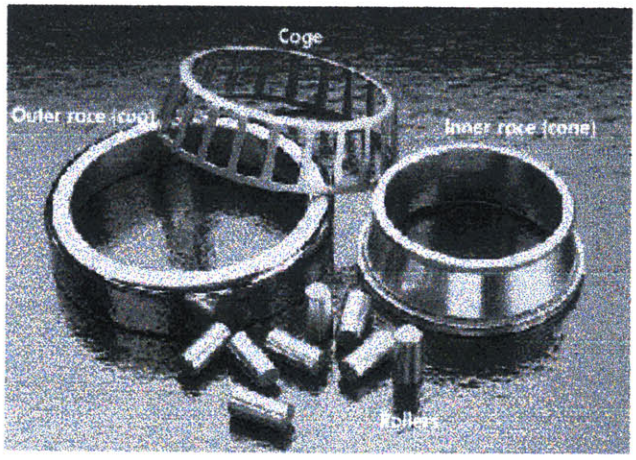

Figure 2.14: Components of tapered roller bearing. Source: The Timken Co.

Furthermore, the cup, cone and rollers bear the actual load, while the cage spaces and holds rollers on the cone. The roller taper and the corresponding angled raceways allow the bearing to withstand both radial and thrust loads. Standard tapered roller bearings can operate at high speeds provided there is proper setting, adequate lubrication, no shock, vibration or unusual loading, and there is adequate heat dissipation.

The bearing was selected based on tooling availability in the Life Test Lab at Timken Research. The test machine also limited the size of the bearing since the available life-test housing could only accommodate a 3"- 5" cup OD. It was therefore determined that a single row pinion bearing would be used. Figure 2.15 shows a schematic of the life test housing.

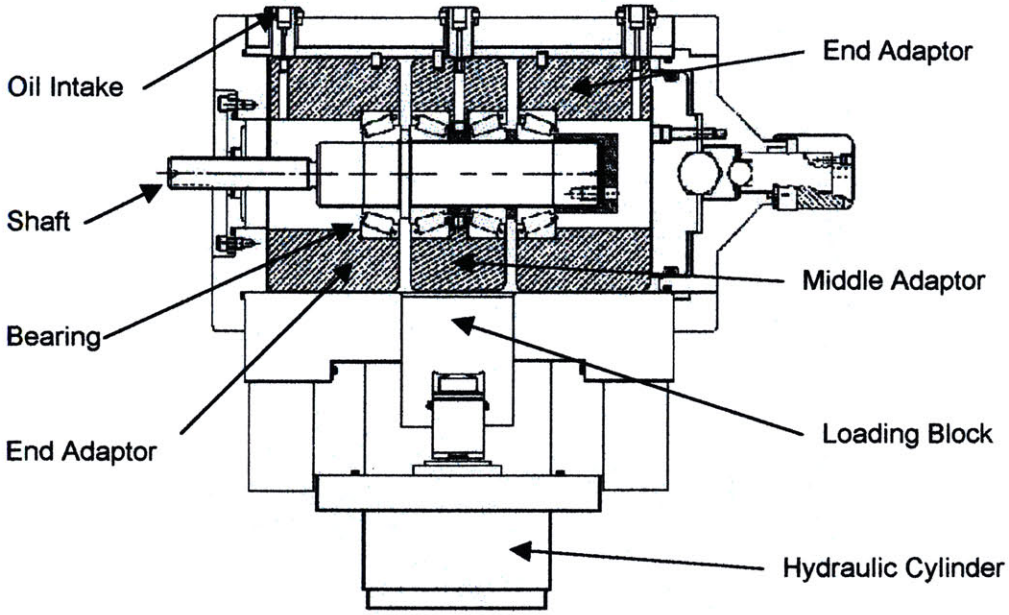

Figure 2.15: Schematic of life test housing

The housing is a casting that can accommodate four single row bearings pressed into their corresponding tooling. The tooling is comprised of two end adaptors, a middle adaptor, and shaft components. In assembling this tooling, the end play is set using shims on the shaft. In addition, the housing is designed such that the 3.75" hydraulic load cylinder causes the loading block to deliver the radial load to the center adaptor. Therefore, load zones will appear in the bottom of the middle adaptor bearings and on the top of the end adaptor bearings. Figure 2.16 shows the type of machine housing to be used.

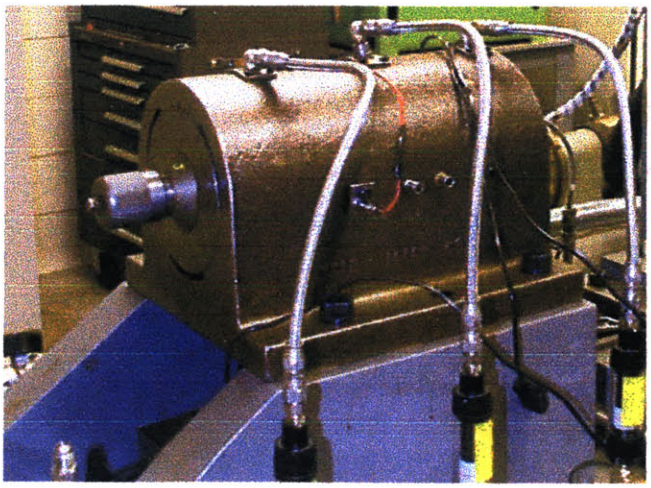

Figure 2.16: Life test housing

The picture also shows the three flexible oil hoses. They connect to the housing at the oil intake in order to fill the housing with the selected lubricant. At the back of the housing, a coupling is then attached via a keyway to the installed shaft, which then connects the rotating components to the machine's motor. The motor can safely reach a maximum speed of 1200 rpms and is controlled with the instrument panel shown in Figure 2.17.

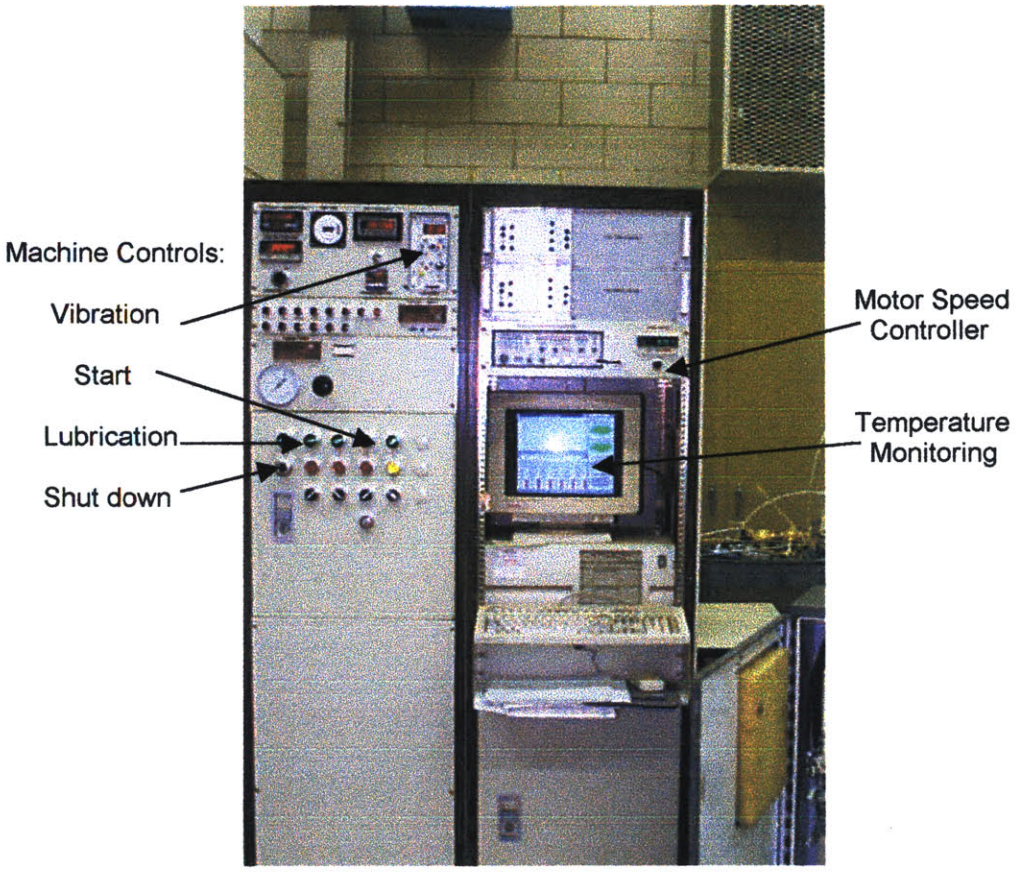

Figure 2.17: Machine Control Console

The start/shut down controls were placed outside of the machine room for safety reasons. Furthermore, temperature and speed monitoring was also carried out in this console. Four thermocouples in the test housing reported bearing temperature in real time for the test duration. Furthermore, in case of high temperature or excessive vibration, the machine will automatically shut down. In order to run the machine; the lubrication hoses first pumped oil into the housing. Subsequently, the motor speed controller was used to bring the shaft speed up to the maximum allowable level. Lastly, the specific load setting was applied using the load system described in Chapter 6.

3 Bearing Tooling

As previously mentioned, the bearing was selected based on tooling availability. Once all of the adaptors and shaft components were obtained, it was decided to place sensors on the cup OD of the bearing. Thus, the three adaptors had to be modified in order to allow space for the sensors.

3.1 Tooling Modifications

The adaptor modifications were made once the sensor selection and placement was determined (see Chapter 4). As shown in Figure 3.1, "pockets" and "channels" were cut out of the adaptors to allow space for the accelerometers and thermocouples mounted on the bearing cup OD.

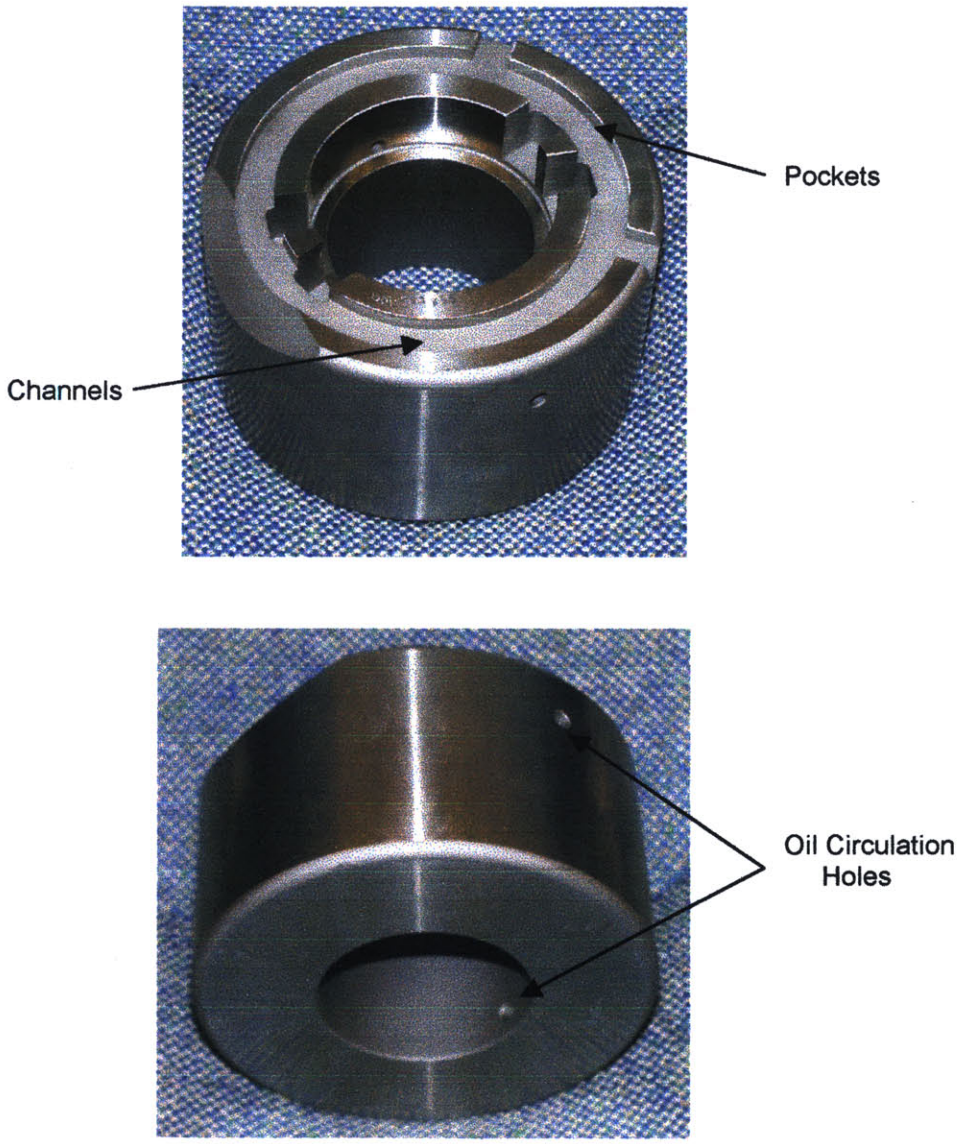

Figure 3.1: Front and back of modified end adaptors

As noted in Figure 3.1, circulation holes were drilled into the adaptors to aid the oil flow during the test. Similarly, the middle adaptor seen in Figure 3.2 was modified as well.

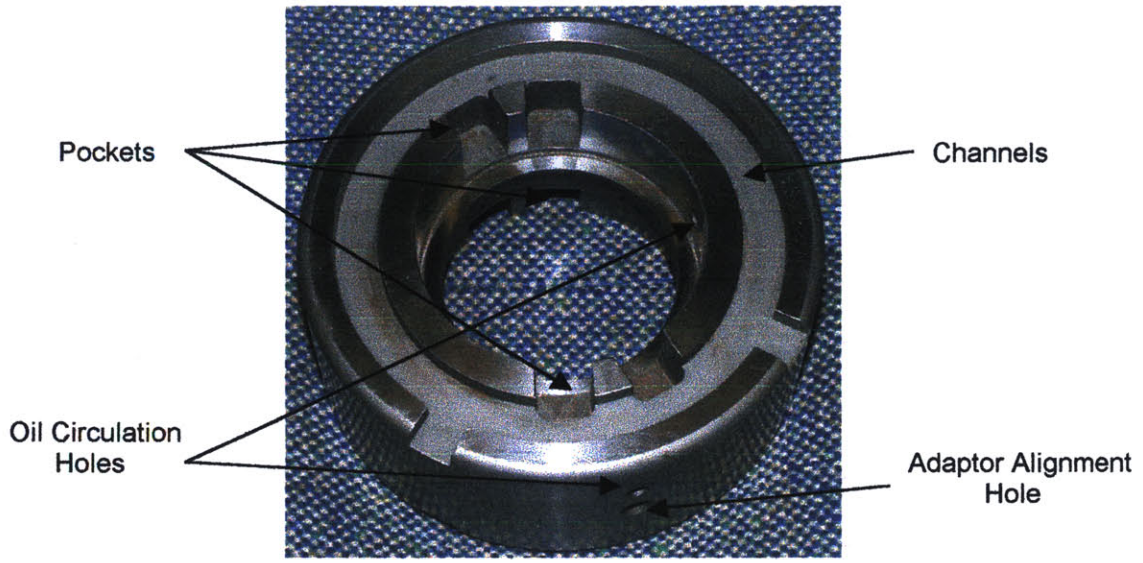

Figure 3.2: Modified middle adaptor

This smaller adaptor had modifications on both faces. The channels were used to neatly route the wires from the sensor positions on the cup OD to the holes in the housing. The wires would come out of the pocket and small pieces of welded metal were used to guide them along the channels to the two top channel exits. Furthermore, the figure shows an adaptor alignment hole. In order to secure the adaptors in place, a small metal pin was used to locate the top of the adaptor using a locating groove along the top of the housing. This in turn helped to consistently orient the bearings when installed.

Taking into account the size of the accelerometers, the pocket dimensions were derived. Figure 3.3 shows the pocket cross-sectional dimensions.

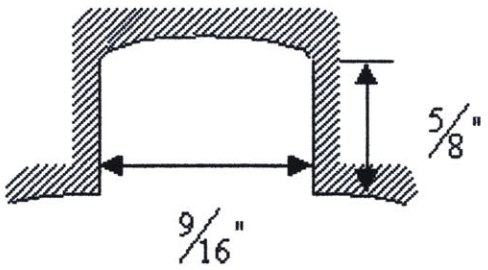

Figure 3.3: Pocket cross-sectional dimensions

Once the accelerometers were selected, it was decided to make all the thermocouple pockets the same size as well in order to minimize the need for further tooling work in case there was any future change in sensor placement. The tolerances on the pocket dimensions were closely held to ensure the removal of material did not affect bearing performance in the life-test machine.

3.2 Housing Modifications

Figure 3.4 shows how the housing was also drilled to take out the sensor wires from the adaptor channels.

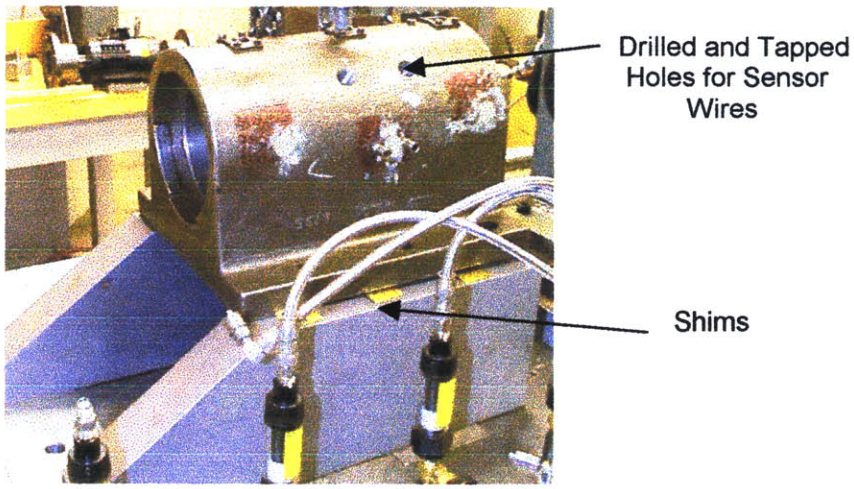

Figure 3.4: Modified housing

The four holes were tapped with a 5/8" thread so those bolts could prevent any leakage of oil during the test when sensors were not used. Once the instrumented bearings were installed, the holes were plugged with rubber stoppers instead. Furthermore, shims were also used at the base of the housing to make sure it was aligned with the machine's motor.

4 Sensor Selection

The advent of sensor technology has made it possible to combine the mechanical and electrical engineering fields and apply such technologies to bearing condition monitoring. For example, computer based systems have been developed to use vibration sensors such as a laser vibrometer.[9] Other systems use industrial accelerometers to monitor vibration in real-time and predict failure.[10-11] Still other approaches use eddy current sensors to set up high-frequency magnetic fields which in turn induce eddy currents in the radii and raceways of the bearing. Therefore, when the magnetic fields are affected by changes in clearance due to wear, a change in the sensor output signal occurs.[12] Yet another approach uses force sensors, whose output signals are relayed to the microprocessor for a programmed comparison to pre-established load limits.[13]

A non-contact sensor was also used in a bearing diagnosis study carried out at the Georgia Institute of Technology by Y.Yang, T. Kurfess, S. Liang, and S. Danyluk.[14] Two types of 'gross defects' were introduced by creating an EDM line on a single roller or by simply taking out one roller. The contact potential difference (CPD) probe generated two main spikes, which decreased with the EDM defect and disappeared with the missing roller defect. Using Timken bearings, it was concluded that the signal is linearly related to operational speed and the spacing between the probe and the roller.

Another study dealing with instrumented bearings was carried out by Brian T. Holm-Hansen and Robert X. Gao at the University of Massachusetts.[15] It addresses several design considerations of a sensor integrated rolling element bearing. The study concludes that a bearing condition monitoring system using a sensor module on the bearing raceway has several advantages when compared to conventional condition monitoring systems. In addition, the use of acoustic, force, or temperature sensors can create a "smart" bearing and replace conventional bearings.

The popularity of "smart" bearings has greatly increased, hence calling for further sensor integration with the bearing. On the issue of imbedding sensors on bearing cups or outer races, a study was published by Robert X. Gao and Prashanth Phalakshan from Louisiana Tech University.[16] This integration requires some material removal in order to fully instrument a bearing. Thus, a slot, in which force and temperature sensors as well as data-processing microelectronics are integrated, was proposed. Using finite element analysis, results showed that the introduction of a slot into the bearing raceway would not cause a significant increase in stress and deflection for up to a 40% reduction on the outer raceway thickness. It is important to note that this study considered a ball bearing with specific dimensions, requiring further analysis for many other types and sizes of bearings. At the same time, the study shows that it is feasible to implement this sensor integration technique.

Whether it is a plastic optical fiber wear sensor,[17] accelerometers, force, eddy current, or temperature sensors, the fundamental idea in all these different approaches is to instrument bearings in order to evaluate their operating condition, thus giving valuable real time information to the operator.

4.1 Sensor Placement

Due to the complexity associated with each type of sensor, it was decided to only use accelerometers and thermocouples in this preliminary study. The number of sensors on the cup OD proved to be the most important decision. It was necessary to take enough data points to characterize the damage progression, but at the same time taking care not to create too much data that would become unmanageable in the end. Figure 4.1 summarizes the sensor placement complexity used to organize and decide on the number of sensors to be used in the various damage tests.

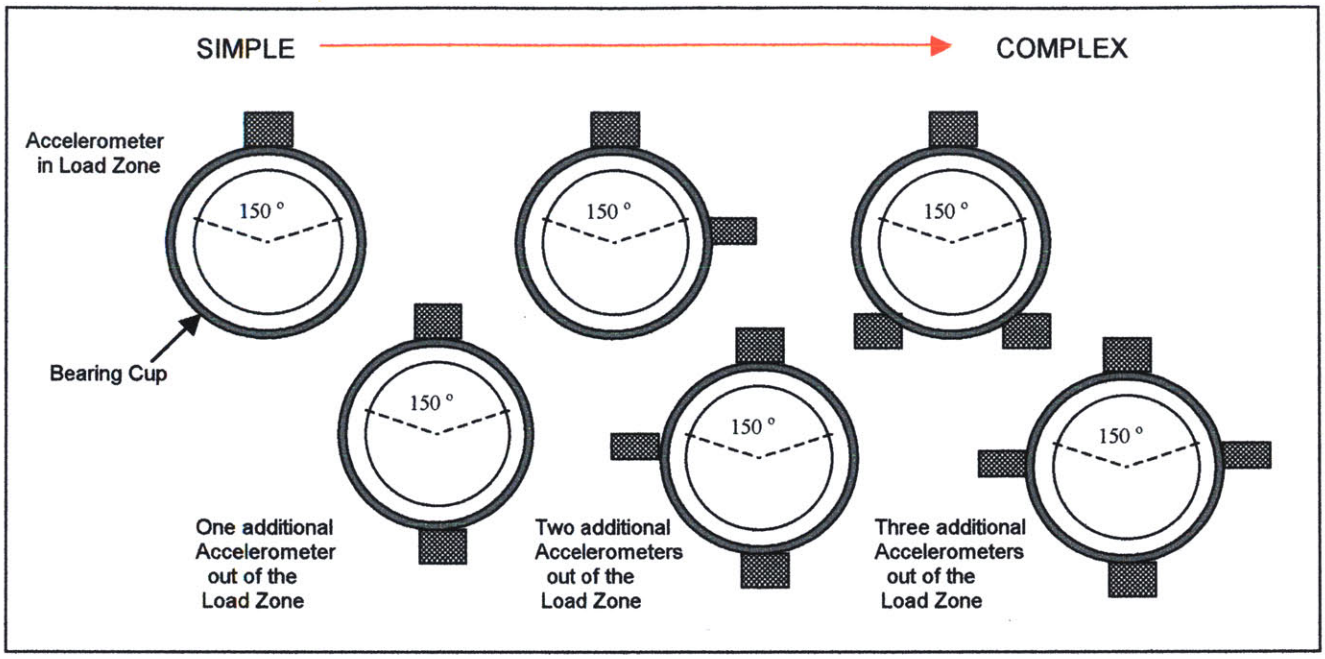

Figure 4.1: Sensor placement complexity for accelerometers

In a similar approach, the thermocouple placement complexity was mapped in order to reach a final instrumentation decision. The most complex configuration was too redundant, while the simplest sensor placement would gather only data points related to the bearing load zone. Thus, Figure 4.2 shows the final sensor placement configuration.

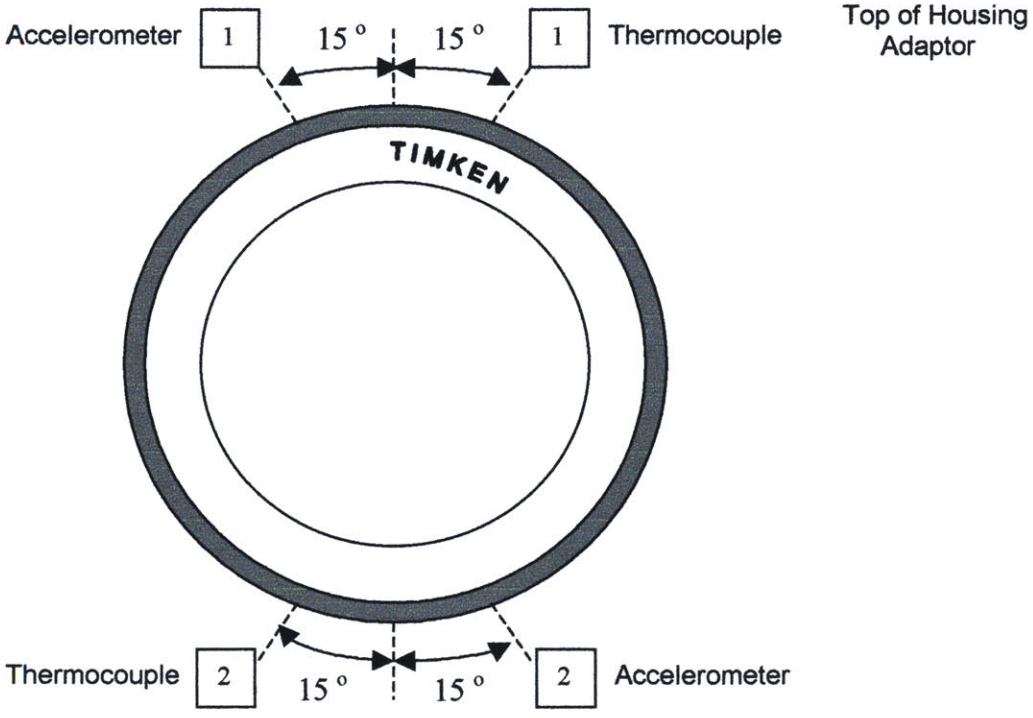

Figure 4.2: Final sensor placement configuration

The schematic shows a thermocouple and an accelerometer inside the cup load zone. Likewise, another thermocouple and accelerometer pair was placed outside the load zone. The sensors would be placed fifteen degrees-off-center, and at vertical angles from each other. This configuration had a twofold purpose: the two thermocouples would determine the existence of "hot spots" in the bearing. On the other hand, the accelerometers would compare the effect of load on the bearing itself. The numbers shown on the sensor locations were then used to label corresponding wires and sensors. Consequently, No. 1 was used to denote the top of the adaptor tooling where the locator pin was inserted, while No. 2 was located on the bottom of the tooling adaptor. Lastly, the letter T in the TIMKEN label stamped on the cup backface was used to consistently locate the bearings with respect to the top of the housing adaptor. Once the two types of sensors and their placement were determined, further detail was needed, such as the manufacturer of the accelerometer and the specific type of thermocouple.

4.2 Sensor Specifications

Accelerometers

It was first suggested to use tri-axial accelerometers, but the amount of data collected would become unmanageable in size. Thus, the selected accelerometer was a 353B17 miniature high-frequency quartz ICP® accelerometer from PCB Piezotronics. Figure 4.3 shows a photo of the proposed accelerometer.

Figure 4.3: 353B17 ICP® accelerometer from PCB Piezotronics

This high-precision, lightweight accelerometer uses a quartz shear sensing element to provide repeatable and reliable vibration measurements. As specified by the manufacturer, the shear mode-sensing element offers reduced sensitivity to thermal transients and base strain. The sensor's small size allows installation in confined or space-restricted areas. This size advantage was one of the main reasons for choosing this type of accelerometer since the smallest amount of material was to be removed from the adaptors. Furthermore, the accelerometer is ideal for measuring higher frequency vibrations. Table 4.1 enumerates the manufacturer's specifications (Appendix A has more detailed list of specifications).

Table 4.1: 353B17 Miniature High-Frequency Quartz ICP® Accelerometer Specs

Voltage Sensitivity (±10%)	10 mV/g (1,02 mV/[m/s2])
Measurement Range	±500 g pk (±4 905 m/s2 pk)
Frequency Range (±5%)	1 to 10 000 Hz
Mounted Resonant Frequency	≥70 kHz
Broadband Resolution	0.005 g rms (0,05 m/s2 rms)
Operating Temperature Range	-65 to +250 °F (-54 to +121 °C)
Sensing Element	Quartz Shear
Size (hex x height)	9/32 x 0.45 inch (7,1 x 11,4 mm)
Weight	0.06 oz (1,7 gm)
Electrical Connector	2-Pin Solder/Top
Mounting Thread	5-40 Male

Source: ®ICP is a registered trademark of PCB Piezotronics Inc.

Thermocouples

Temperature sensors called thermocouples are based on the principle that when two dissimilar metals are joined a predictable voltage will be generated that relates to the difference in temperature between the measuring junction and the reference junction. The selection of the optimum thermocouple type, mainly the metals used in their construction, is based on application temperature, atmosphere, required length of service, accuracy and cost. Different thermocouple types have very different voltage output curves. It is also required that thermocouple or thermocouple extension wire, of the proper type, be used all the way from the sensing element to the measuring element. Selecting the wire size used in the thermocouple sensor depends upon the application. Usually, when longer life is required for the higher temperatures, the larger size wires should be chosen. On the contrary, when sensitivity is the prime concern, the smaller sizes should be used.

The selection of the thermocouple was simply determined by the existing type in the signal conditioning box. Hence, a type J thermocouple was selected. Nevertheless, it is important to point out that this particular type is made up of iron (+) and constantan (-) metals and has a useful application range of 200-1400°F. (Source: ISE Inc.)

4.3 Sensor Preparation and Installation Procedure

Thermocouples Preparation and Installation:

4.3.1 Using TT-J-24-TWSH-SLE thermocouple wire, attach a male connector (1261-J) with ground to one end of the 2' pigtail. Thermocouple wiring is color coded by thermocouple types. Different countries utilize different color coding (see Figure 4.4).

Figure 4.4: Color coding for type J thermocouple. Source: United States ASTM

4.3.2 On the other end, strip 0.170" of insulation. Cut the ground wire off and strip 0.070" off the remaining two wires.

4.3.3 Use a vise to flatten the exposed wires and then line them up over one another to spot-weld them together at a setting of 6% in the Unitek welder. The spring tension should be set at 34 oz.

4.3.4 After welding them together, use a Q-tip to coat the brown insulation with M-Line Tetraetch without coating the inside of the wire. Then proceed to clean once more with soapy water and then with alcohol or acetone.

4.3.5 Cut and etch 0.250" long sleeves of fluoroplastic teflon 12-6 (FEP).

4.3.6 Once the sleeves have been cleaned as well, Insert them into the thermocouple wires and bend the welded pair in the same direction.

4.3.7 Use a heat gun to shrink the sleeve over the thermocouple wire. Make sure to cover any exposed metal shield.

4.3.8 Check that the thermocouples are functioning properly by using a heat gun and a Fluke meter.

4.3.9 Prepare a mixture of thermally conductive epoxy (Aremco 860 FSLV) with MEK. Coat the bent tips and follow the cure schedule on the can. (2 hrs. @ 150°F)

4.3.10 Cut 0.002" thick μ-metal into 0.300" wide strips. Fold the strips to be 0.150" wide and weld over the thermocouple wires using the Unitek welder with the welding setting set at 20% full energy of 125 W-s.

4.3.11 Weld a small strip 0.050" wide to the secure the tip of the thermocouple is touching the bearing surface.

4.3.12 Apply a coat of Aremco 568 high thermally conductive epoxy to attached thermocouple and cure for 1 hour at 150°F.

Accelerometer Installation and Coating Procedure

4.3.13 Attach accelerometers by using Aremco 860 FSLV epoxy and follow cure schedule on the can (2 hrs. @ 150°F). Make sure the accelerometers are centered on the bearing cup. Secure them with mylar tape and with spring clamps.

4.3.14 Apply one coat of MCOAT-B and air dry for 2 hrs. Apply a second coat, wait for 2 hrs. and bake at 200°F for 1 hour.

5 Bearing Damage

Bearing damage may occur while handling, before, and during installation. Improper installation, setting, and operating conditions can also cause damage. In many cases, the damage is easily identified by the appearance of the bearing, but it is not easy and sometimes it is impossible, to determine the exact cause of that damage. Simple examination of a bearing will not reveal the cause of the trouble. It can reveal if the bearing is good for further service, but often it is necessary to make a thorough and complete investigation of the mounting, installation and parts affecting the bearing operation to determine the cause of the damage. Unless the true cause of the damage is found and corrected, the replacement bearing will be damaged in the same manner and again there will be premature trouble. Hence, with proper precautions during the handling, assembly and operation of bearings, almost all damage can be prevented.

In a bearing vibration study by A.G. Herraty, a former Maintenance Manager for SKF, the modes of failure are summarized. First, it is established that the classical mode of failure is rolling contact fatigue. These defects are normally 0.2-0.3mm deep and have a surface area of $2mm^2$. Furthermore, failure most often occurs on the inner ring of bearings where contact fatigue stresses are higher. Although, this study primarily discussed ball bearings, similar failure characteristics can be seen with tapered roller bearings. Finally, other root causes of bearing failure are preloading, misalignment, and lubrication problems.[18]

5.1 Types of Damage

In the following section, examples are shown of the most common types of damage and some of the causes of this damage.

Mode of Contact Fatigue

Figure 5.1 shows how fatigue results from locally increased stress at the ends of roller/race contact.

Figure 5.1: Geometric stress concentration. Source: The Timken Co.

Fatigue damage may also develop after repeated cyclic stress causes a crack beneath the surface of a bearing race. Figure 5.2 explains how cracks propagate and when they reach the surface, spalling occurs.

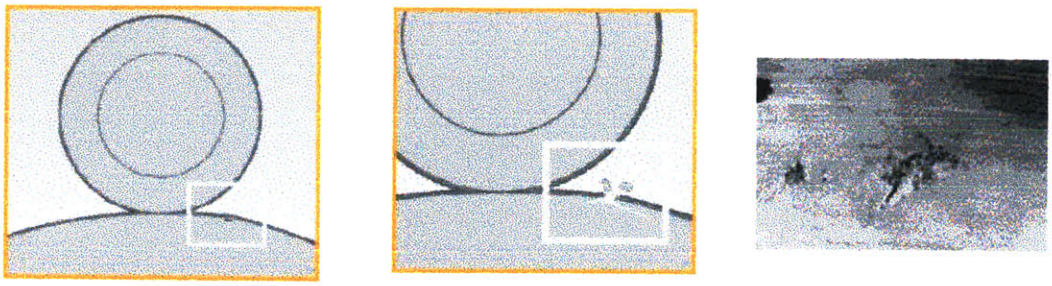

Figure 5.2: Point Surface Origin damage progression. Source: The Timken Co.

A Point Surface Origin (PSO) is categorized as fatigue damage, which has its origin, associated with the surface asperities, which act as local stress concentrations resulting in surface spalling.

Figure 5.3: Peeling. Source: The Timken Co.

Figure 5.3 shows how peeling is characterized by a shallow < 2.5 mm deep, spalling which sometimes occurs locally around bruises, grooves, or ends of roller/race contacts.

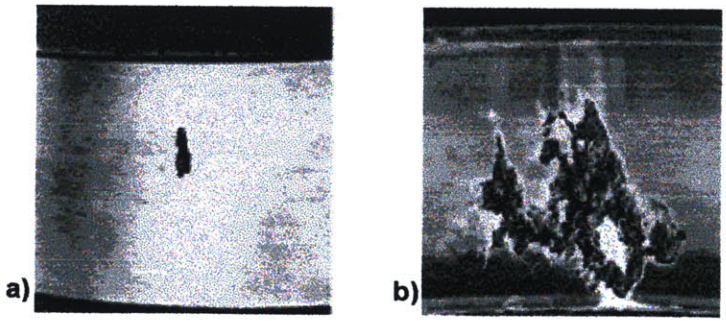

Figure 5.4: Inclusion origin spall: a) Non-propagating spall, b) spall propagated by hydraulic pressure. Source: The Timken Co.

Inclusions generally occur due to impurities in the steel. As seen in Figure 5.4, the bearing is placed under load in its particular application, this "dirty" steel gives rise to small spalls that do not propagate or to spalls that propagate and can create catastrophic failure of not only the bearing but the application as well.

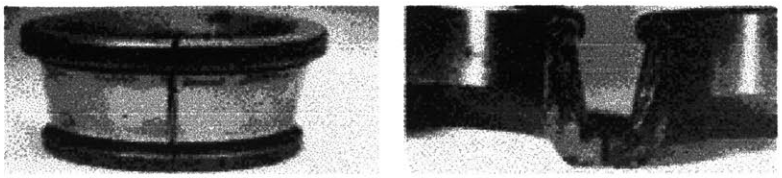

Figure 5.5: Transverse cracking fatigue. Source: The Timken Co.

Figure 5.5 presents a severe stage of cracking that extends through the length of the bearing.

Damage by Mechanisms Other Than Contact Fatigue

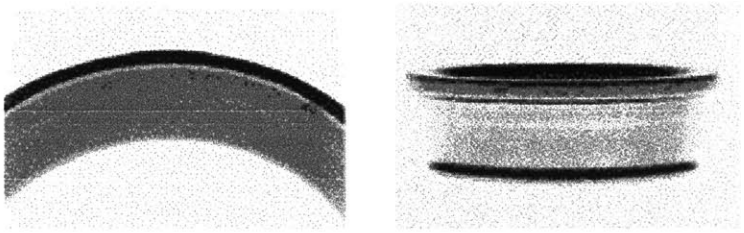

Figure 5.6: Abrasive Wear. Source: The Timken Co.

Sand, fine metal from grinding or machining, and fine metal or carbides from wear of gears will wear the bearing. As seen in Figure 5.6, this wear can result in an increase in endplay, resulting in misalignment and reducing fatigue life.

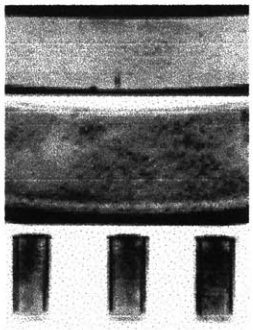

Figure 5.7: Wear from foreign material. Source: The Timken Co.

Figure 5.7 shows how foreign debris bruises or "dents" all contact surfaces due to hard particles in the lubricant. This particular type of damage can be controlled for laboratory experimentation and will be further discussed in this chapter.

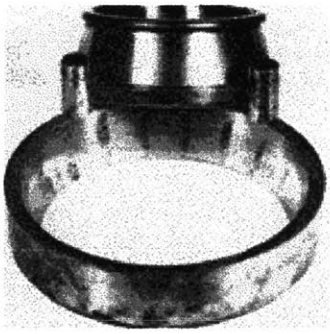

Figure 5.8: Etching in the initial stage. Source: The Timken Co.

Etching or corrosion, seen in figure 5.8, is caused by moisture at the roller/raceway contact line. This condensate initially collects in the bearing housing due to temperature changes. Subsequently, water or moisture may enter the bearing through a damaged or worn seal.

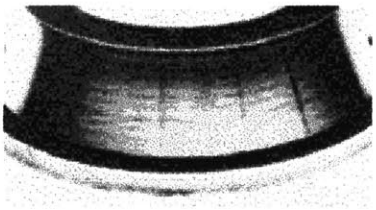

Figure 5.9: Brinelling. Source: The Timken Co.

Figure 5.9 gives an example of brinelling. This type of damage is the plastic deformation of bearing element surfaces due to extreme or repeated shock loads. A snug or light preload setting will eliminate this type of brinelling caused by the pounding action in the bearing.

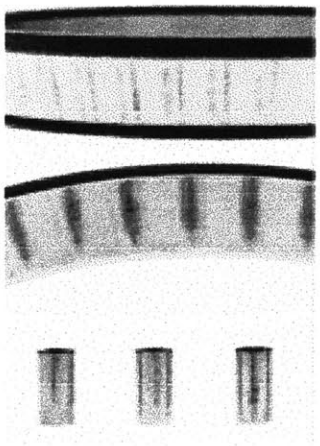

Figure 5.10: False brinelling. Source: The Timken Co.

For the case of false brinelling, as seen in Figure 5.10, the damage is recognizable by the grooves worn into the raceways by axial movement of the rollers during transportation. It can be eliminated or at least greatly reduced by blocking up shafts or axles so as to move the weight from the bearings.

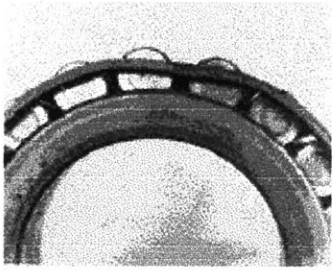

Figure 5.11: Cage damage. Source: The Timken Co.

This type of damage can be caused by careless handling and use of improper tools during installation of the bearings. Figure 5.11 is an example cage that was dropped. This damage will cause the rollers to bind in the cage and skew, creating stresses along the sides of the cage pockets. This will also cause bad roller end contact against the rib resulting in scoring of the rib. Eventually, the cage will break as seen in Figure 5.12.

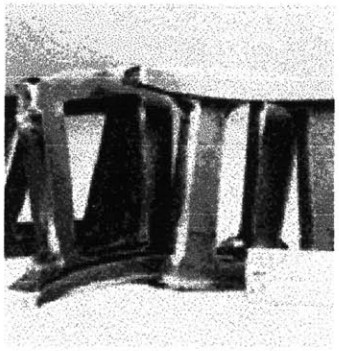

Figure 5.12: Cage breakage. Source: The Timken Co.

In the preceding examples, the results of bad handling, improper assemblies, adjustments and operating conditions have been stressed and the resulting damage shown.

5.2 Damage Severity and Isolation

Artificial damage can be easily created in the laboratory. For example, a grinding mark of a certain length and depth can be made on a raceway in order to be picked up by the sensor. The problem here is that an artificial damage will not depict the true nature of bearing failure. Thus, a natural damage is advantageous since it gets as close as possible to a real life situation. In order to detect the incipient damage in a bearing, tests would last a very long time. Therefore, the process of debris denting can accelerate this.

In the past, many have documented how a bearing damaged by debris has a shorter life when compared to an undamaged bearing.[19-21] The debris represents the introduction of foreign particles or the generation of wear particles, as mentioned in the previous section. Moreover, there are several mechanisms that decrease bearing fatigue life. First, the process of indentation causes plastic flow of the bearing material and the formation of shoulders on the bearing surface. These shoulders then create a stress concentration region under the surface of the bearing as well as accompanying lubricant starvation.[22-23] Yet another mechanism that explains fatigue life reduction is the formation of microcracks upon indentation, which may eventually propagate during operation and develop into spalls (macrocraks).[24]

In the case of debris particles, their behavior in the bearing contact region suggests that first; the particle plastically deforms or flattens into a platelet. In the process, this particle deformation causes plastic deformation on the bearing raceway surface. Subsequently, the particle can fracture and cause further plastic deformation of the bearing surface. As a final option, the particle may not be embedded into the raceway since it does not deform or fracture, having a minute or no effect at all on bearing fatigue life.[25]

In debris denting, there are a variety of materials that can be used to reduce bearing life. The most common types are SiC, TiC, Al_2O_3, and T-15 tool steel. In addition, the friable particle size ranges from 25-53 μm (984-2087μin) and 90-125 μm (3543-4921 μin). Evaluation of the debris particles and the bearings indicate that the most severe damage to the bearings is generated by ductile particles, which reduce fatigue life by 98%. T-15 tool steel, regardless of particle size and probably due to its ductility, has a consistently harmful effect of 97-99% bearing fatigue life reduction.

Bearings were "dented" with 71.4 mg of T15 tool steel having a particle size of 90-125 μm and a Vickers hardness of 850 MPa. The debris denting was carried out in the Lubrication Evaluation Machine (LEM) at Timken Research. In this machine, the bearing cups were pressed into the corresponding adaptor and attached to a spindle, which extended from the pillow block. The lubricant ISO 32 (SAE 10) life test oil with the Timken proprietary R&O additive package was poured into the cup cavity along with the previously specified tool steel particles. The housing of the LEM was then moved upward by the load cylinder and the bearing was seated. The bearing was then rotated for 2.5 minutes at 800 rpm for 2000 revolutions. Finally, each bearing was examined after denting to verify that it had been dented with the specified number of dents of a given size per unit surface area. In this way, the amounts of each debris type were established so that all the bearings would be dented identically.

Once this preliminary damage was done, bearing life was reduced considerably and laboratory tests could take place in shorter time slots. The following pictures show a dented raceway along with its corresponding orthographic plot.

a)

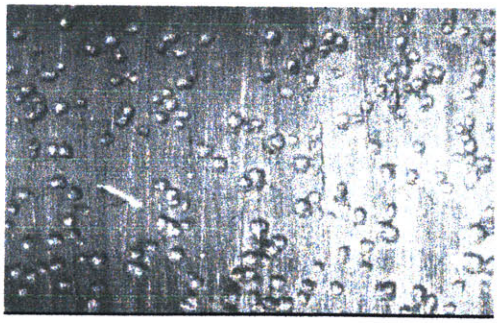

b)

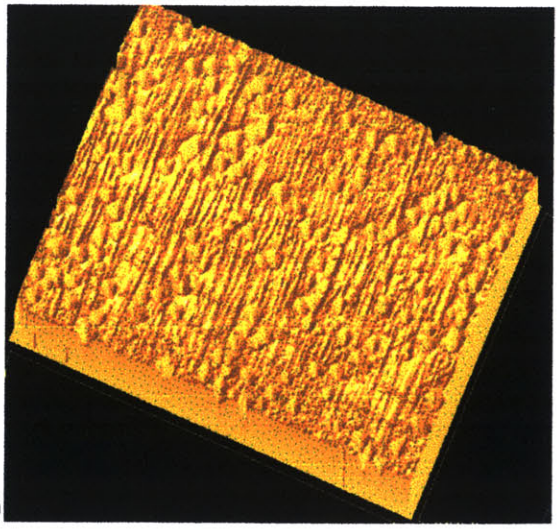

Figure 5.13: a) Dented raceway surface b) orthographic plot of dented surface

Figure 5.13b was analyzed to reveal the detailed orthographic plot in figure 5.14.

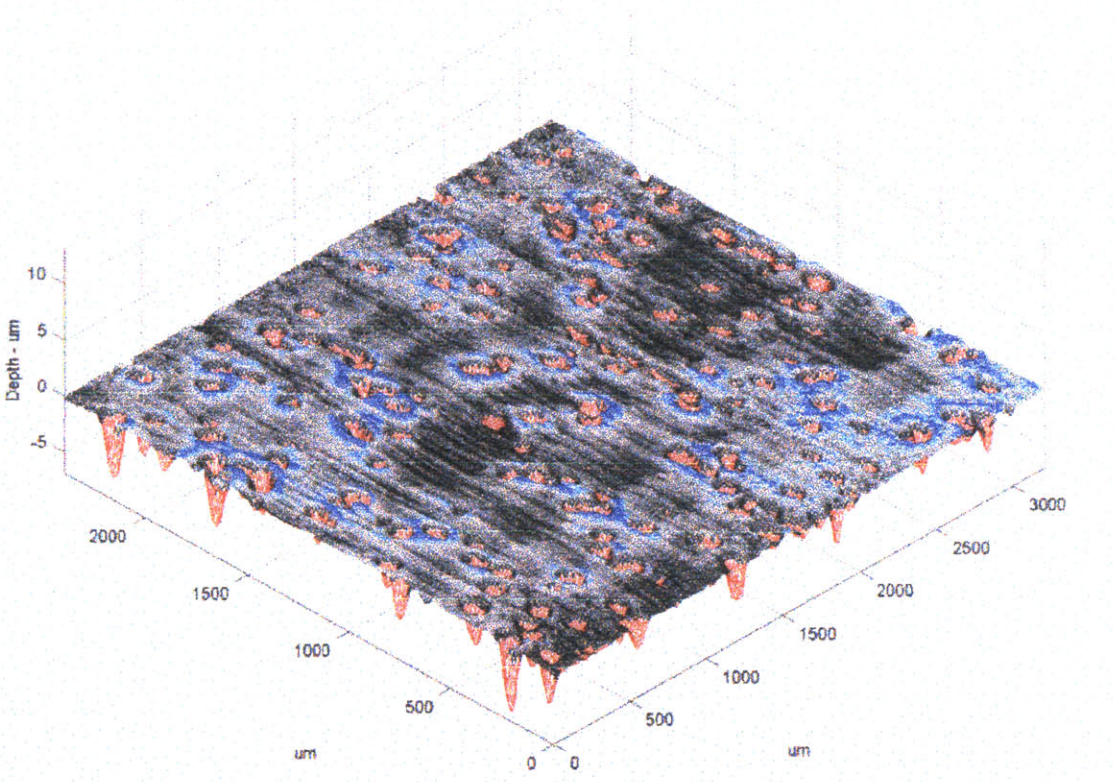

Figure 5.14: Detailed orthographic plot of dented bearing race. Magnification (25X) Source: D.A. Clouse, 03-Dec-1999, Timken Research.

A further look at the orthographic plot shows the depth of the "dents". Although the data range in the direction of depth is –6.831/0.723 μm, most dents are about 5μm in depth and the surface appears to be uniformly dented. This same technique will be used to study the surface topography of damaged bearings when failure occurs in the baseline tests.

In addition to denting the bearings, the damaged component will be isolated. For example, in order to associate a particular signal signature with cone damage, a dented cone will be used with other undented components so that failure is most likely to occur in the damaged cone. Similarly, all other components, namely cups and rollers will be tested separately.

6 Load System

6.1 Life-Test Requirements

The 5" life-test machine designated for this project had a maximum load output of 800 psi and a maximum speed of 1200 rpm. The test also requires a one-in-four measure to declare a bearing failure. Normally, failure occurs at a speed of 1600 RPM and a maximum load of 2700 psi. In addition, the time at which this failure occurs for the chosen part number greatly varies but it still exceeds the two-week length. Thus, the described debris denting is intended to reduce bearing life into the two-week time span.

6.2 Machine Limitations and Changes

Apart from the debris denting, the machine was modified to increase its flexibility and shorten the bearing failure time. Increasing its speed would require a new motor and a costly overhaul. Hence, a portable load system was installed to increase the load capacity from 800 psi to 2700 psi. Although the modified housing can only take about 1350 to 1400 psi, the increased load capacity can accelerate bearing failure.

In order to construct the portable load system, several parts were needed. As shown in figure 6.1, an 18" life-test machine was dismantled.

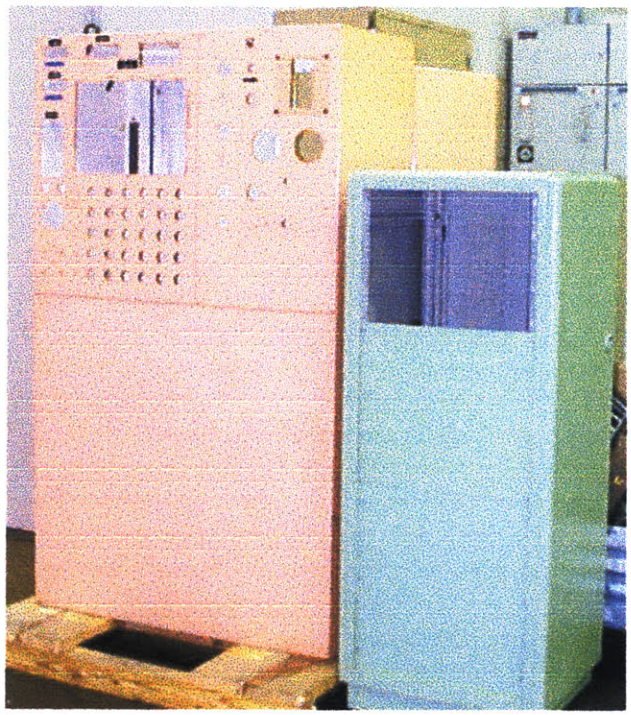

Figure 6.1: Old and new load system cabinets

The large cabinet was stripped of all its components, since the green cabinet would now contain the new portable load system. In the beginning stages, the parts were in complete disorder as seen in the figure 6.2.

Figure 6.2: 18" load system components

Afterwards, a custom made steel panel was ordered to mount the different components. Figure 6.3 shows the planned system layout.

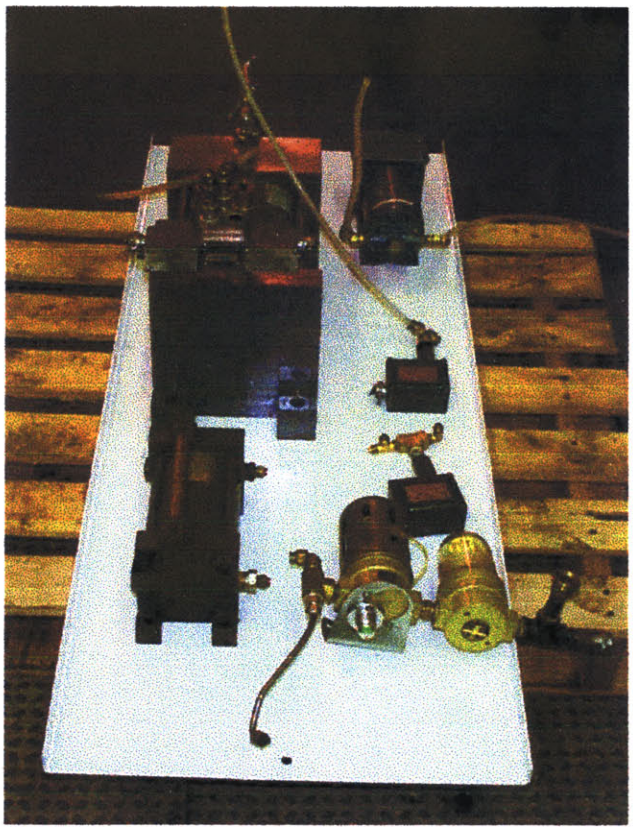

Figure 6.3: Steel panel with load system components

Hex bolts were welded to the steel panel in order to mount the heavy 64:1 booster. Subsequently, the transmitter, air filter, oil reservoir, and pressure switches were mounted. Figure 6.4 shows the mounted component panel in the green cabinet.

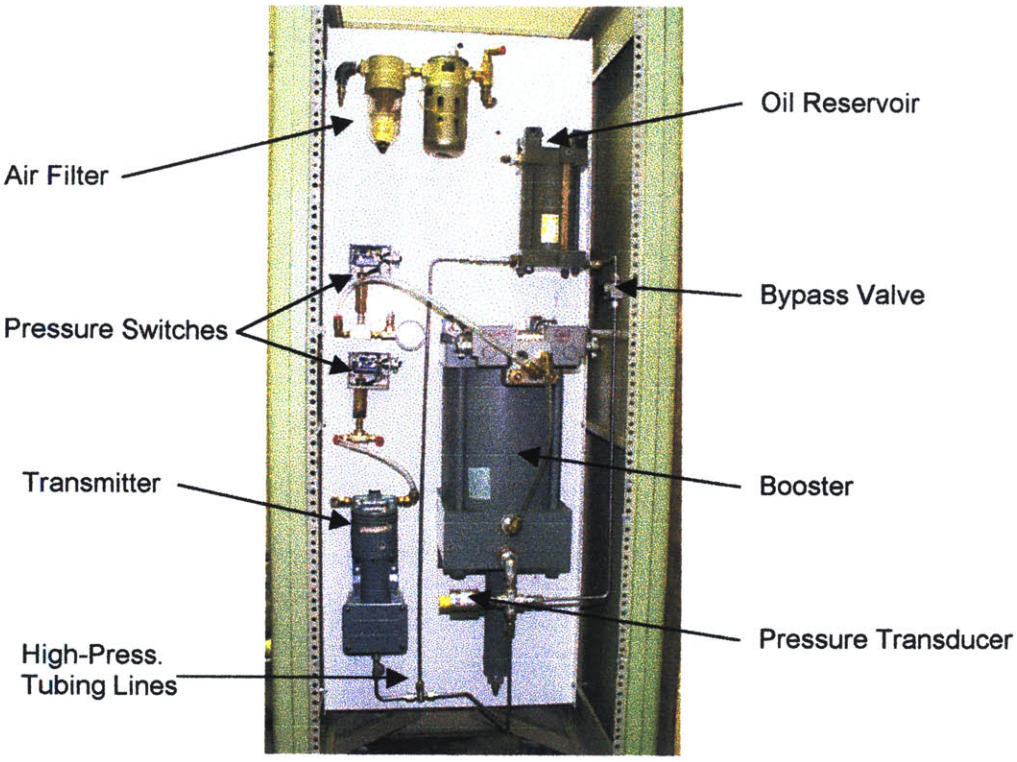

Figure 6.4: Mounted steel panel

A door was ordered for the new cabinet. The rest of the components, namely: a Moore controller, dial gages, a Sensotec load reader, and electronic controls were laid out on the door. The corresponding holes were then drilled. Finally, after mounting the rest of the components and plumbing the system using polypropylene tubing, the electrical components were wired. Figure 6.5 shows the completed load system.

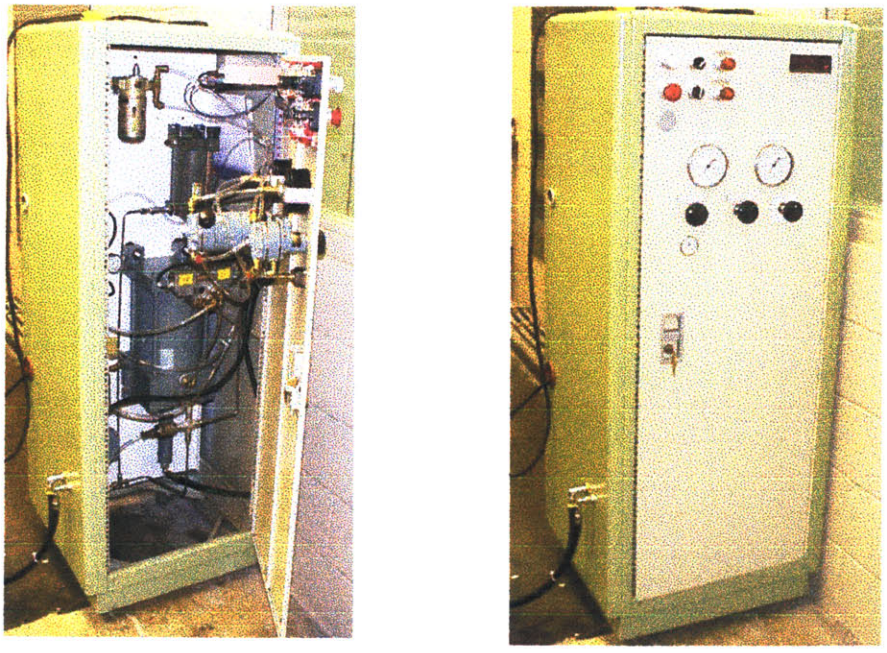

Figure 6.5: Completed portable load system

7 Lubricant Selection

Proper lubrication is essential to successful performance of any bearing. This requires the selection of an adequate type of lubricant, the right amount of lubricant and the correct application of the lubricant on the bearing. The three fundamental functions of a lubricant are to separate mating surfaces and reduce friction, to transfer heat (with oil lubrication), and to protect from corrosion and, in the case of grease lubrication, from dirt ingress. According to elastohydrodynamic effects, all these functions directly deal with rib/roller end contact and the generation of a film thickness on the raceway.

Elastohydrodynamic Lubrication

The formation of the lubricant film between the mating bearing surfaces is called the elastohydrodynamic (EHD) mechanism of lubrication. The two major considerations in EHD lubrication are: the elastic deformation of the contacting bodies under load and the hydrodynamic effects forcing the lubricant film to separate the contacting surfaces while the pressure is deforming them. Figure 7.1 shows the different parameters involved in determining the bearing film thickness.

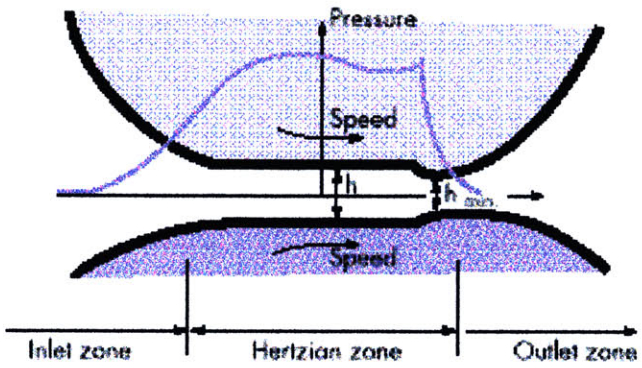

Figure 7.1: Elastohydrodynamic (EHD) lubrication. Source: The Timken Co.

Film Thickness on the Raceway

The importance of the EHD lubrication mechanism lies in the fact that the lubricant film thickness between the two contacts can be related to the bearing performance. The thickness of the generated film depends on the operating condition parameters such as: velocity, loads, lubricant viscosity, and pressure/viscosity relationship. Analytical relationships for calculating the minimum and the average film thickness have been developed. In order to calculate the minimum film thickness, the following equation can be used (based on the Dowson Equation):

$$h_{\min} = KD(\mu_o V)(0.7)a(0.54)W - (0.13)R(0.43) \ , \qquad (1)$$

where h_{min} is the minimum lubricant film thickness (mm), KD is the constant containing moduli of elasticity, and μ_o is the lubricant viscosity at atmospheric pressure. The variable V is the relative surface velocity, a is the lubricant pressure viscosity coefficient, W is the load per unit length, and R is the equivalent radius.

Subsequently, in order to obtain the average film thickness, h, use the following expression (based on Grubin Equation):

$$h = 0.039(\mu Va)0.728(P/l) - 0.091(S/R)0.364, \quad (2)$$

where μ is the lubricant's viscosity, V the surface velocity, and a is the lubricant pressure viscosity coefficient. The new variables are P, which is the load between inner race and rollers, l is the effective length contact between rollers and inner race, and S / R is the sum of inverses of contact radii. Hence, the major factors influencing the lubricant film thickness are viscosity and speed whereas load has less importance. Source: The Timken Co.

It is also important to note that the fatigue life of a bearing is related in a complex way to speed, load, lubrication, temperature, setting and alignment. Consequently, speed, viscosity and temperature determine the bearing lubricant requirements. For example, table 7.1 shows how two bearing test groups were subjected to conditions of constant speed and load.

Table 7.1: Temperature effects on lubricant film thickness

Test Group	Temperature °C	Visc. @ Test Temp. mm2 / sec (cSt)	EHD Film (h_{min}) µm	Life %
A - 1	135	2.0	0.038	13 - 19
A - 2	66	19.4	0.264	100

Source: The Timken Co.

By varying the operating temperature and oil grade of the test groups, different film thicknesses were created. As expected, the results showed that bearing life dramatically decreased with high temperatures, since a lower viscosity and a thinner film was produced. On the contrary, two similar bearing test groups were subjected to constant viscosity and load conditions, but the speed was varied. The results are shown in table 7.2.

Table 7.2: Speed effects on lubricant film thickness

Test Group	Speed rev/min	EHD Film (h_{min}) µm	Life %
B - 1	3600	0.102	100
B - 2	600	0.028	40

Source: The Timken Co.

The study concluded that higher speeds produced thicker films and longer lives. Therefore, the damage mapping tests will be run at 1200 rpm, which is much lower than the normal speeds of 2700 rpm.

Film Thickness at Rib/Roller End Contact

The contact between the large end of the roller and the inner race rib experiences much lower loads than the roller/race contact. Thus, the lubricant film thickness at the rib/roller end contact is usually larger. In spite of that, scoring and/or welding of the rib/roller asperities can occur in severe conditions. This damage may be related to speed, oil viscosity, load or inadequate oil supply to the rib/roller end contact. In these cases, the use of Extreme Pressure (EP) lubricant additives may help prevent bearing damage.

7.1 Types of Lubricant related Bearing Damage

As an example, bearings with scored and heat discolored roller ends and rib are easily identified as a burned up bearing and damaged beyond further use. The cause of the burning or damage, however, might be traced to any one of a number of things such as insufficient or improper lubricant. It may also be the wrong type of lubricant or the wrong system for supplying lubricant. Perhaps a lighter or a heavier lubricant is needed or an extreme pressure type of lubricant rather than a straight mineral oil and a circulating oil system needed rather than an oil level or splash system. Furthermore, an excessively tight bearing setting or a combination of a preload setting and inadequate lubrication could cause this type of damage as well.

According to A.G. Herraty, a former Maintenance Manager for SKF, failure due to incorrect lubrication depends on the creation of oil film between the rolling elements and raceways, preventing metal to metal contact. Thus, oil viscosity is the most important factor for ensuring adequate bearing lubrication. Furthermore, the lubricant must be clean and free from liquid or solid contaminants. In the event of a low viscosity lubricant or insufficient lubrication, the raceway surfaces will quickly crack resulting in pitting and fatigue flaking. [18]

7.2 Lubricant Selection Criteria

There are numerous types of lubricants used in life-test machines. As previously discussed the higher viscosity the oil has, the longer the life of the bearing. The machine to be used originally had 50W oil in its housing oil reservoir. As seen in Figure 7.2 oil pumped from the bottom reservoir and heated to 180°F enters the housing through three orifices on the top. The oil is heated to simulate operational conditions.

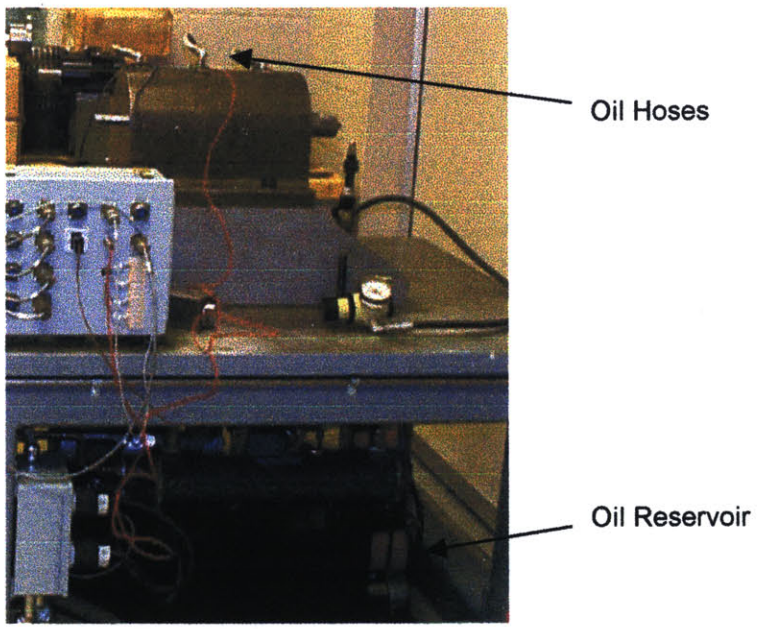

Figure 7.2: Housing oil intake valves

The test assembly is constantly lubricated to reduce the risk of burn up due to lubricant starvation. In order to fail the bearings even quicker, a change in the lubricant was needed. Therefore, 10W (SAE 10) oil was used to accelerate bearing failure.

8 Data Acquisition System

8.1 Hardware Requirements

The sensor wires were connected to extensions that in turn connected into a signal conditioning box. First of all, most of the hardware components used to link the sensors to the software were from National Instruments. The signal conditioning box had Omega 3M signal conditioners for the thermocouples and a PCB module for the accelerometers. These conditioners were wired such that the amplified output, using BNC cables, plugged into two BNC break out boxes. Finally, using a special shielded cable, the BNC boxes plugged into an AT-MIO-64-E3 DAQ card in a PC with the Lab Windows/CVI software (see Figure 8.1).

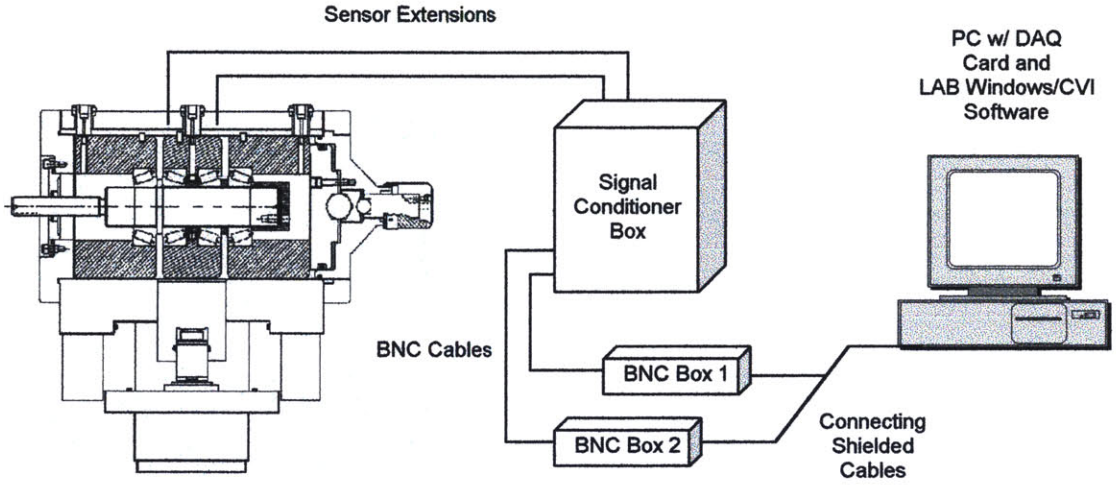

Figure 8.1: Schematic of Data Acquisition System

As presented in the preceding schematic, BNC Box 1 had the accelerometer inputs while BNC Box 2 had the thermocouple inputs. Furthermore, figure 8.2 shows the experimental setup.

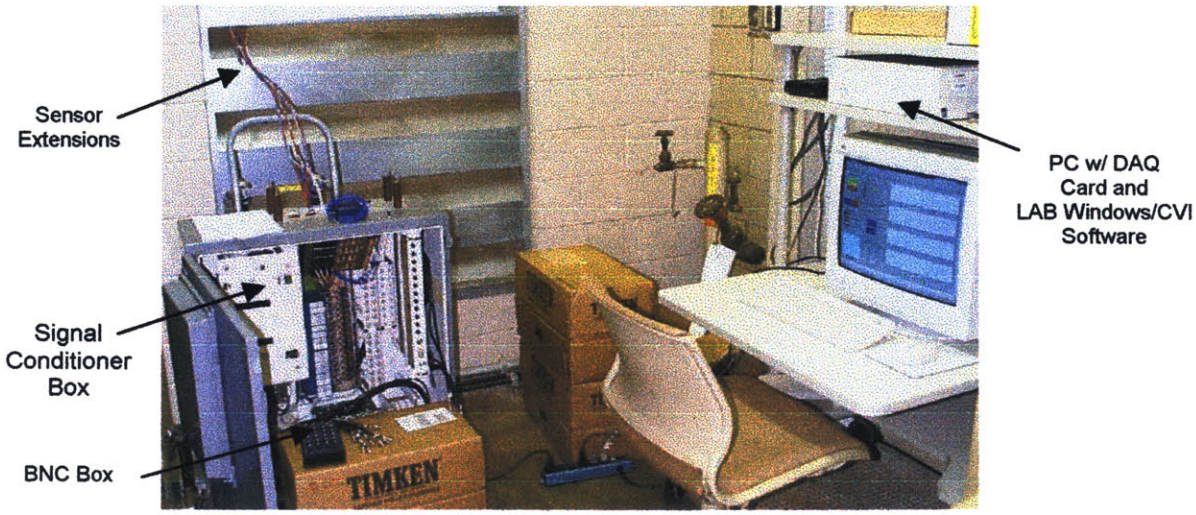

Figure 8.2: Data Acquisition Station

8.2 Software Requirements

The data acquisition software needed to capture the incipient damage and its propagation, ultimately leading to catastrophic failure. Therefore, since it is impractical to continuously record data over long periods of time, the software was designed to record a 1-sec. waveform every hour. Furthermore, once the standard deviation of the measured signal changed by a specified percentage, the acquisition rate was cut in half. Hence, data samples were taken more frequently as the bearing began to fail. All of these parameters were user defined and could be changed at the beginning of each test. It is also important to note that any changes made to the software must be made in the LabWindows/CVI environment. The data acquisition system was developed with the help of Advanced Integration, L. L. C., a software consultant firm.

In order to keep track of all the different sensors, a detailed labeling system was developed. First of all, each sensor (accelerometer or thermocouple) had a top (1) or bottom (2) position as explained in chapter 4. This position was then associated with the label of the particular bearing part being tested (N1, D1, R1, etc.). Next, each sensor was associated with a signal conditioner, a BNC label, a hardware channel (on the BNC box), and a software channel. Table 8.1 shows the different sensors and the corresponding labels for the 9 proposed tests.

Table 8.1: Sensor Labeling System

					TEST NUMBER									
	SOFTWARE CHANNEL	HARDWARE CHANNEL	BNC LABEL	SIGNAL COND.	1	2	3	4	5	6	7	8	9	LOAD ZONE
BNC BOX 1	CH 1	CH 0	A 1	PCB 1	N 1-1	N 2-1	N 3-1	N 4-1	N 5-1	N 6-1	N 7-1	N 8-1	N 9-1	Inside
	CH 2	CH 1	A 2	PCB 2	N 1-2	N 2-2	N 3-2	N 4-2	N 5-2	N 6-2	N 7-2	N 8-2	N 9-2	Outside
	CH 3	CH 2	A 3	PCB 3	D 1-1	D 4-1	D 7-1	11-1	14-1	17-1	21-1	24-1	27-1	Outside
	CH 4	CH 3	A 4	PCB 4	D 1-2	D 4-2	D 7-2	11-2	14-2	17-2	21-2	24-2	27-2	Inside
	CH 5	CH 4	A 5	PCB 5	D 2-1	D 5-1	D 8-1	12-1	15-1	18-1	22-1	25-1	28-1	Outside
	CH 6	CH 5	A 6	PCB 6	D 2-2	D 5-2	D 8-2	12-2	15-2	18-2	22-2	25-2	28-2	Inside
	CH 7	CH 6	A 7	PCB 7	D 3-1	D 6-1	D 9-1	13-1	16-1	19-1	23-1	26-1	29-1	Inside
	CH 8	CH 7	A 8	PCB 8	D 3-2	D 6-2	D 9-2	13-2	16-2	19-2	23-2	26-2	29-2	Outside
BNC BOX 2	CH 9	CH 16	T 1	OMEGA O	N 1-1	N 2-1	N 3-1	N 4-1	N 5-1	N 6-1	N 7-1	N 8-1	N 9-1	Inside
	CH 10	CH 17	T 2	OMEGA 1	N 1-2	N 2-2	N 3-2	N 4-2	N 5-2	N 6-2	N 7-2	N 8-2	N 9-2	Outside
	CH 11	CH 18	T 3	OMEGA 2	D 1-1	D 4-1	D 7-1	11-1	14-1	17-1	21-1	24-1	27-1	Outside
	CH 12	CH 19	T 4	OMEGA 3	D 1-2	D 4-2	D 7-2	11-2	14 - 2	17-2	21-2	24-2	27-2	Inside
	CH 13	CH 20	T 5	OMEGA 4	D 2-1	D 5-1	D 8-1	12-1	15-1	18-1	22-1	25-1	28-1	Outside
	CH 14	CH 21	T 6	OMEGA 5	D 2-2	D 5-2	D 8-2	12-2	15-2	18-2	22-2	25-2	28-2	Inside
	CH 15	CH 22	T 7	OMEGA 6	D 3-1	D 6-1	D 9-1	13-1	16-1	19-1	23-1	26-1	29-1	Inside
	CH 16	CH 23	T 8	OMEGA 7	D 3-2	D 6-2	D 9-2	13-2	16-2	19-2	23-2	26-2	29-2	Outside

The chart shows the eight accelerometers (A1 to A8) and the eight thermocouples (T1 toT8). In addition, the chart also shows which sensors will be inside or outside the bearing load zone during the test cycle.

8.3 Data Acquisition Procedure

The following section describes the procedure used when using the National Instruments' LabWindows/CVI software developed with the help of Advanced Integration, L.L.C.

Lab Windows/CVI: Set-up and Run Application

Once the LabWindows/CVI software was running, three different program files needed to be loaded: a source (*.c) file, an include (*.h) file, and a user interface (*.uir) file. In order for the data to be saved in a desired directory, the source code files needed to be in that same directory as well. Once the desired files were loaded and the program was running, the application front panel in figure 8.3 would then appear.

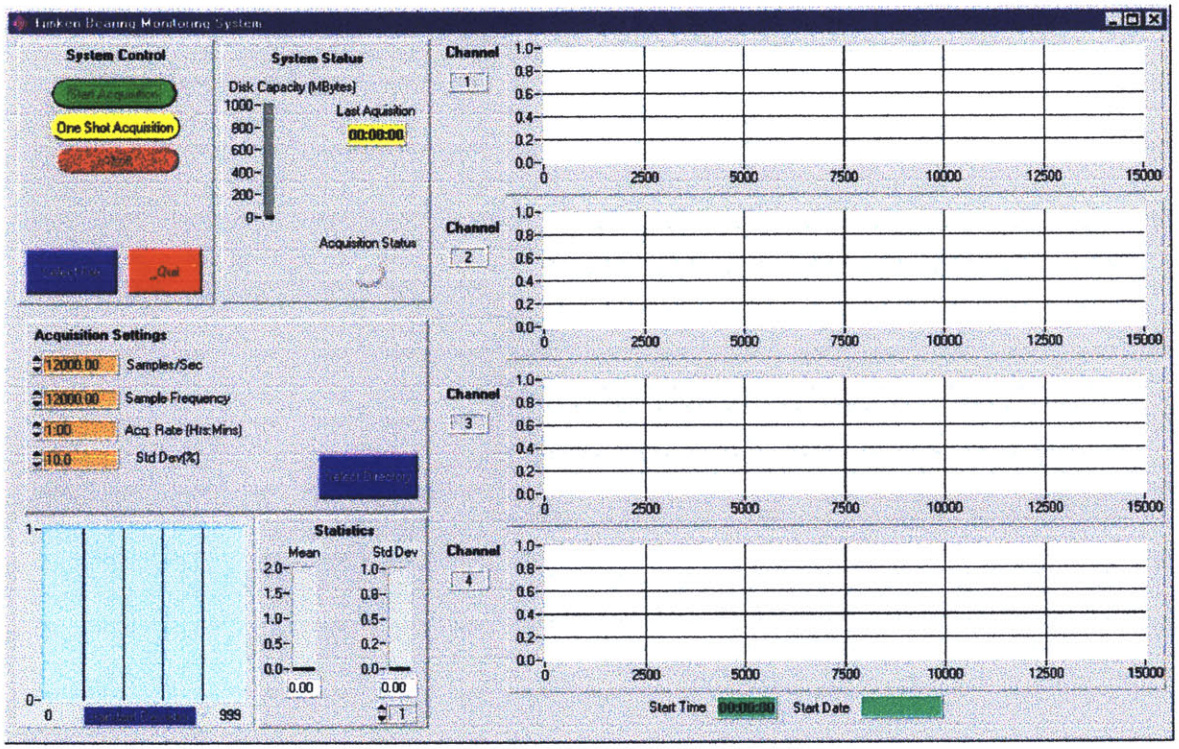

Figure 8.3: DAQ application front panel

The four waveform graphs in the front panel had channel toggles in order to view different channels at the same time. There was also a channel toggle and a corresponding graph for the standard deviation value in the bottom left corner of the front panel. Before taking any data, the acquisition settings were specified. These values were the number of samples per second (12,000), the sample frequency (12 kHz), the acquisition rate (1:00 hrs:mins), and the standard deviation percentage change (10.0%); the default values are respectively shown in parenthesis. There was also the option of loading any particular setting values used in a previous acquisition. The next step was to start the acquisition. Once the machine was running and under load, the operator would select the file destination of the data to be acquired. Once started, the application could be aborted in order to obtain data samples at irregular time intervals in order to record the effect of load on the sensor signals.

8.4 SONY PC SCAN: Signal Evaluation

This software package could be used to analyze the acquired data during and after the dented bearing tests. In addition, the software required a specific binary format as well as a .log file in order to open the data file. Once the data file was opened, the screen capture shown in figure 8.4 would appear.

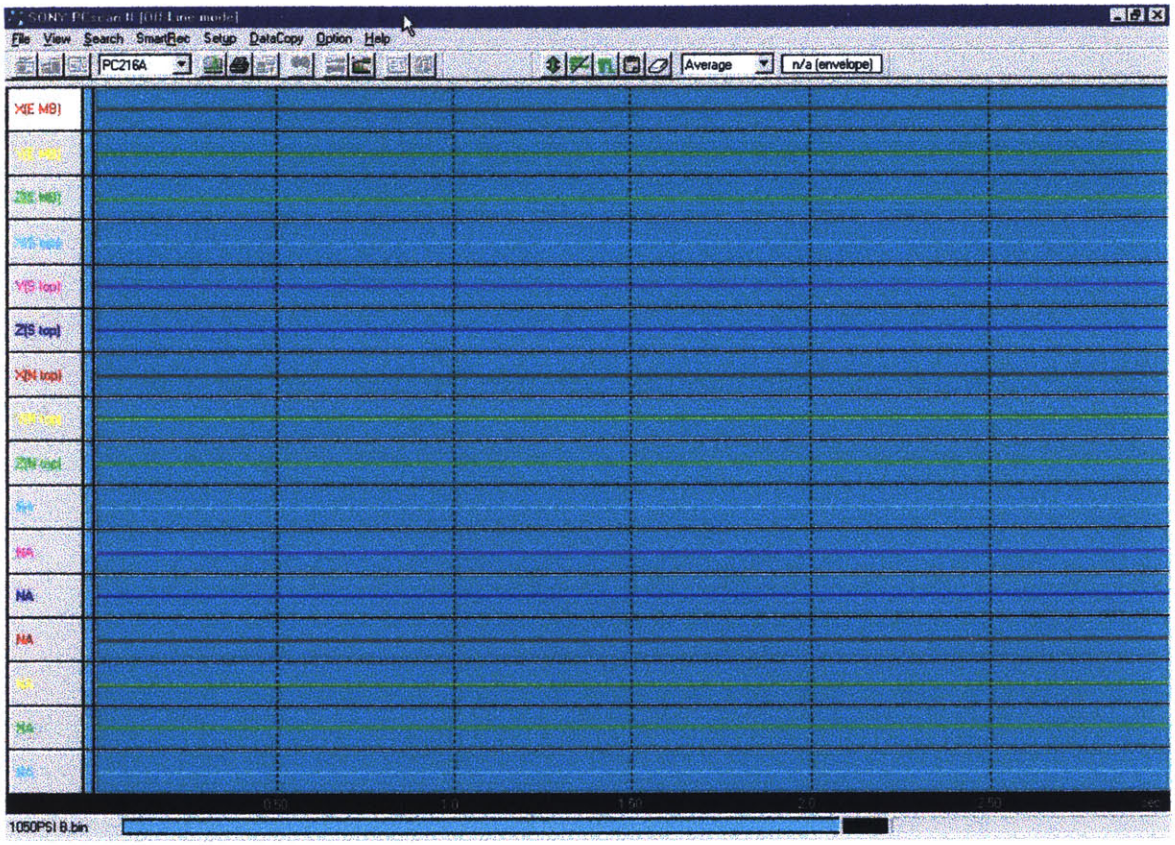

Figure 8.4: SONY PC SCAN software

Next, click on the Auto Scale button to view the signals (see figure 8.5).

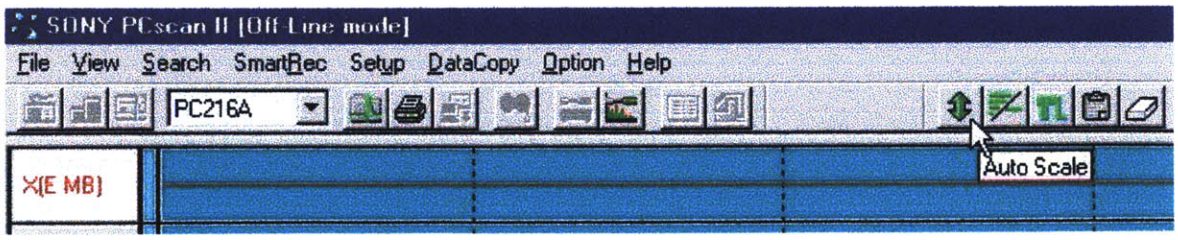

Figure 8.5: Auto Scale function

This will allow the operator to check on the signals being obtained during the test. The operator can further analyze these signals using this software or any other signal analysis programs already developed for this application. As a final note, this software was used in conjunction with a SONY DAQ recorder to obtain the baseline test results in the following chapter.

8.5 Defect Frequency Equations

Bearing Geometry

The following drawing in figure 8.6 explains the geometric relationship of various bearing parameters.

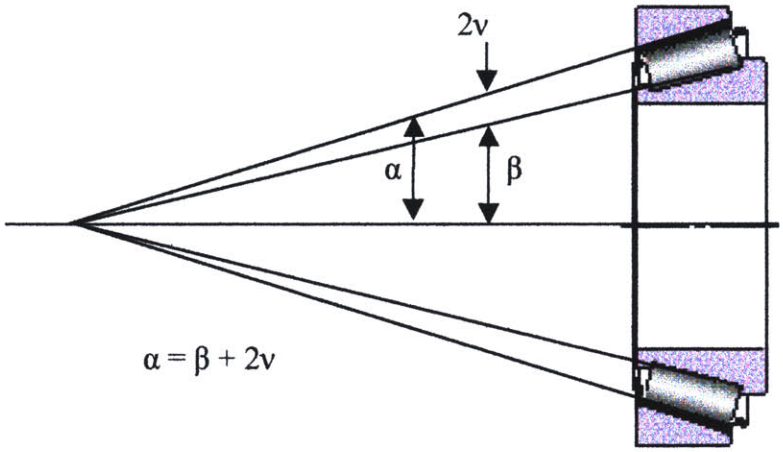

Figure 8.6: Bearing geometry. Source: The Timken Co.

In this case, α is the half-included cup angle, β is the half-included cone angle, and v is the half-included roller angle. Using the concept of a planetary gear system, the following bearing defect, frequency equations can be derived.

$$F_{roller} = \frac{\left(S/60\right)\left(\sin\alpha\right)\left(\sin\beta\right)}{\left(\sin v\right)\left(\sin\alpha + \sin\beta\right)}, \tag{1}$$

$$F_{cup} = \frac{\left(S/60\right)Z\left(\sin\beta\right)}{\left(\sin\alpha + \sin\beta\right)}, \tag{2}$$

$$F_{cone} = \frac{\left(S/60\right)Z\left(\sin\alpha\right)}{\left(\sin\alpha + \sin\beta\right)}, \tag{3}$$

where Z is the number of rollers and S is the bearing rpm. Knowing all these parameters for the selected bearing and at a speed of 1200 rpm:

$$F_{roller} = 68.63Hz \qquad F_{cup} = 155.46Hz \qquad F_{cone} = 204.54Hz$$

These theoretical frequencies can then be compared to the frequencies obtained from the damage mapping tests. Thus, this study will begin to fill the gap between theory and engineering practice by comparing the derived defect frequency and the signal obtained by the sensors.

8.6 Data Acquisition Techniques for Signal Evaluation

R. H. Bannister from the Cranfield Institute of Technology reviewed the different techniques for monitoring rolling element bearings.[26] First of all, a bearing that has been correctly selected for a particular application, carefully fitted, and supplied with the adequate lubrication will produce random vibration signatures after the initial running-in period. In the early stages of bearing failure, fatigue spalls are created and every time an element passes over the defect, a discrete shock wave is generated. Once this occurs, the data acquisition portion of a condition monitoring system can begin to collect data relevant to bearing degradation. The following list briefly outlines the different DAQ techniques that can be used in bearing condition monitoring.

- Low Frequency, Narrow Band Analysis, (0 to 300 Hz)
- High Frequency Spectrum Analysis, (1kHz to 40 kHz)
- Envelope – Spectrum Analysis
- Non – Contact Measurements
- Statistical Analysis
- Shock Pulse Metering (SPM)
- Acoustic Emission
- Adaptive Noise Canceling (ANC)

Further analytical capabilities are: acceleration, velocity, displacement, spike energy, and time waveforms.[6] In addition, other tools in analyzing bearing signature data are crest factors, kurtosis analysis, spectral analysis, fiber optic sensor technique, eddy current sensor technique, and temperature monitoring.[27] Moreover, in the proceedings of the 41st Meeting of the Mechanical Failures Group at the Naval Air Test Center another list of promising approaches was presented. This list included some of the previously mentioned techniques as well as others like Fourier analysis and Cepstrum analysis.[28] Thus, there exists a large variety of methods or techniques which may prove more advantageous for some studies than for others. In any case, only experience will determine which approach is the most successful in bearing condition monitoring.

9 Baseline Tests

9.1 External Damage Acquisition

Baseline tests were carried out in order to predict how long a dented bearing would last under the new load and lubricant conditions. Therefore, four dented cone assemblies were placed into the life-test machine and ran for about 240 hours until a defect was detected using a sounding rod. Tri-axial accelerometers were then placed on the outside of the housing to record the vibration created by the defect. Figure 9.1 shows the experimental setup.

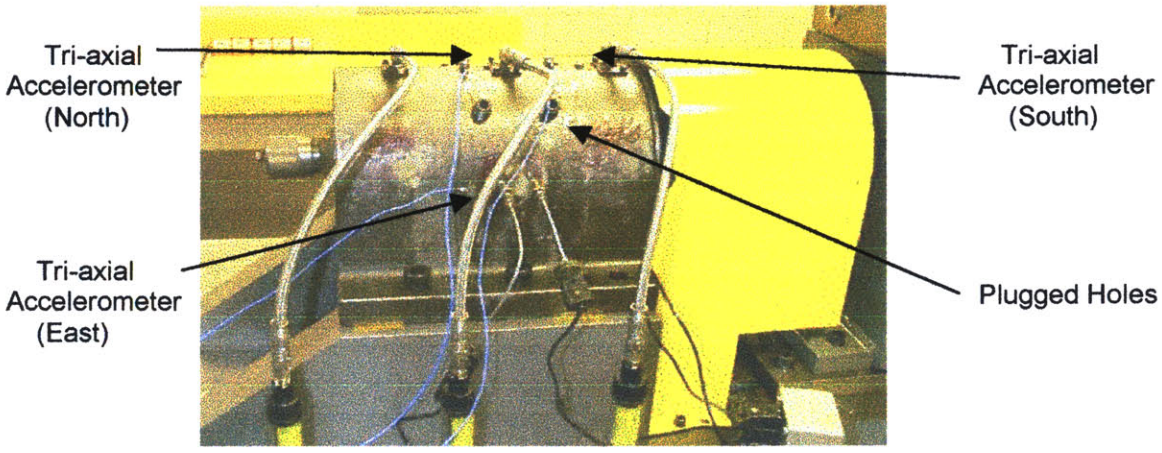

Figure 9.1: External Data Acquisition

Under normal conditions, these selected bearings would run for several months. Thus, the lubricant, load, and debris denting accelerated the onset of contact failure fatigue.

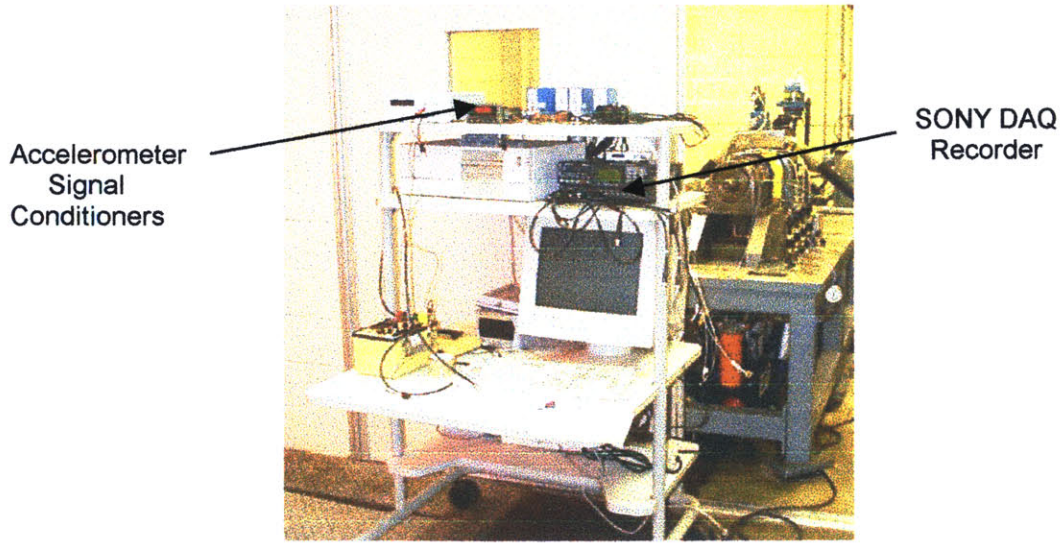

Figure 9.2: DAQ Hardware

This DAQ set up used the SONY PC SCAN software to compare the dented baseline test with the undented version. The data also picked up the bearing defect frequency (see Appendix B for 'Failed BRG Baseline' vibration data of various load settings).

On an additional note, the data files differentiate the type baseline test data along with the specified load setting at which time the sample was taken. Figure 9.3 gives an example of the data as well as the correlation between the signal plots and the accelerometer positions on the housing.

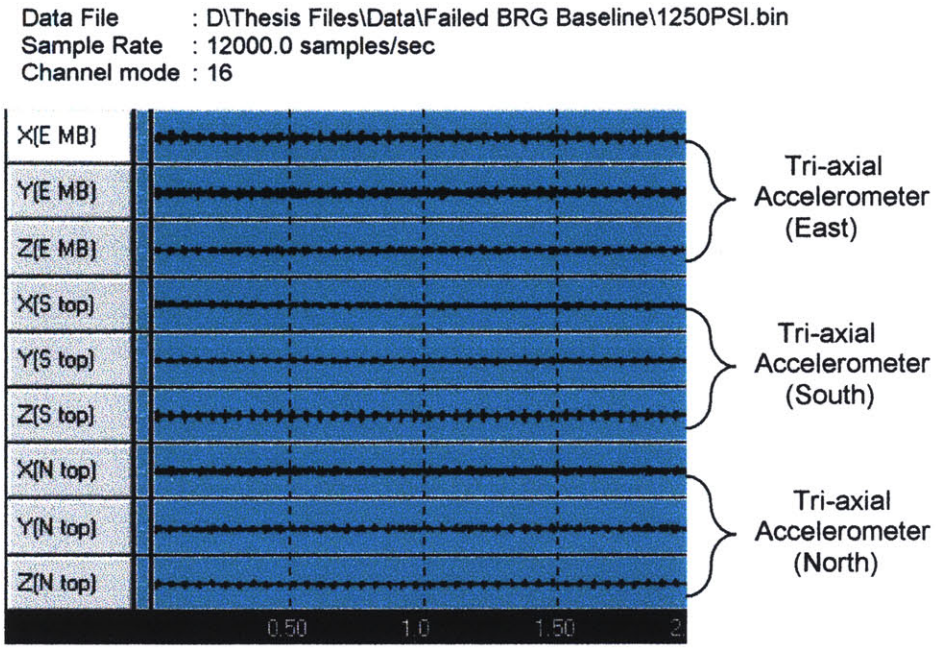

Figure 9.3: SONY PC SCAN results of bearing damage baseline test

9.2 Damaged Bearings

When the test components were disassembled, a spall was detected on one of the dented cone raceways. Figure 9.4 shows the cone spall along with its corresponding orthographic plot.

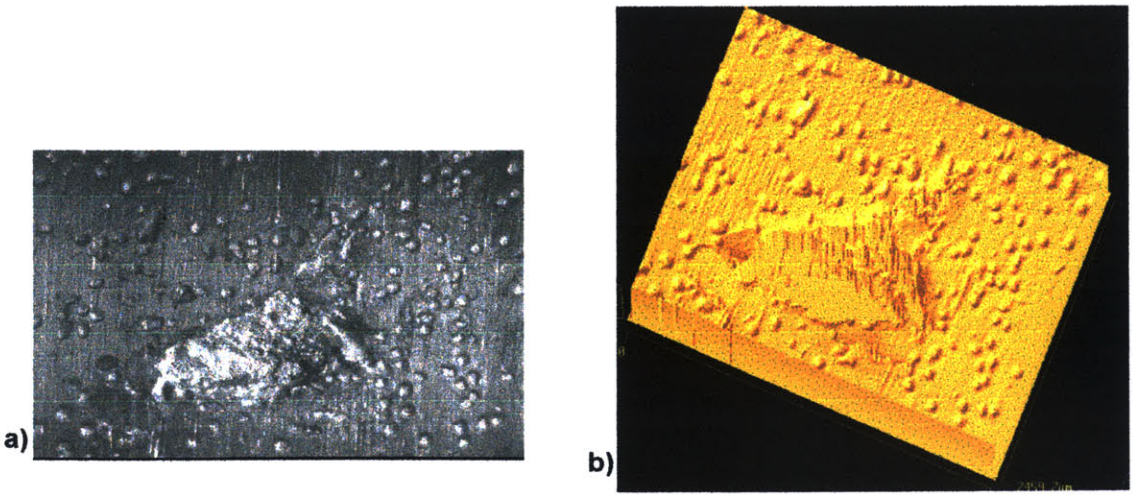

Figure 9.4: a) Spall on dented raceway surface. b) Orthographic plot of fatigue spall.

Furthermore, figure 9.4b was analyzed in the detailed orthographic plot in figure 9.5.

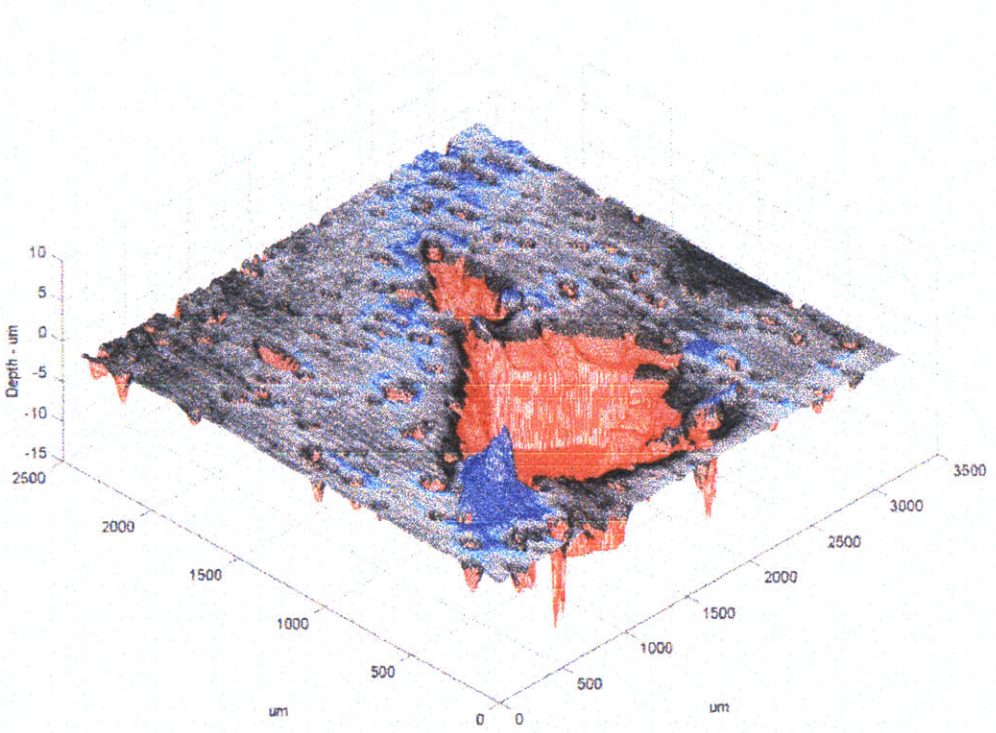

Figure 9.5: Detailed orthographic plot of bearing spall. Magnification (25X)
Source: D.A. Clouse, 03-Dec-1999, Timken Research.

A further look at the orthographic plot shows the depth of the spall. Although the data range in the direction of depth is –68.108 / 7.019 µm, the bottom of the orthographic plot was truncated at –15.0 µm. In this case the orthographic microscope ran out of range since the spall was so large.

On an additional note, bearing defects can be derived from the general appearance of a bearing signature. For example, smooth, continuous geometry defects, such as out-of-roundness, lobing, and chatter tend to excite a single frequency. Hence, this signal would appear to be sinusoidal in the time-domain. For sharp, localized discontinuities, such as nicks, flats, or cracks, excite all the harmonics, which show up in the time-domain as a series of impulses. A third type of defect is caused by frictional problems, such as severe sliding, or metal to metal contact. This defect will tend to excite all frequencies resulting in a baseline increase of the signature. Hence, in the time-domain, this would show up as a set of random movements. (Source: The Timken Co.)

9.3 Undamaged Bearings

Similarly, a baseline test was conducted using undented bearings. Based on the previous test, the machine was run for about 240 hours and the same external vibration readings were taken. Only this time, there appeared to be no distinct defect frequencies as in the dented case (see Appendix C for 'Good BRG Baseline' vibration data of various load settings).

10 Test Procedure

10.1 Component Assembly and Disassembly

The assembly procedure for the instrumented bearing cups was very delicate. Once the cups were pressed and secured into the modified adaptors, the end adaptor was inserted in to the life-test housing (see figure 10.1).

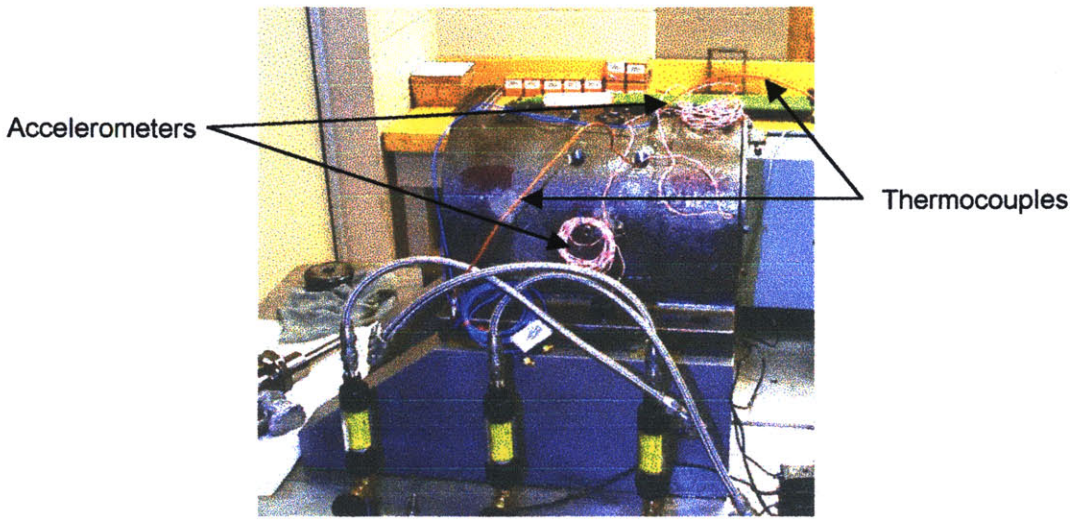

Figure 10.1: Installation of instrumented end adaptor

The wires were then pulled out of the corresponding hole. The shaft was then built-up using the corresponding cones and middle adaptor. The important part was to slowly pull the sensor wires as the shaft was placed into the housing or else they could get pinched. Finally the last adaptor was installed in the same manner. Figure 10.2 shows the instrumented test set up.

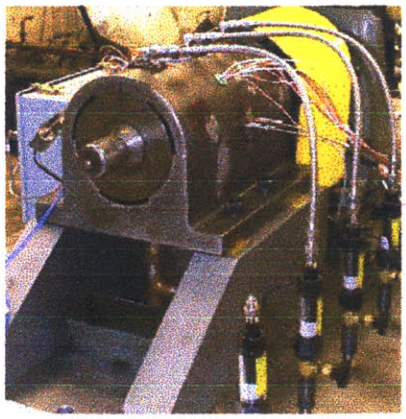

Figure 10.2: Instrumented life-test housing

The holes in the housing were plugged with rubber stoppers, which provided a tight seal for the oil inside the housing and at the same time guided the wires from the respective adaptor channels. The labeled extensions were then connected to the sensor wires.

Similarly, the machine disassembly required the removal of the different adaptors and pressing out the bearing cups and cones from the tooling.

10.2 Instrumented Cup Installation Order

The subsequent tests required a procedure to standardize the installation order of the bearing cups. Therefore, figure 10.3 and the accompanying table show this organization for the different bearing damage tests.

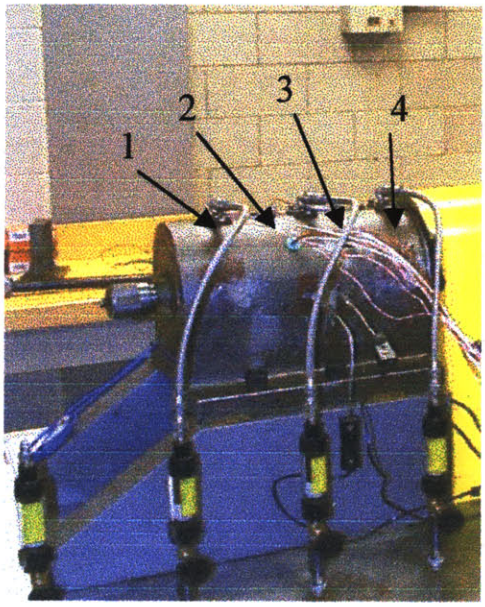

	Cup Position			
	1	2	3	4
TEST 1	N1	D1	D2	D3
TEST 2	N 2	D 4	D 5	D 6
TEST 3	N 3	D 7	D 8	D 9
TEST 4	N 4	11	12	13
TEST 5	N 5	14	15	16
TEST 6	N 6	17	18	19
TEST 7	N 7	21	22	23
TEST 8	N 8	24	25	26
TEST 9	N 9	27	28	29

Figure 10.3: Installation order for bearing damage tests

Using the 240-hour baseline test, the shown test schedule was developed. The different damage tests (1-9) are aimed to associate a particular bearing defect with a distinct signal signature. Although there exist theoretical ways to determine cup, cone and roller defect frequencies, there is a lack of experimental data to correlate this theory to engineering practice. Thus, tests 1-3 will only contain dented cups, tests 4-6 will use dented cones, and tests 7-9 will require dented rollers. Similarly, the three dented cup tests will require undented rollers and cones, and so on. This way, damage will be isolated to a single component in order to begin the damage mapping of tapered roller bearings.

11 Conclusions

At the end of this project, a fully functional and automated data acquisition system for bearing damage mapping was completed. Although some software changes may be needed in the future, the approach lays the foundation for future condition monitoring work at Timken Research. In addition, a bearing condition monitoring test procedure has been established as well. Lubricants, bearings, and sensors have been selected. The instrumentation procedure has also been documented along with the assembly and disassembly of the test housing. One of the most important contributions of this particular study is the accelerated damage test using debris denting. This can recreate typical bearing fatigue failure much better than conventional grinding or EDM marks. Furthermore, using the modified load system, bearings can be run at high loads in order to fail them in a shorter period of time. Hence, where this project ends another begins. The procedure and apparatus have been completed in order carry out a variety of test scenarios and eventually reach a better understanding of bearing condition monitoring.

11.1 Discussion: Working in Industry

The opportunity to work in industry has proven to be priceless. There are many things that a classroom environment can teach the student, but nothing compares to the real life exposure of working alongside engineers with years of expertise. In addition, having the chance to carry out some program management has given the author confidence in facing future challenges in engineering practice.

The most rewarding moment took place when the instrumented machine and data acquisition system was delivered to the company engineer who would use this machine for damage mapping and bearing condition monitoring studies. This moment provides a sense of completion and achievement unmatched by any situation in a university environment. It not only gives the engineer a feel for the complexity of real life industry problems and solutions, but the process by which projects are organized and completed.

As mentioned in the introduction, the intended scope of this project had two phases. The first phase was to design the test apparatus, the test procedure, and data acquisition system. The second phase would carry out the damage mapping tests and analyze the sensor data. In the six-month time frame for this thesis project, only the first phase was completed. Phase two is currently underway at Timken Research in Canton, OH. There were several factors that attributed to the difference between the intended and the actual scope of the project. The following sections will explain these factors and the learning experience gained by the author.

11.2 Organizational Barriers

First of all, the author realizes that engineers and technicians have a number of projects that keep them overwhelmingly busy. When the project was beginning to take shape, it lacked the weight of a team endeavor. More often, it was a personal struggle to obtain technical support, since the project completion responsibility fell on the hands of only one person. Many times, the project was growing in size and complexity, but the corresponding technical support was not allocated since it was not a high priority. For example, the new portable load system needed a front door for its cabinet. This door was not ordered until very late in the project. Although the inside of the cabinet had been plumbed, the outside components could not be mounted until the door arrived and was modified. Therefore, only when real deadlines threatened the life of the project, management stepped in to force change and a quick response time.

Miscommunication between engineers and technicians was another obstacle since many technicians were not briefed on the project progress, nor were they made aware about the full scope of the engineering effort.

11.3 Technological Barriers

At the beginning to the project, the test components were outlined (i.e. load system, life test machine, tooling, bearings, etc.). Some of these components could not be used in their present state and were therefore modified for the specific requirements of this project. For example, a lot of time was spent upgrading the machine. In order to fail the bearings in a reasonable amount of time, a new load system was needed. This proved to be a necessity but quickly became a bottleneck for the project. Another bottleneck was the lengthy instrumentation of the bearing cups. The manufacture and installation of the thermocouples for each bearing set took a lot of time from the rest of the project and it was inevitably decided to outsource such a time consuming task.

11.4 Knowledge Barriers

The data acquisition system proved to be the biggest oversight on the part of the author. Due to the complexity of the project, the DAQ system was left to the end. With only two months left before the delivery date, the DAQ system was designed. The specifications required a course in LabView, since the author had no previous programming experience. After a full week of training, another engineer suggested that LabWindows/CVI was a more powerful tool than LabView due to its C based coding. Since this engineer would inherit the project, the necessary software changes were needed. Therefore, a consultant (Advanced Integration, L.L.C.) was contracted to aid in the creation of the data acquisition software since time was running out. In retrospect, this situation could have been avoided with more careful planning and by running different tasks in parallel. Furthermore, it pointed out the need to have a wider multidisciplinary training in order to tackle similar obstacles in the future. In the end, the project was successfully transferred with the new Lab Windows/CVI software.

Although many obstacles sprang up along the length of this project, it was undoubtedly a great learning experience. As a result, the author has greater appreciation of a professional engineering environment, where deadlines and project milestones are a reality and not just some topic mentioned in a classroom. The demands of the job are very real, making this experience a great stepping stone in preparing the author for a career in engineering.

References

Gao, Robert X.; Jin, Yucheng; Warrington, Robert O., "Microcomputer-based real-time bearing monitor," IEEE Transactions on Instrumentation and Measurement, v43, n2, April 1994.

Gao, Robert X.; Holm-Hansen, Brian T.; Wang, Changting, "Design of a mechatronic bearing through sensor integration," The International Society for Optical Engineering Proceedings of the 1998 Conference on Sensors and Controls for Intelligent Machining, Agile Manufacturing, and Mechatronics, Boston, MA.

Anon,"Condition monitoring puts the squeeze on plant downtime," *Noise and Vibration Worldwide*, v26, n9, October 1995.

Anon, "Preventive maintenance bearing fruits," *Manufacturing Engineer*, v68, n9, January 1989.

Courtright, Michael L., "Instrumented bearings get rolling with ABS," *Machine Design*, v64, n1, January 1992.

Anon, "Health Maintenance for machines?," *Tooling & Production*, v57, n8, November 1991.

Hutton, Roger W., "Condition monitoring and reliability management – how dow they fit together?, " Proceedings for the 12th International Congress on Condition Monitoring and Diagnositc Engineering Management, July 1999.

Dow, Scott E., "The future of training for condition based monitoring," Proceedings for the 12th International Congress on Condition Monitoring and Diagnositc Engineering Management, July 1999.

Neun, John A.; Watts, Robert J., "Automated system to diagnose the condition of machinery using vibration analysis," American Society of Mechnanical Engineers, January 1990.

Anon, "I/N Tek installs system to monitor vibration and predict failures," *Iron and Steel Engineer*, v75, n6, June 1998.

Lösl, J.; Franke, D., "Industrial accelerometers for machine and rolling bearing monitoring," Sensor and Transducer Conference at MTEC Measurement Technology, 1997.

Wozniak, J., "The Rothe Erde current condition monitoring system," *Technische Mitteilungen Krupp*, n1, April 1993.

Coleman, J. R., "Life extension through tool-condition monitoring," *Machine and Tool Blue Book*, March 1987.

Yang, Y.; Kurfess, T.; Liang, S.; Danyluk, S., "Application of a specialized capacitance probe in the bearing diagnosis," Wear Proceedings of the 1999 12th International Conference on Wear of Materials.

Holm-Hansen, BrianT.; Gao, Robert X., "Smart bearing utilizing embedded sensors: design considerations," The International Society for Optical Engineering Smart Structures and Materials, March 1997.

Gao, Robert X.; Phalakshan, P., "Design considerations for a sensor-integrated roller bearing," Rail Transportation Proceedings of the 1995 ASME International Mechanical Engineering Congress and Exposition, November 1995.

Cohen, Edward I.; Mastro, Stephen A.; Nemarich, Christopher P.; Korczynski, Joseph F. Jr; Jarret, Andrew W.; Jones, Wayne C., "Recent developments in the use of plastic optical fiber for an embedded wear sensor," The International Society for Optical Engineering Proceedings of the 1999 Smart Structures and Materials – Sensory Phenomena and Measurement Instrumentation for Smart Structures and Materials.

Herraty, A. G., "Bearing vibration. Failures and diagnosis," *Mining Technology*, v75, n862, February 1993.

Sayles, R. S.; Hamer, J. C.; Ioannides, E., "The effects of particulate contamination on rolling bearings - a state of the art review," Proc. Instn. Mech. Engrs., 1990.

Fitzsimmons, B.; Clevenger, H. D., "Contaminated lubricants and tapered roller bearing wear," *ASLE Transactions*, 1975.

Perroto, J. A., "Effect of abrasive contamination on ball bearing performance," *Lubricatoin Engineering*, 1979.

Chao, K. K.; Saba, C. S.; Centers, P. W., "Effects of lubricant borne solid debris in rolling surface contacts," *Tribology Transactions*, 1996.

Sayles, R. S.; Macpherson, P. B., "Influence of wear debris on rolling contact fatigue," Rolling Contact FatigueTesting of Bearing Steels, ASTM STP 771, 1982.

Holzhauer, W., "Surface changes around large raceway indentations during run-in of tapered roller bearings," STLE Preprints, 1990.

Dwyer-Joyce, R. S.; Hamer, J. C.; Sayles, R. S.; Ioannides, E., "Lubricant screening for debris effects to improve fatigue and wear life," Proceedings of 18th Leeds-Lyon Symposium on Tribology, 1992.

Bannister, R.H., "A review of rolling element bearing monitoring techniques," *Condition Monitoring*, n6, 1986.

Kim, P. Y.,"A review of rolling element bearing health monitoring (II) preliminary test results on current technologies," Proceedings on Machinery Vibration Monitoring & Analysis Meeting, 1984.

Pratt, J., "Engine and transmission monitoring – a summary of promising approaches," Proceedings from 41st Meeting of the Mechanical Failures Prevention Group, Naval Air Test Center, October 1986.

Appendix A: Accelerometer Manufacturer Specifications

353-2130-95

APPLICATION		
NEXT ASS'Y	USED ON	VAR

REVISIONS				
REV	DESCRIPTION	ECN	DATE	APP'D
F	UPDATED CABLE CALL OUT	8809	3/4/98	
G	DRAFTING ERROR	9153	5/26/98	Kml.

PIN CONFIGURATION

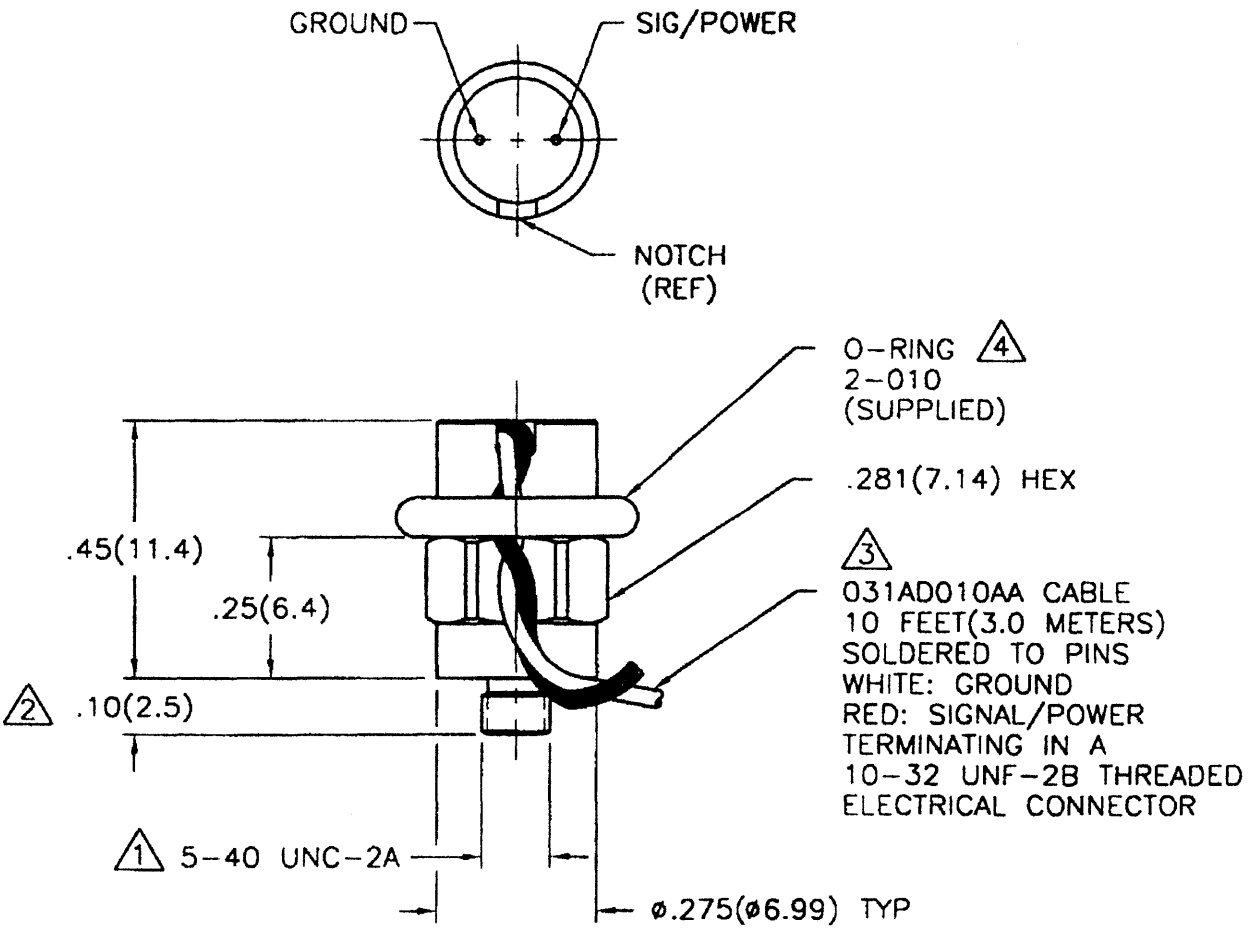

4 IF O-RING IS REMOVED, TAKE PRECAUTIONS TO STRAIN RELIEVE CABLE.

3 FOR "W" OPTION, CABLE REPLACED BY 018 TYPE CABLE 10 FT (3.0 METERS) LONG TERMINATING IN 10-32 THREADED ELECTRICAL CONNECTOR. CENTER CONDUCTOR SIGNAL/POWER, SHIELD GROUND.

2 STUD REMOVED FOR SENSOR WITH ADHESIVE MOUNT OPTION.

1 M3 X 0.50-6g FOR SENSOR WITH METRIC OPTION.

UNLESS SPECIFIED TOLERANCES						
DIMENSIONS IN INCHES DECIMALS XX ±.01 XXX ±.005 ANGLES ±2 DEGREES	DIMENSIONS IN MILLIMETERS (IN PARENTHESIS) DECIMALS XX ±0.3 XXX ±0.13 ANGLES ±2 DEGREES	DRAWN	RM 5/27/98	MFG	LDA	5-27-98
FILLETS AND RADII .003 - .005	FILLETS AND RADII (0.07 - 0.13)	CHK'D	Kml 5/27/98	ENGR	DS	5/27/98
D0011 REV. B 03/13/98		APP'D	5/27/98	SALES	CSO	5/27/98

PCB PIEZOTRONICS INC.
3425 WALDEN AVE. DEPEW, NY 14043
(716) 684-0001 EMAIL: SALES@PCB.COM

TITLE: OUTLINE DRAWING
MODEL 353B13, B17 & B67
ACCELEROMETER

CODE IDENT. NO. 52681 | DWG. NO. 353-2130-95 | SCALE: 3X | SHEET 1 OF 1

081-XXXX-90

APPLICATION		
NEXT ASS'Y	USED ON	VAR

STANDARD STUD MOUNT

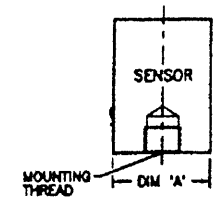

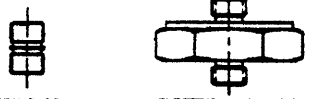

STUD MODEL	SENSOR THREAD	MOUNTING THREAD	SEE DRAWING
081A27	5-40	5-40	A
M081A27	5-40	M3 X 0.50	B
081B05	10-32	10-32	C
M081B05	10-32	M6 X 0.75	F
081B20	1/4-28	1/4-28	E
M081B20	1/4-28	M6 X 0.75	F
M081B23	10-32	M5 X 0.80	D
081A08	10-32	1/4-28	E
081A90	10-32	5-40	A
081A21	10-32	10-32	C
M081A61	1/4-28	M6 X 1.00	F
M081A62	10-32	M6 X 1.00	F
081A39	10-32	10-32	C
081A40	1/4-28	1/4-28	E

INTEGRAL STUD MOUNT

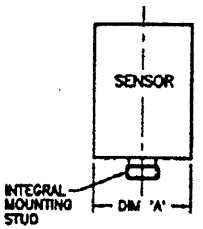

MOUNTING THREAD	SEE DRAWING
10-32	C
1/4-28	E
M3 X 0.50	B
M5 X 0.80	D
M6 X 0.75	F

"THRU-BOLT" MOUNT

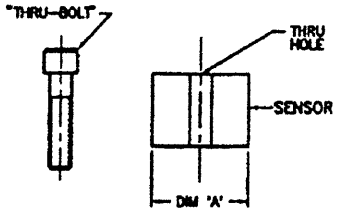

(METRIC DIMENSIONS IN PARENTHESIS)

BOLT MODEL	BOLT LENGTH	BOLT THREAD	SEE DRAWING
081A25	.63(16.0)	10-32	C
081A50	.80(20.3)	10-32	C
081A51	.87(22.1)	10-32	C
M081A25	(16.0).63	M5 X 0.80	D
M081A50	(20.3).80	M5 X 0.80	D
M081A51	(22.1).87	M5 X 0.80	D
081A55	1.00(25.4)	10-32	C
081A56	.75(19.1)	1/4-28	E
081A57	1.00(25.4)	1/4-28	E
M081A58	(25.4)1.00	M6 X 1.00	F
M081A59	(20.0).79	M6 X 1.00	F
M081M94	(30.0)1.18	M6 X 1.00	F
081M96	1.12(28.4)	1/4-28	E
081M110	1.10(28.0)	M8 X 1.25	F
M081A67	1.18(30.0)	M6 X 1.00	F
081A67	1.12(28.4)	1/4-28	E
M081A73	(34.0)1.34	M6 X 1.06	F
081A73	1.34(34.0)	1/4-28	E
081A68	.90(22.86)	1/4-28	E
M081A68	(22.86).90	M6 X 1.00	F

X — 5-40 MOUNTING INSTRUCTIONS

(METRIC DIMENSIONS IN PARENTHESIS)

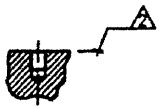

MOUNTING HOLE PREPARATION:
DRILL ø.101(ø2.57) ⚠
X .20(5.1) ∓ MIN.
TAP 5-40 UNC-2B
X .15(3.8) ∓ MIN.

4.) RECOMMENDED MOUNTING TORQUE, 4-5 INCH POUNDS (45-55 NEWTON CENTIMETERS).

B — M3 X 0.50 MOUNTING INSTRUCTIONS

(ENGLISH DIMENSIONS IN PARENTHESIS)

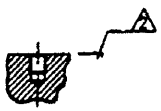

MOUNTING HOLE PREPARATION:
DRILL ø2.5(ø.099) ⚠
X 4.6(.18) ∓ MIN.
TAP M3 x 0.50-6H
X 3.3(.13) ∓ MIN.

4.) RECOMMENDED MOUNTING TORQUE, 45-55 NEWTON CENTIMETERS(4-5 INCH POUNDS).

C — 10-32 MOUNTING INSTRUCTIONS

(METRIC DIMENSIONS IN PARENTHESIS)

MOUNTING HOLE PREPARATION:
DRILL ø.159(ø4.04) ⚠
X .23(5.8) ∓ MIN.
TAP 10-32 UNF-2B
X .15(3.8) ∓ MIN.

4.) RECOMMENDED MOUNTING TORQUE, 10-20 INCH POUNDS (113-225 NEWTON CENTIMETERS).

D — M5 X 0.80 MOUNTING INSTRUCTIONS

(ENGLISH DIMENSIONS IN PARENTHESIS)

MOUNTING HOLE PREPARATION:
DRILL ø4.22(ø.166) ⚠
X 7.62(.300) ∓ MIN.
TAP M5 x 0.8-6H
X 5.06(.200) ∓ MIN.

4.) RECOMMENDED MOUNTING TORQUE, 113-225 NEWTON CENTIMETERS(10-20 INCH POUNDS).

E — 1/4-28 MOUNTING INSTRUCTIONS

(METRIC DIMENSIONS IN PARENTHESIS)

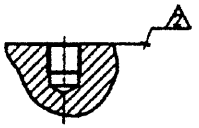

MOUNTING HOLE PREPARATION:
DRILL ø.218(ø5.54) ⚠
X .300(7.62) ∓ MIN.
TAP 1/4-28 UNF-2B
X .200(5.08) ∓ MIN.

4.) RECOMMENDED MOUNTING TORQUE 2-5 FOOT POUNDS (3-7 NEWTON METERS).

F — M6 X 0.75, M6 X 1.00,& M8 X 1.25 MOUNTING INSTRUCTIONS

(ENGLISH DIMENSIONS IN PARENTHESIS)

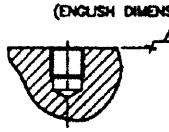

M6 X 0.75
DRILL ø5.31(ø.209) ⚠
X 7.62(.300) ∓ MIN.
TAP M6x 0.75-6H
X 5.06(.200) ∓ MIN.

MOUNTING HOLE PREPARATION:

M8 X 1.25
DRILL ø6.75(ø.266) ⚠
X 8.64(.340) ∓ MIN.
TAP M8x 1.25-6H
X 5.00(.197) ∓ MIN.

M6 X 1.00
DRILL ø5.05(ø.199) ⚠
X 17.00(.670) ∓ MIN.
TAP M6 x 1.00-6H
X 10.00(.394) ∓ MIN.

4.) RECOMMENDED MOUNTING TORQUE 3-7 NEWTON METERS (2-5 FOOT POUNDS).

3.) FOR BEST RESULTS, PLACE A THIN LAYER OF SILICONE GREASE (OR EQUIVALENT) ON INTERFACE PRIOR TO MOUNTING.

⚠ MOUNTING SURFACE SHOULD BE FLAT TO WITHIN .001(0.03) TIR OVER DIM 'A' WITH A MINIMUM 63(1.6) FINISH FOR BEST RESULTS.

NOTES: ⚠ DRILL PERPENDICULAR TO MOUNTING SURFACE TO WITHIN ±1°.

REVISIONS				
REV	DESCRIPTION	ECN	DATE	APP'D
J	REVISED PER ECN	8717	2/12/98	
K	REVISED PER ECN	9090	5/5/98	
L	MODEL NUMBER UPDATE	9732	11/5/98	
N	MODEL NUMBER UPDATE	10222	3/17/99	
N	MODEL NUMBER UPDATE	10255	3/24/99	PMS/94

DRAWINGS NOT TO SCALE

UNLESS SPECIFIED TOLERANCES	
DIMENSIONS IN INCHES	DIMENSIONS IN MILLIMETERS
DECIMALS XX ±.01 XXX ±.005 ANGLES ±2 DEGREES	DECIMALS XX ±0.3 XXX ±0.13 ANGLES ±2 DEGREES
FILLETS AND RADII .003 - .005	FILLETS AND RADII 0.07 - 0.13

00012 REV. B 03/13/96

DRAWN	TW	4/15/99	MFG	TBS	3/26/99
CHK'D	DSM	3/25/99	ENGR	JMB	3/25/99
APP'D		3/24/99			

TITLE: INSTALLATION DRAWING FOR STANDARD 081 SERIES MOUNTING

PCB PIEZOTRONICS
3425 WALDEN AVE. DEPEW, NY 14043
(716) 684-0001 EMAIL: SALES@PCB.COM

CODE IDENT. NO.	DWG. NO.
52681	081-XXXX-90

SCALE: 1=1.5 | SHEET 1 OF 1

Model Number
353B67

QUARTZ SHEAR ICP® ACCELEROMETER SPECIFICATIONS

Revision: K
ECN #: 8299

DYNAMIC PERFORMANCE			
Voltage Sensitivity	mV/g [mV/(m/s²)]	100 [10,2]	[1]
Measurement Range	±g pk [±m/s² pk]	50 [491]	
Frequency Range: (±5%)	Hz	5 to 10,000	
(±10%)	Hz	3 to 18,000	
(±3 dB)	Hz	1 to 25,000	
Mounted Resonant Frequency	kHz	≥40	
Resolution - Broadband	g pk [m/s² pk]	0.007 [0,07]	
Amplitude Linearity	%	±1	[2]
Transverse Sensitivity	%	≤5	[3]
ENVIRONMENTAL			
Shock Limit (maximum)	±g pk [±m/s² pk]	5,000 [49 050]	
Operating Temperature Range	°F [°C]	-65 to +250 [-54 to +121]	
Temperature Response		See Graph	[4]
Strain Sensitivity	g/με [(m/s²)/με]	≤0.005 [≤0,05]	
ELECTRICAL			
Excitation Voltage/Constant Current	VDC/mA	24 to 30/2 to 10	
Output Impedance	ohms	<100	
Output Bias	VDC	15 to 19	
Discharge Time Constant	sec	≥0.5	
Warm Up Time (within 10% of output bias)	sec	<5	
Broadband Electrical Noise (1-10 kHz)	μV rms	300	
Spectral Noise: (1 Hz)	μg/√Hz [(μm/s²)/√Hz]	1,600 [15 696]	[5]
(10 Hz)	μg/√Hz [(μm/s²)/√Hz]	320 [3 139]	
(100 Hz)	μg/√Hz [(μm/s²)/√Hz]	150 [1 386]	
(1 kHz)	μg/√Hz [(μm/s²)/√Hz]	50 [491]	
Ground Isolation	ohms	None (Optional)	
MECHANICAL			
Sensing Element	material/geometry	Quartz/Shear	
Housing	material/sealing	Titanium/Welded Hermetic	
Size (hex x height)	inch [mm]	0.28 x 0.54 [7,1 x 13,7]	
Weight	oz [gm]	0.06 [1,8]	
Electrical Connector	type/location	2-Pin Solder/Top	
Cable (standard 10 ft supplied)	type/termination	031D010W Twisted Pair/10-32	
Mounting Thread	size	5-40 Male	
Mounting Torque	**in-lb [N-cm]**	**8-12 [90-130] Must Be Applied**	

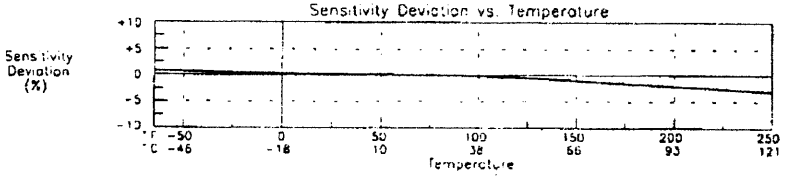

PCB® PIEZOTRONICS

In the interest of constant product improvement, we reserve the right to change specifications without notice.

ICP® is a registered trademark of PCB Piezotronics, Inc.

OPTIONAL VERSIONS

Optional versions have identical specifications and accessories as listed for the standard model except where noted by the letter prefixes below. More than one option may be used.

X A - Adhesive Mount
Additional Accessory: (1) Model 080A90 "quick bonding gel"
Note: Mounting stud removed - Adhesive mounting base is not required.

☐ J - Ground Isolated

High Frequency Range: (+5%)/(+10%)	Hz	8,000/15,000
Mounted Resonant Frequency	kHz	≥35
Electrical Base Isolation	ohms	>10⁸
Size (hex x height)	inch [mm]	0.37 x 0.69 [9,5 x 17,5]
Weight	oz [gm]	0.10 [2,9]

☐ M - Metric

Mounting Thread	size	M3 x 0.50 Male
Supplied Accessories:	(1) Model M080A15 base replaces Model 080A15	

☐ W - Water Resistant

Cable (standard 10 ft supplied)	type/termination	018D010A/10-32

NOTES:
[1] Supplied with a sensitivity tolerance of ±10%.
[2] Zero based best straight line method.
[3] Transverse sensitivity is typically ≤3%.
[4] Specification within ±2% of typical curve.
[5] Acceleration level equivalent.

SUPPLIED ACCESSORIES:
080A15 Adhesive Mounting Base (1)
(except A option)
080A24 Petro Wax Sample (1)
NIST Traceable Calibration Certificate

Drawn:	Engineer:	Sales: CSA	Approved:	Spec Number:
Date: 10/1/97	Date: 10/1/97	Date: 10/1/97	Date: 10/14/97	353-2670-80

Appendix B: Failed Bearing Baseline Test

Data File : D:\Thesis Files\Data\Failed BRG Baseline\1250PSI B.bin
Sample Rate : 12000.0 samples/sec
Channel Mode : 16

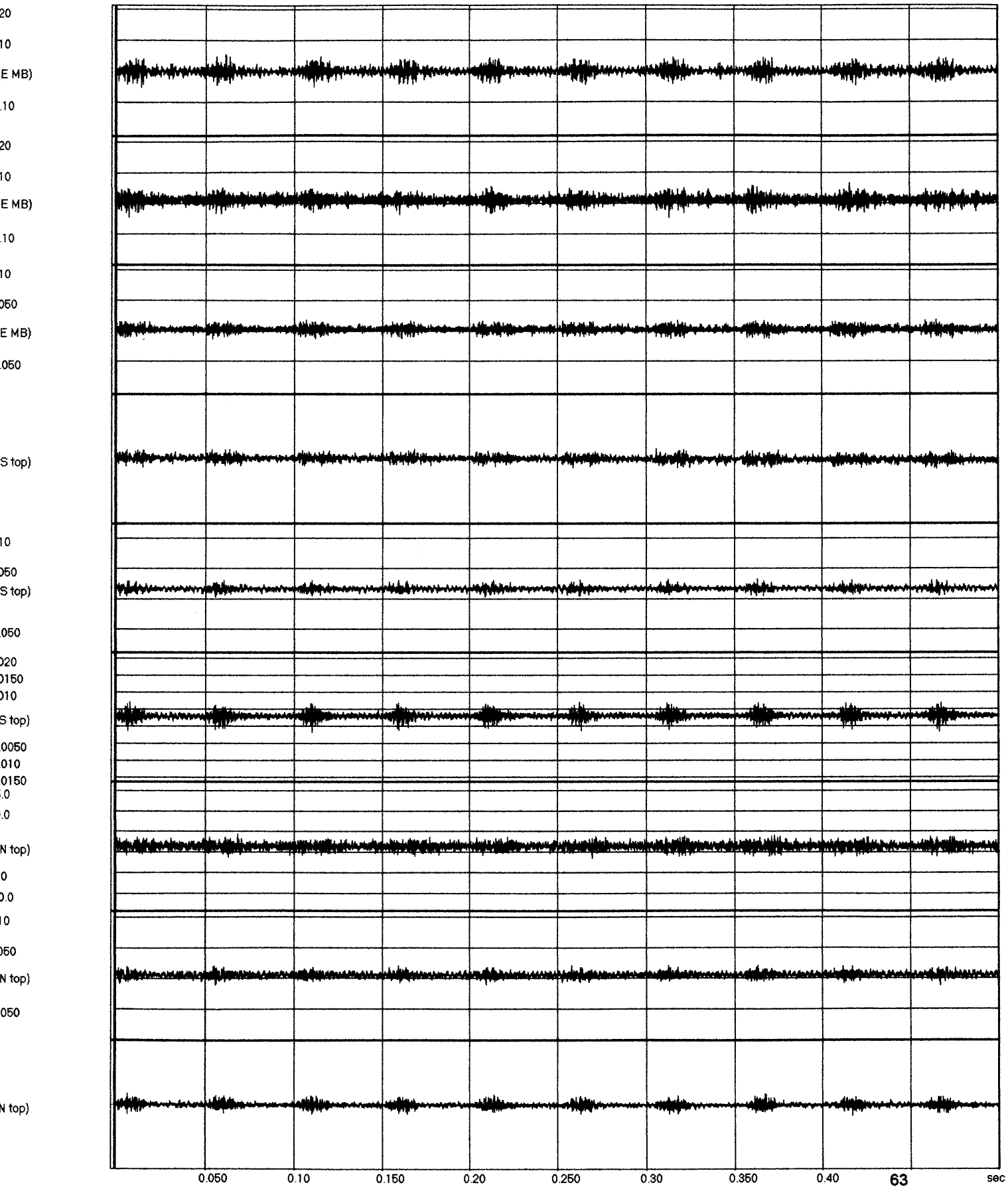

Data File : D:\Thesis Files\Data\Failed BRG Baseline\1050PSI B.bin
Sample Rate : 12000.0 samples/sec
Channel Mode : 16

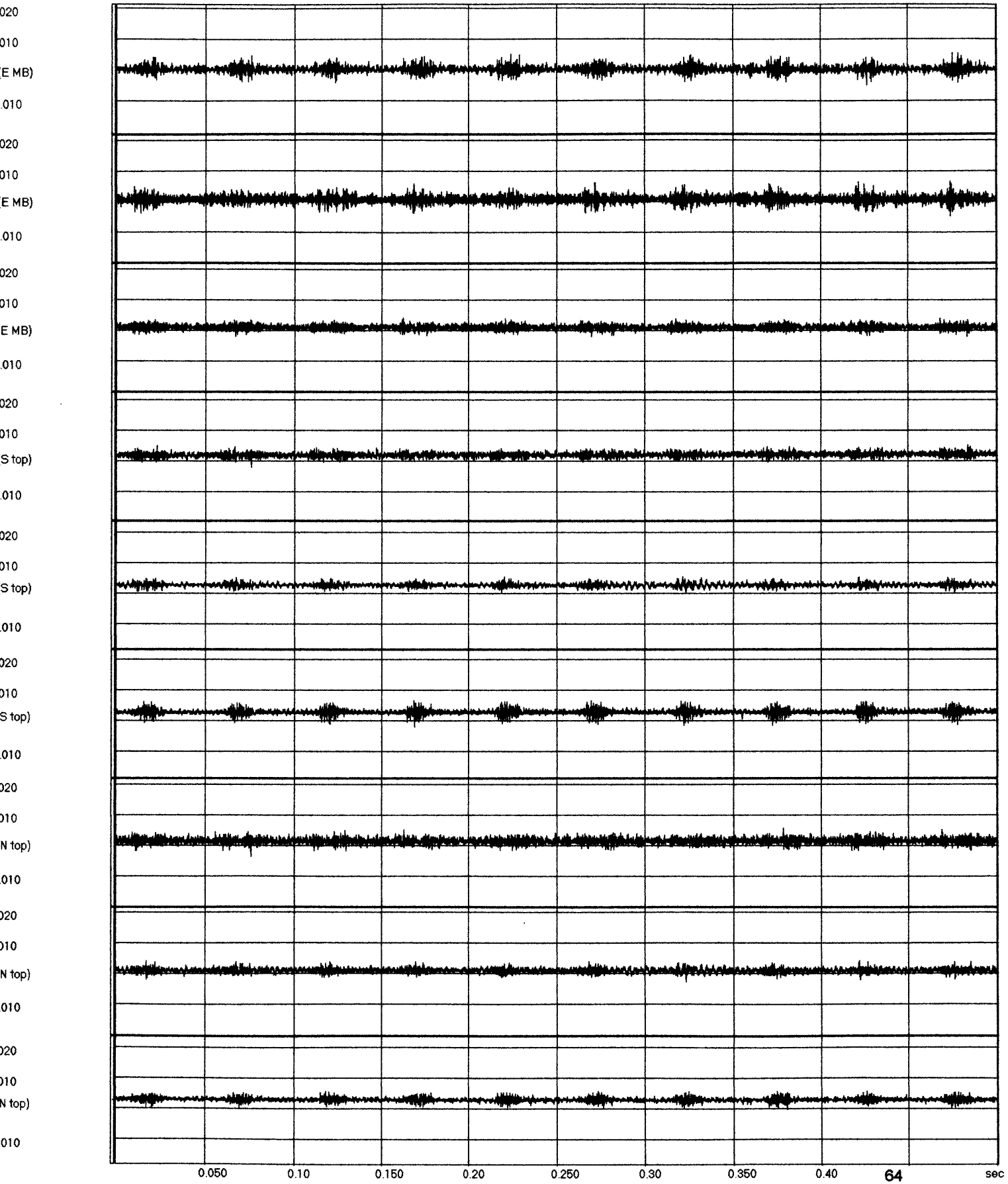

Data File : D:\Thesis Files\Data\Failed BRG Baseline\900PSI.bin
Sample Rate : 12000.0 samples/sec
Channel Mode : 16

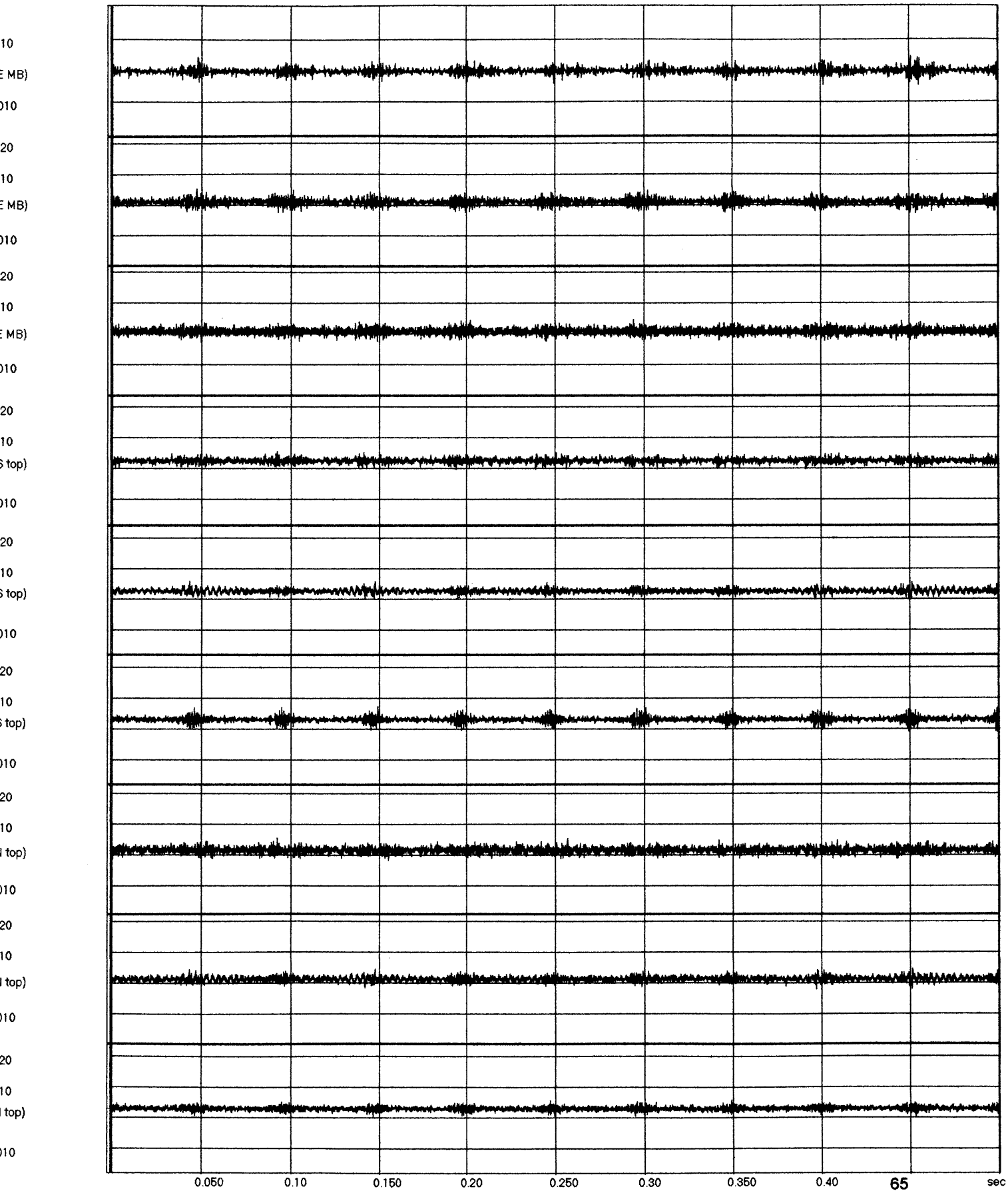

Data File : D:\Thesis Files\Data\Failed BRG Baseline\830PSI B.bin
Sample Rate : 12000.0 samples/sec
Channel Mode : 16

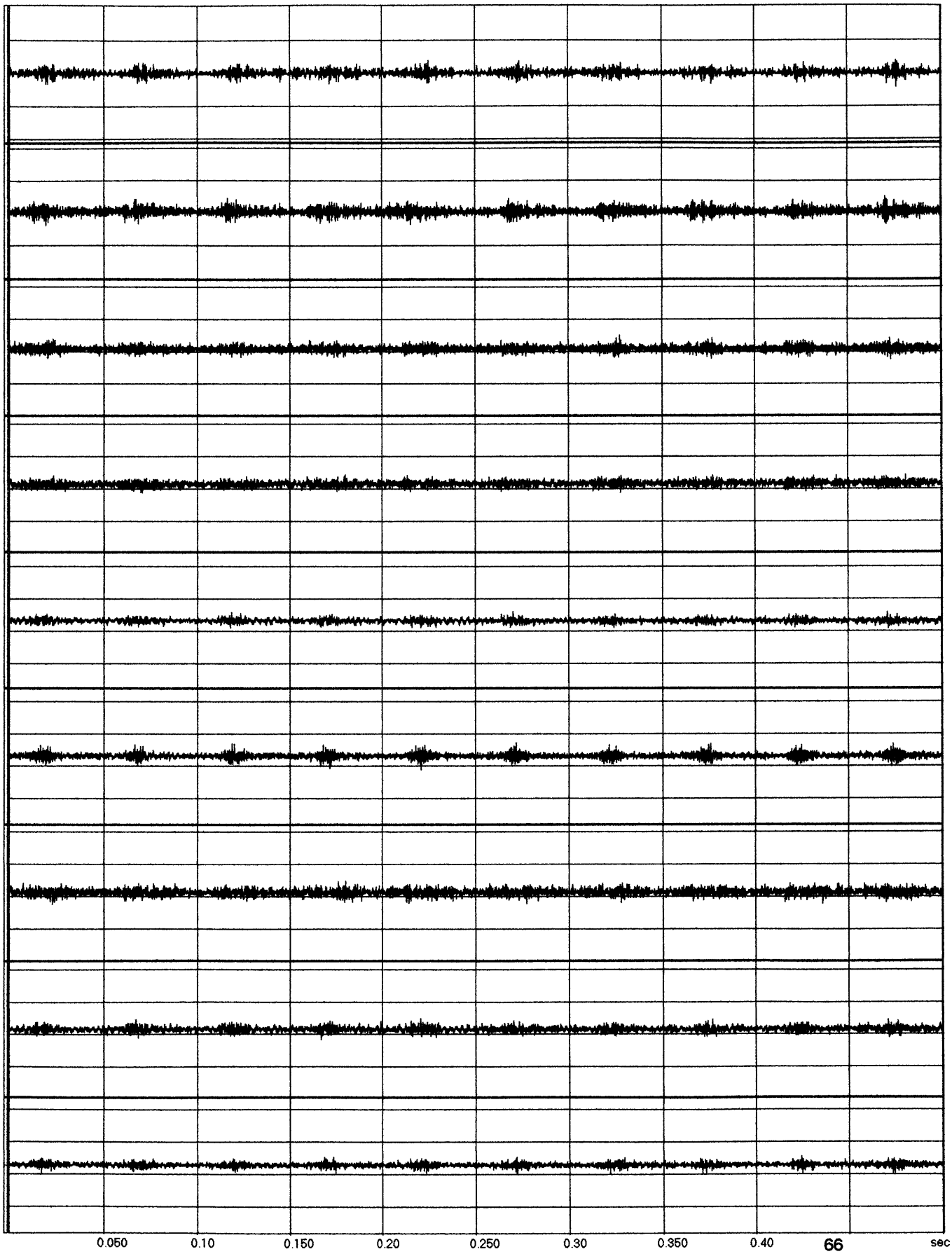

Data File : D:\Thesis Files\Data\Failed BRG Baseline\760PSI B.bin
Sample Rate : 12000.0 samples/sec
Channel Mode : 16

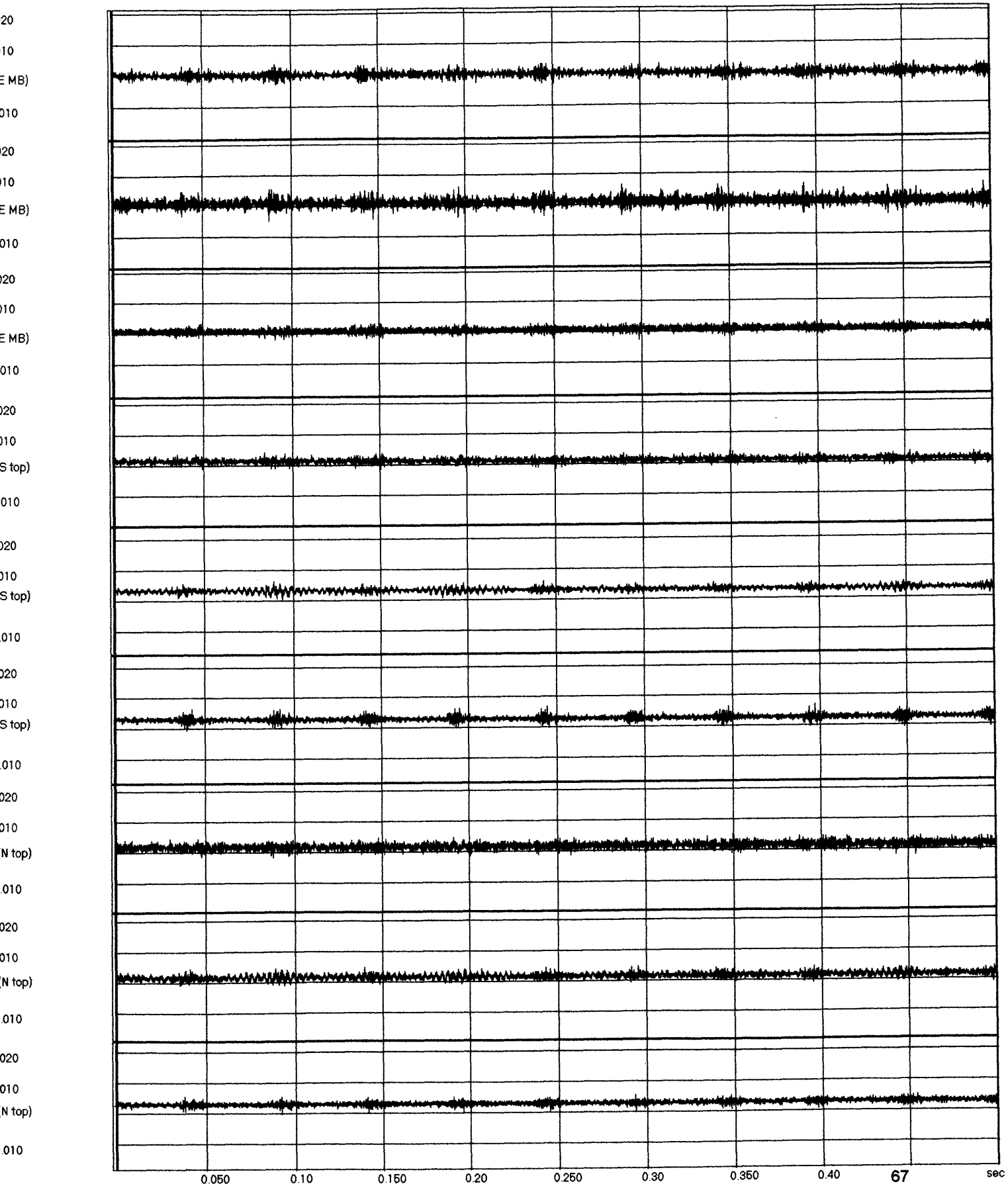

Data File : D:\Thesis Files\Data\Failed BRG Baseline\608PSI.bin
Sample Rate : 12000.0 samples/sec
Channel Mode : 16

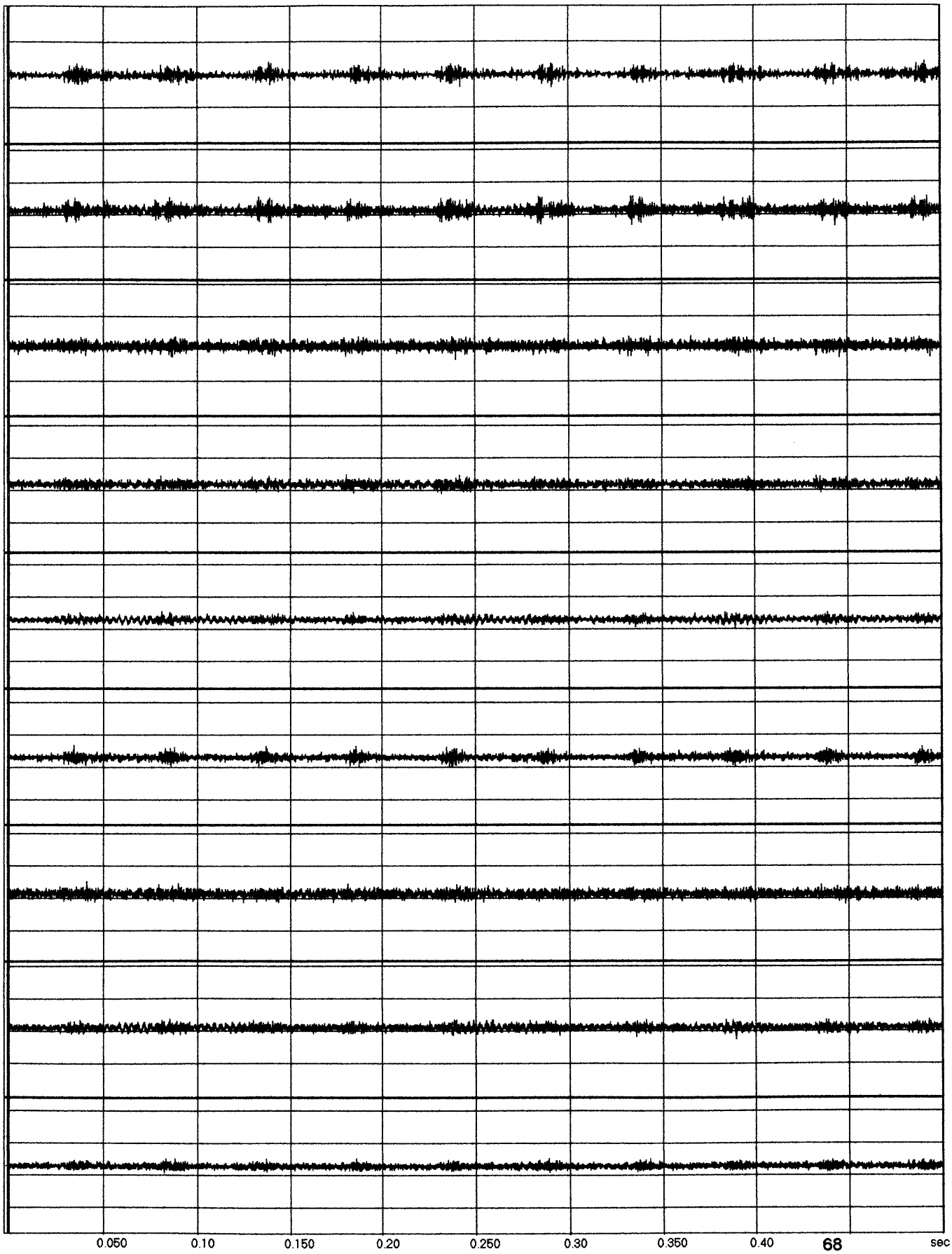

Data File : D:\Thesis Files\Data\Failed BRG Baseline\468PSI B.bin
Sample Rate : 12000.0 samples/sec
Channel Mode : 16

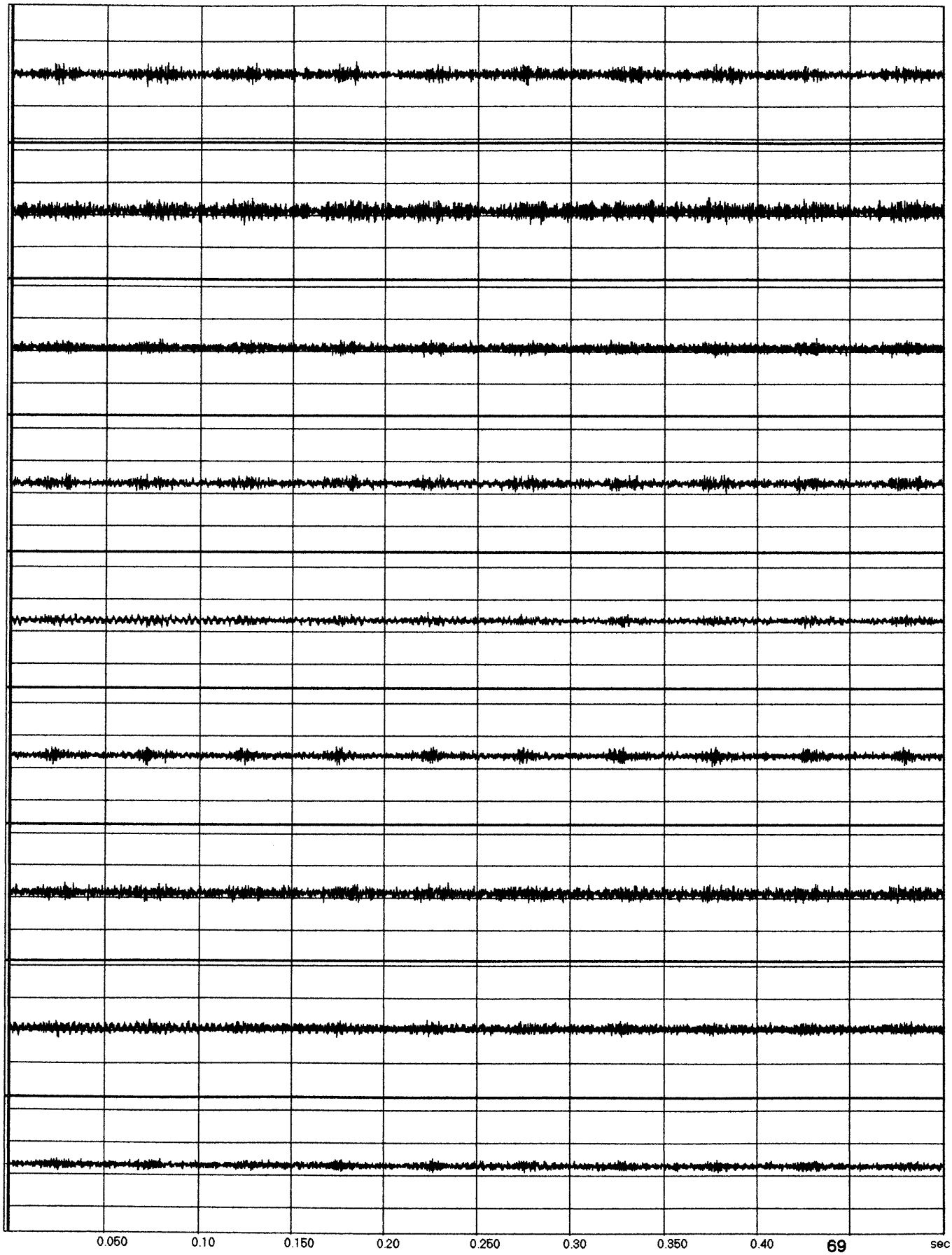

Data File : D:\Thesis Files\Data\Failed BRG Baseline\308PSI.bin
Sample Rate : 12000.0 samples/sec
Channel Mode : 16

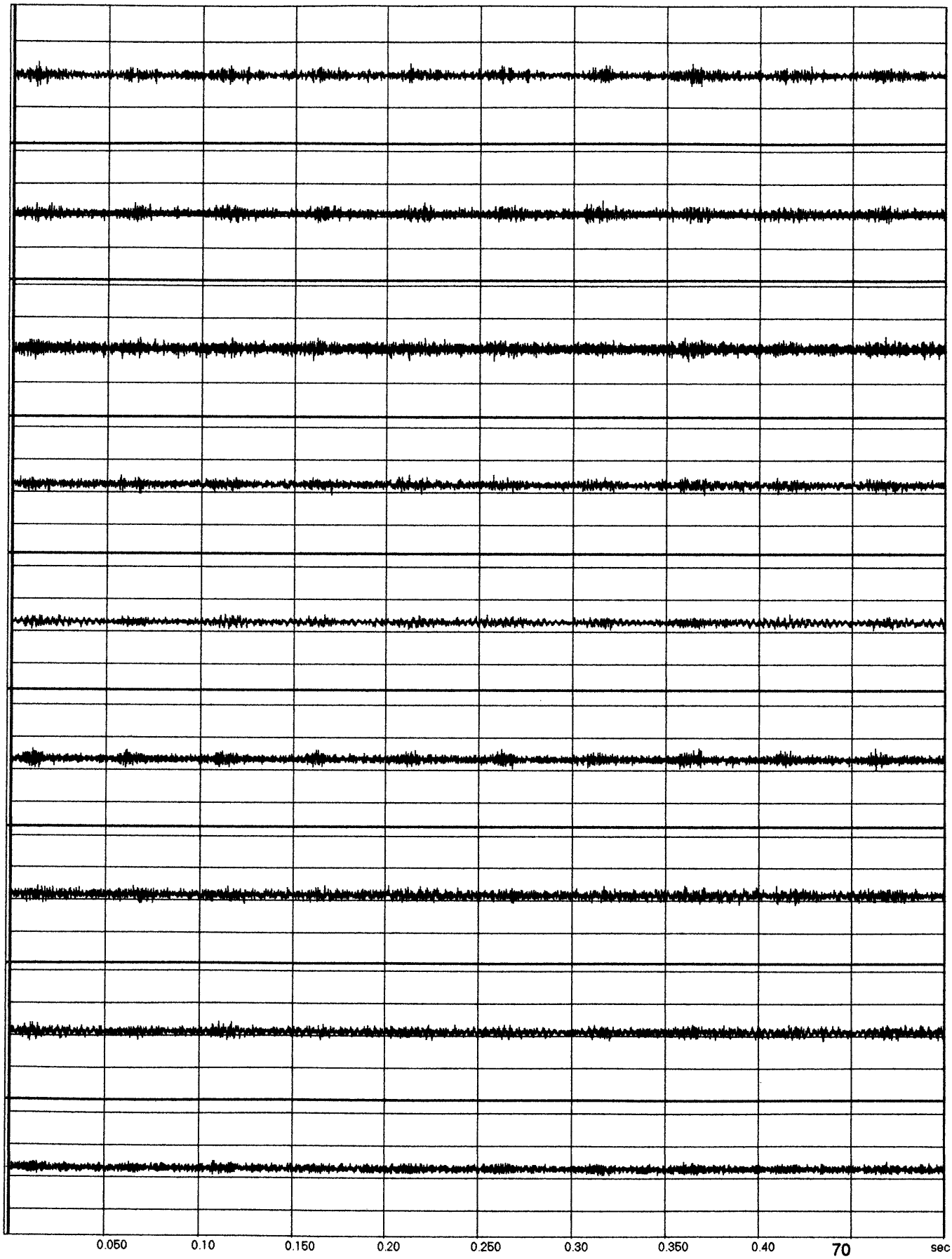

Appendix C: Good Bearing Baseline Test

Data File : D:\Thesis Files\Data\Good BRG Baseline\1250.bin
Sample Rate : 12000.0 samples/sec
Channel Mode : 16

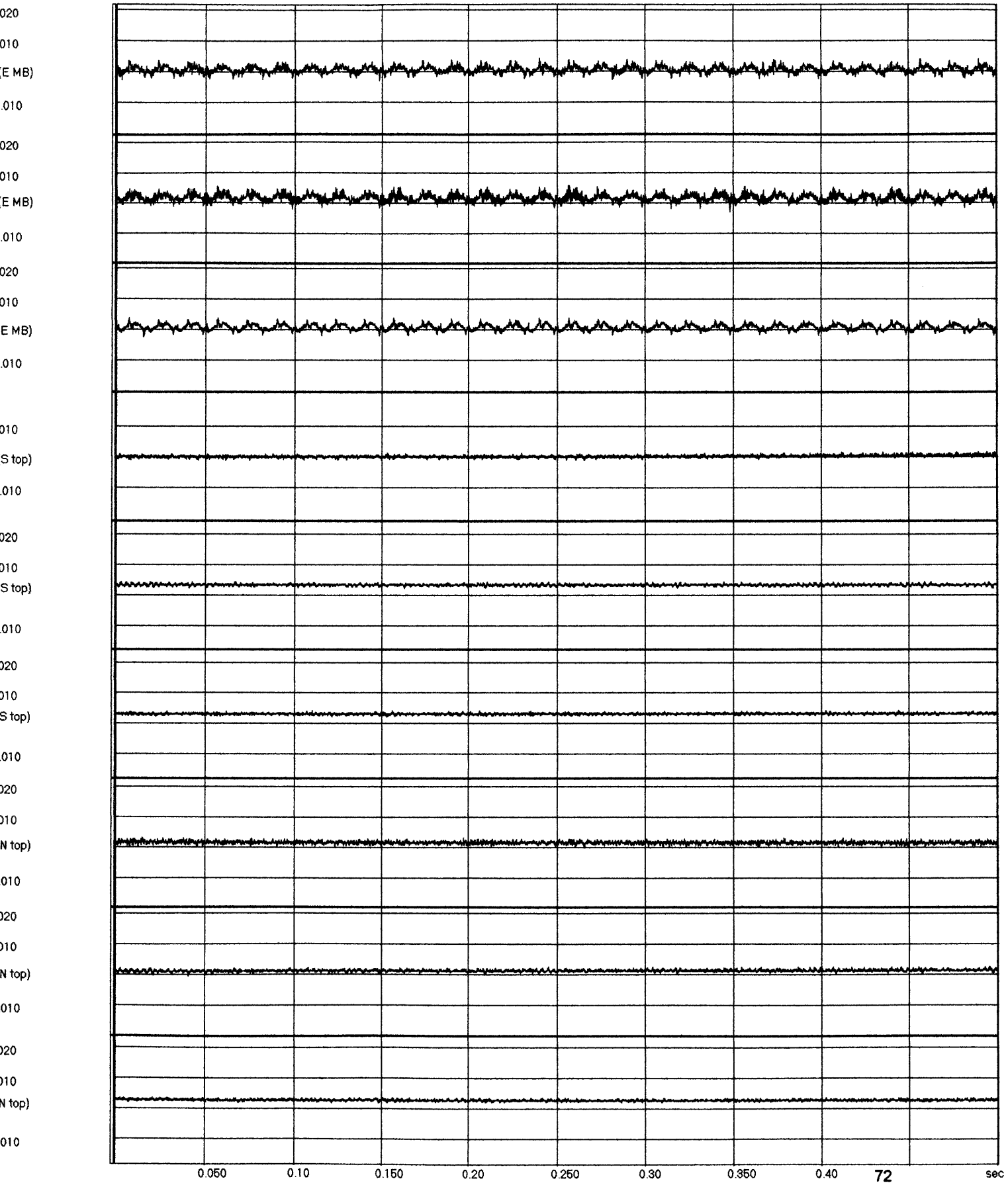

Data File : D:\Thesis Files\Data\Good BRG Baseline\1050.bin
Sample Rate : 12000.0 samples/sec
Channel Mode : 16

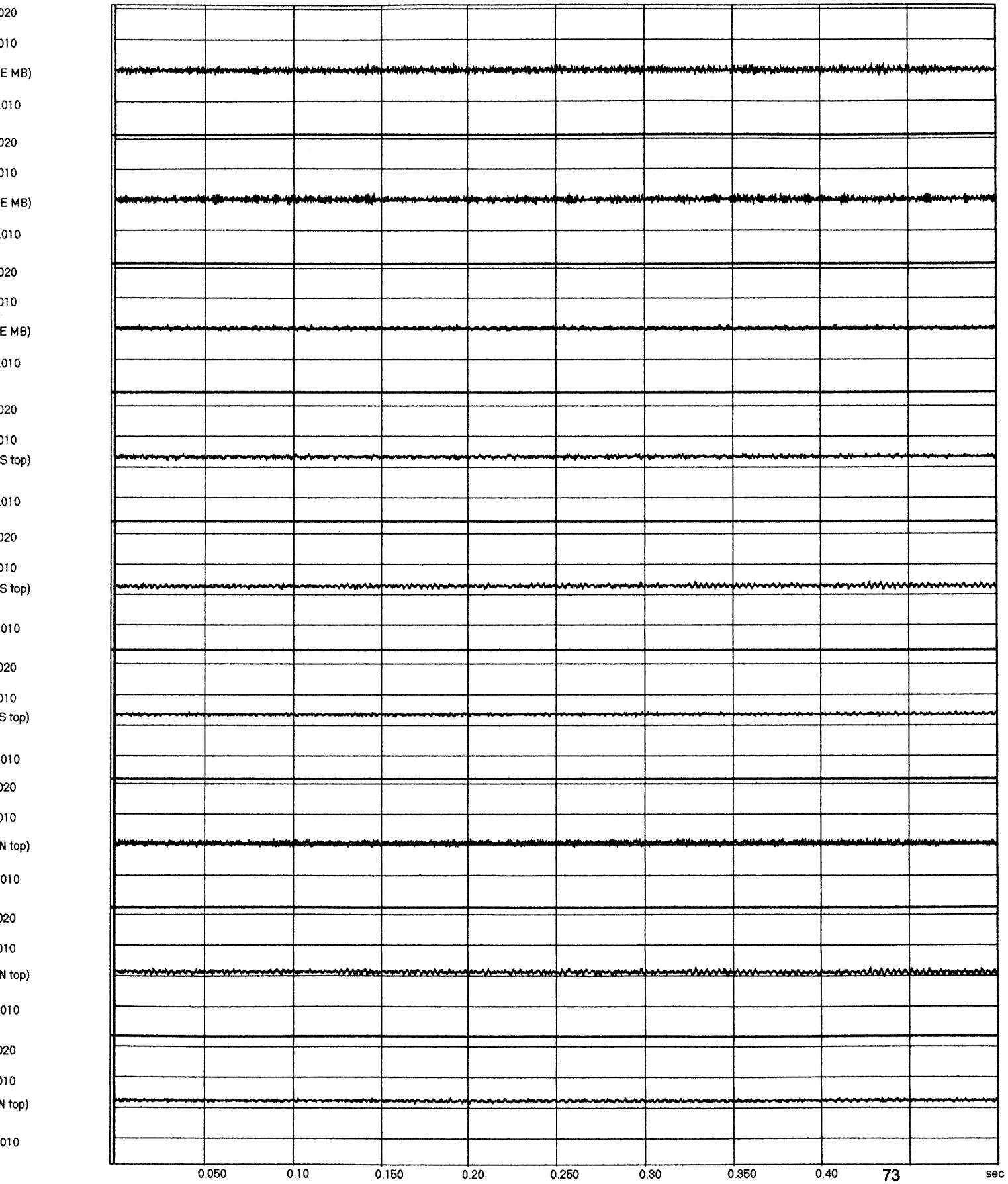

Data File : D:\Thesis Files\Data\Good BRG Baseline\900.bin
Sample Rate : 12000.0 samples/sec
Channel Mode : 16

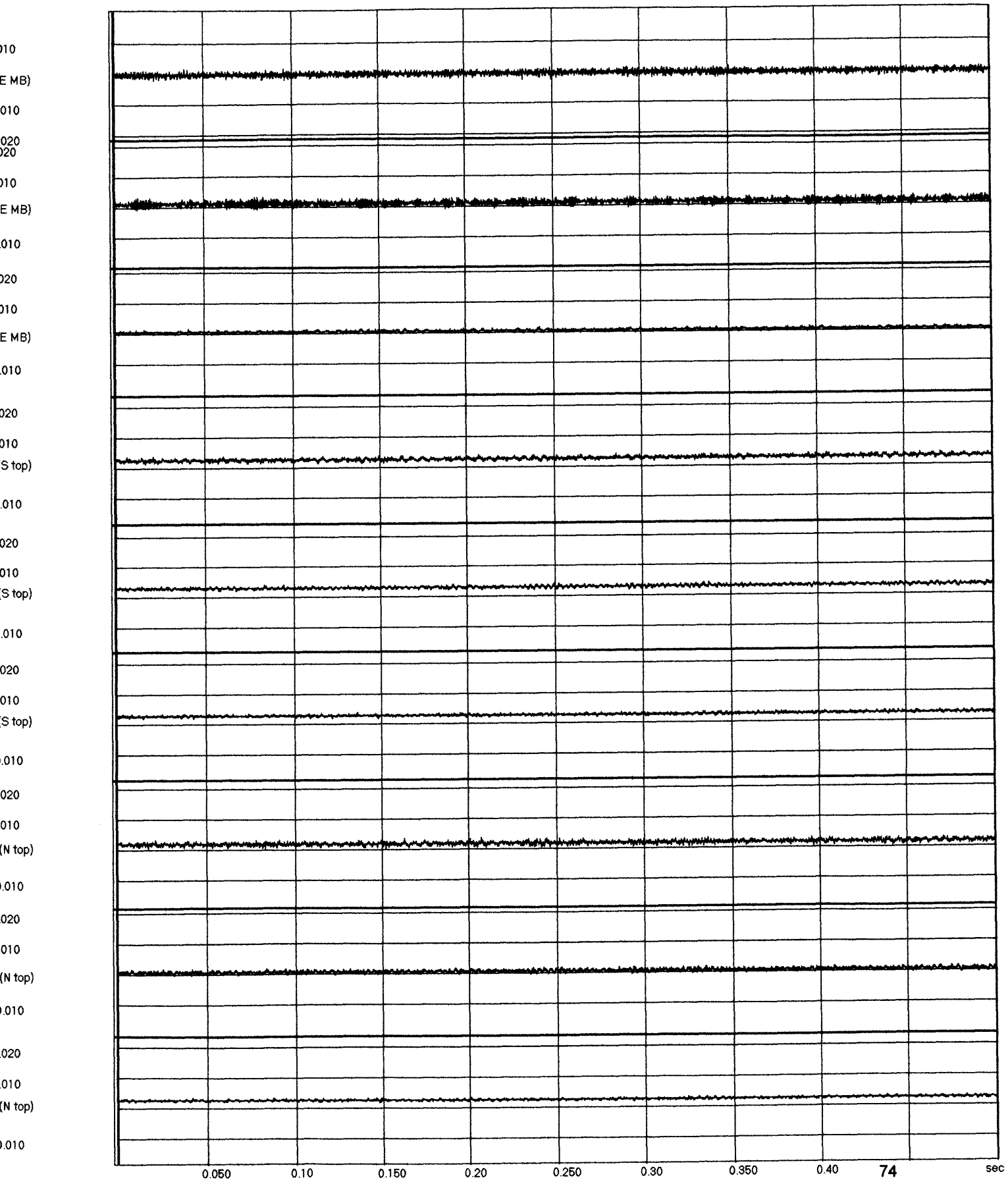

Data File : D:\Thesis Files\Data\Good BRG Baseline\800.bin
Sample Rate : 12000.0 samples/sec
Channel Mode : 16

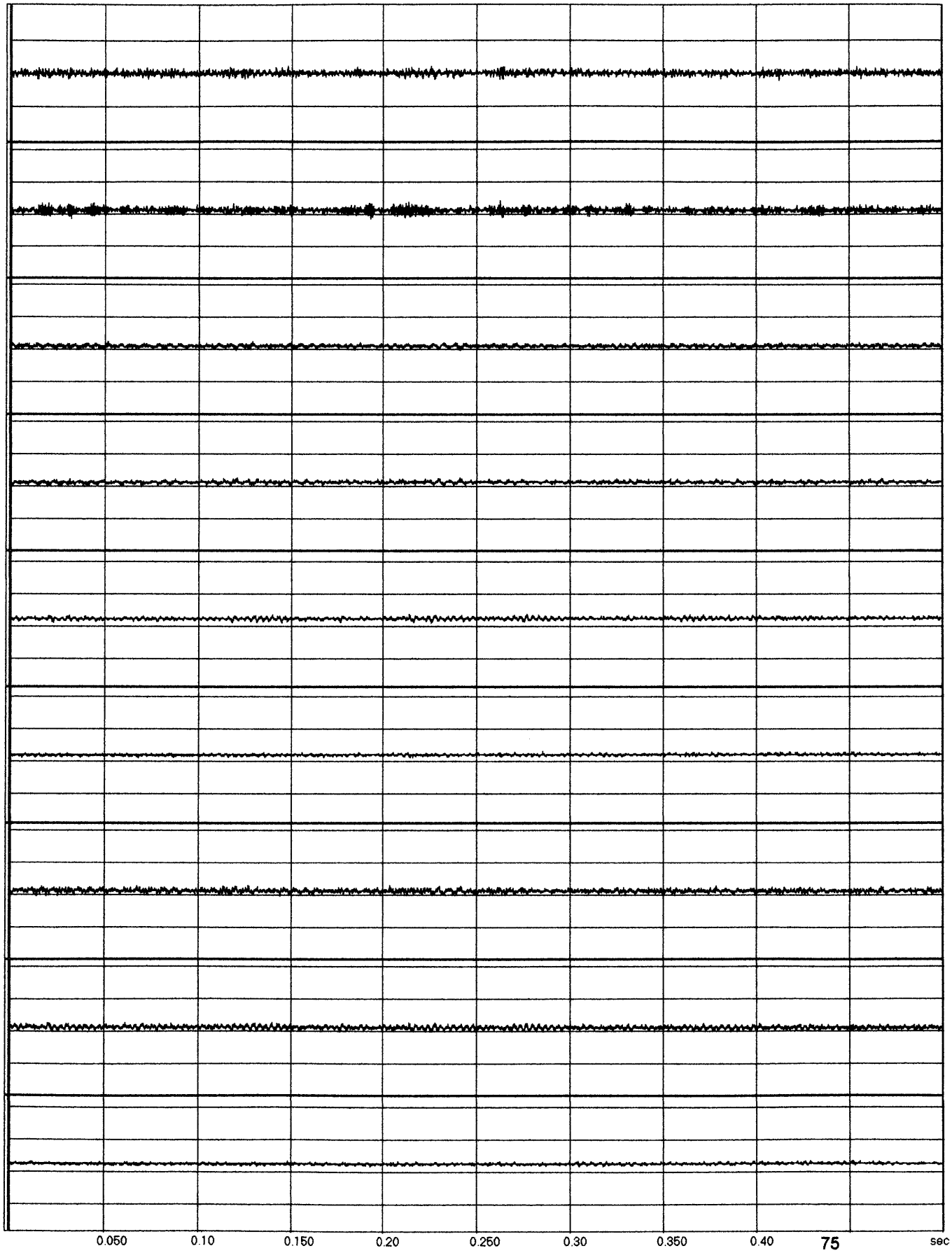

Data File : D:\Thesis Files\Data\Good BRG Baseline\700.bin
Sample Rate : 12000.0 samples/sec
Channel Mode : 16

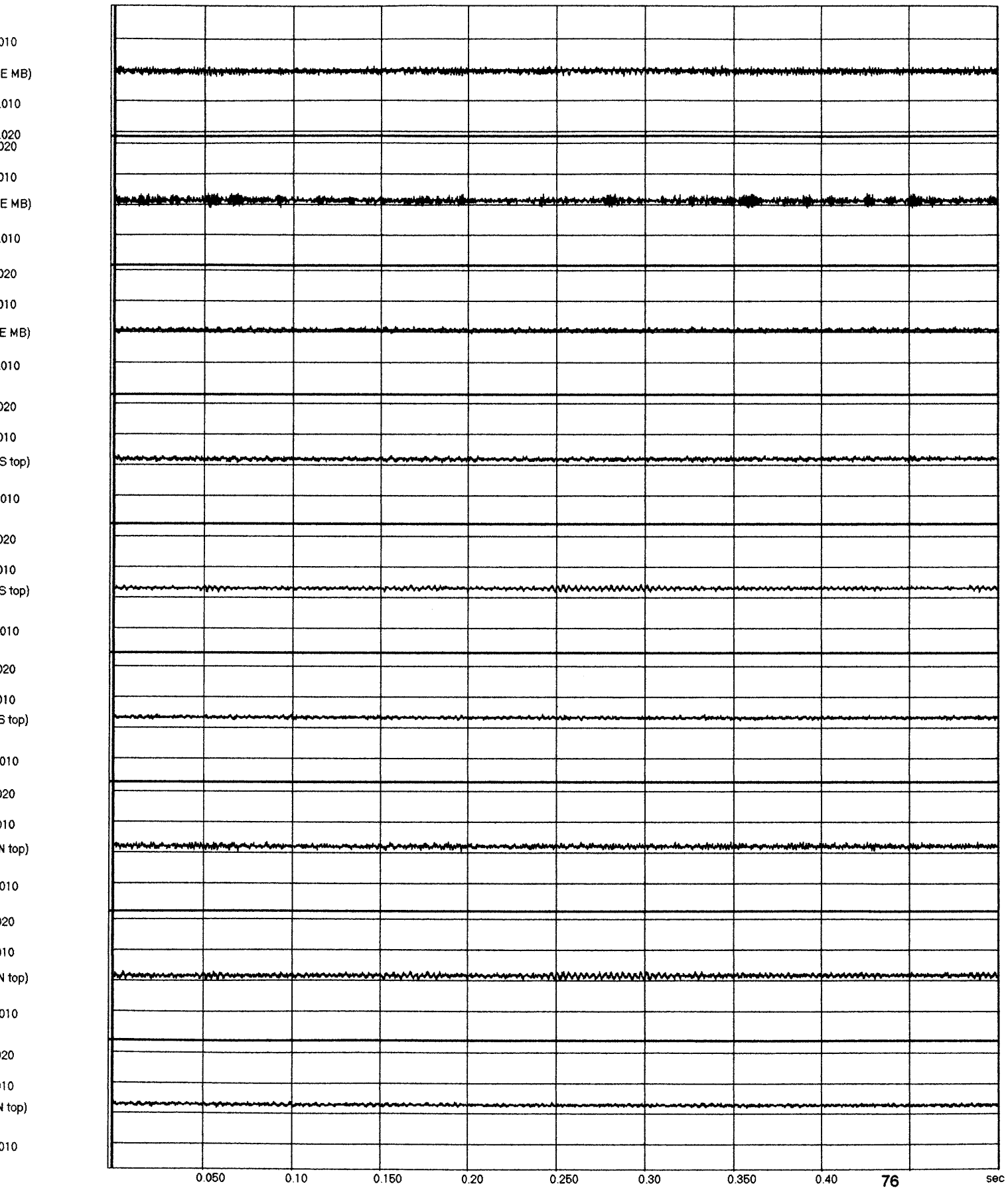

Data File : D:\Thesis Files\Data\Good BRG Baseline\600.bin
Sample Rate : 12000.0 samples/sec
Channel Mode : 16

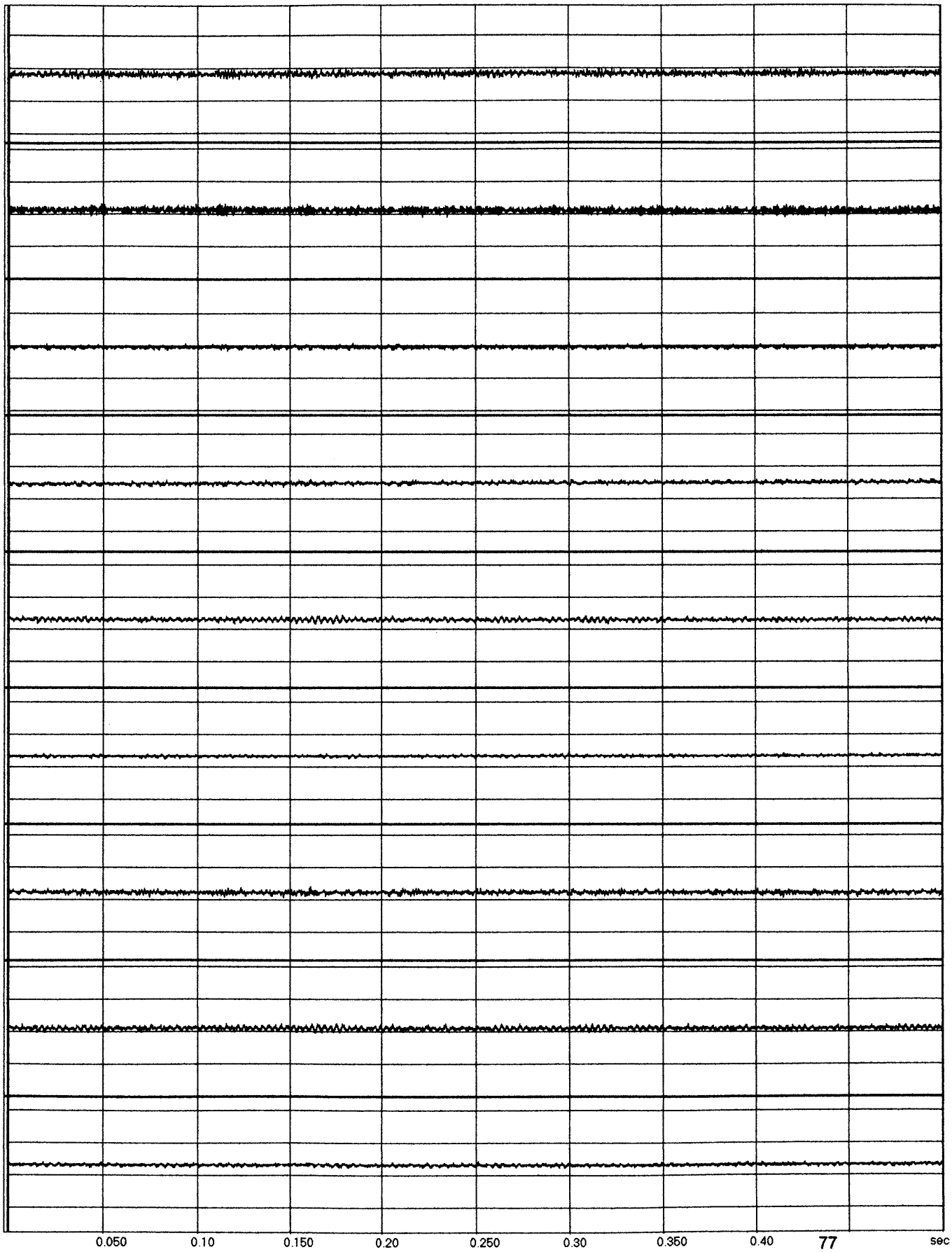

Data File : D:\Thesis Files\Data\Good BRG Baseline\450.bin
Sample Rate : 12000.0 samples/sec
Channel Mode : 16

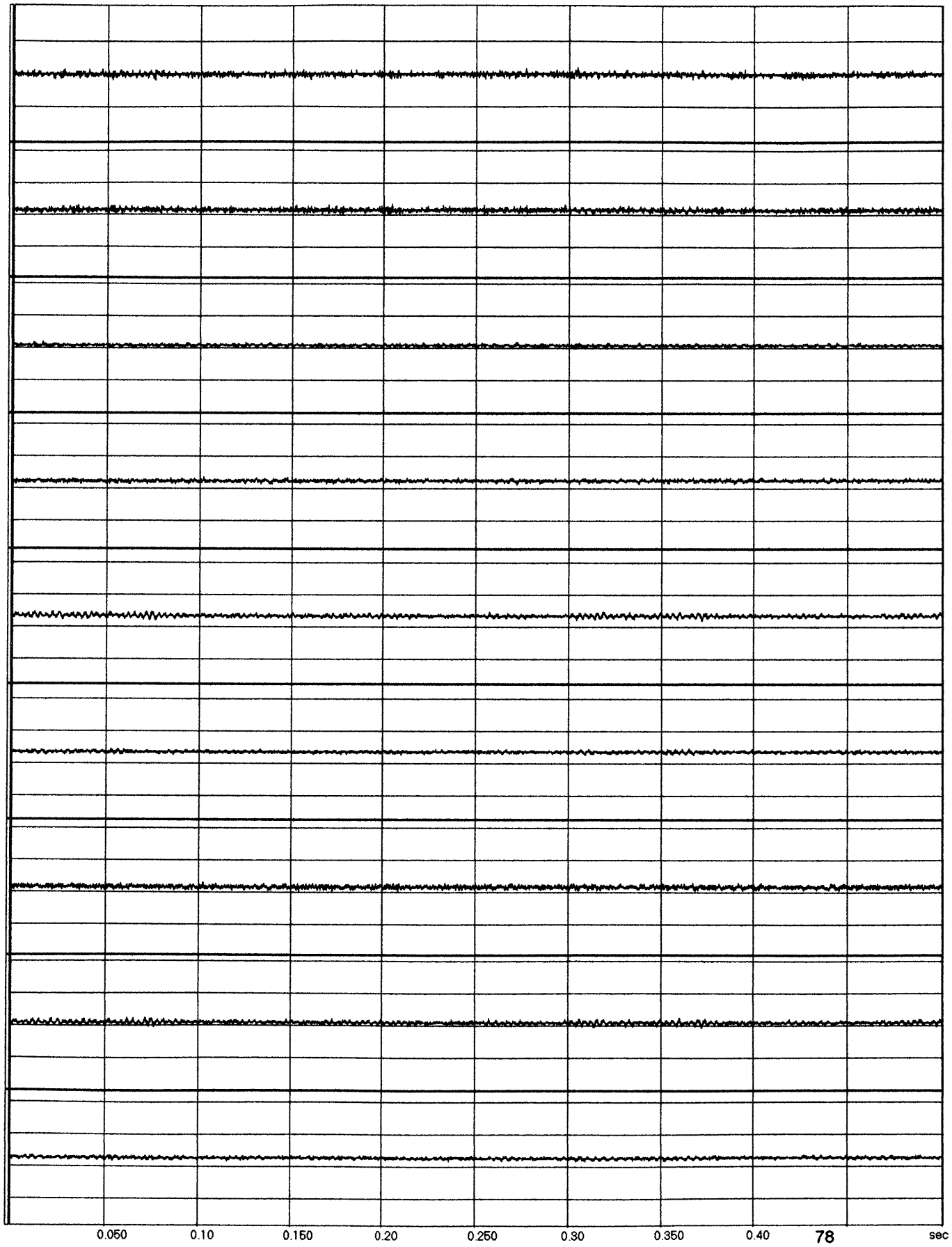

Data File : D:\Thesis Files\Data\Good BRG Baseline\300.bin
Sample Rate : 12000.0 samples/sec
Channel Mode : 16